Technical Report

"Ultrafast X-Ray Sources"

Grant No. AFOSR-89-0476

August 1989 to August 1993

Professor Roger W. Falcone
Principal Investigator

Department of Physics
University of California at Berkeley
Berkeley, California 94720

510-642-8916

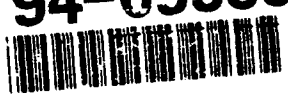

REPORT DOCUMENTATION PAGE

Approved for public release; distribution unlimited.

Form Approved OMB No. 0704-0188

1. AGENCY USE ONLY (Leave blank)	2. REPORT DATE	3. REPORT TYPE AND DATES COVERED
		Final Report 8/89 - 8/93

4. TITLE AND SUBTITLE

Ultrafast X-Ray Sources

5. FUNDING NUMBERS

AFOSR-89-0476

6. AUTHOR(S)

Professor Roger W. Falcone

7. PERFORMING ORGANIZATION NAME(S) AND ADDRESS(ES)

Department of Physics
University of California
Berkeley CA 94720

8. PERFORMING ORGANIZATION REPORT NUMBER

AFOSR-TR- 94 0063

9. SPONSORING/MONITORING AGENCY NAME(S) AND ADDRESS(ES)

AFOSR/NE
110 Duncan Avenue Suite B115
Bolling AFB DC 20332-0001

10. SPONSORING/MONITORING AGENCY REPORT NUMBER

2301/AS

11. SUPPLEMENTARY NOTES

12a. DISTRIBUTION/AVAILABILITY STATEMENT

UNLIMITED

Approved for public release; distribution unlimited.

12b. DISTRIBUTION CODE

13. ABSTRACT *(Maximum 200 words)*

During the contract period we made progress in six areas:

-- development of ultrashort pulse x-ray sources
-- generation of subpicosecond, unicycle elentromagnetic pulses
-- propagation of intensee, short pulse lasers in plasmas
-- new x-ray lasers
-- new high-intensity, short pulse lasers
--diagnosis of multiphoton ionized plasmas.

Our work resulted in thirty-one publications, which are listed in Section III of this report. Publications not previously been sent to AFOSR are included in thisreeport.

Our work has resulted in forty-five conference presentations, which are listed in sectionIV of this report. Four additional invited talks are currently scheduled.

14. SUBJECT TERMS			15. NUMBER OF PAGES
			16. PRICE CODE
17. SECURITY CLASSIFICATION OF REPORT	18. SECURITY CLASSIFICATION OF THIS PAGE	19. SECURITY CLASSIFICATION OF ABSTRACT	20. LIMITATION OF ABSTRACT
UNCLASSIFIED	UNCLASSIFIED	UNCLASSIFIED	UL

Contents

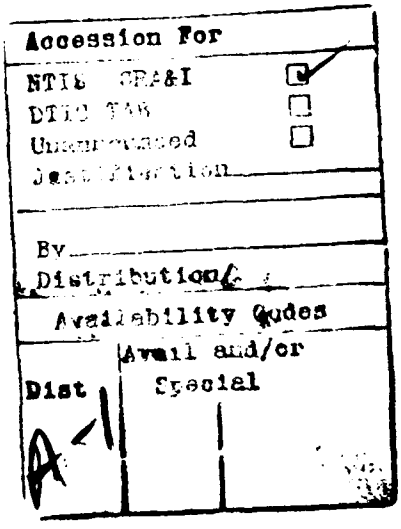

I. Introduction

During the contract period we made progress in six areas:

-- development of ultrashort pulse x-ray sources
-- generation of subpicosecond, unicycle electromagnetic pulses
-- propagation of intense, short pulse lasers in plasmas
-- new x-ray lasers
-- new high-intensity, short pulse lasers
-- diagnosis of multiphoton ionized plasmas.

Our work resulted in thirty-one publications, which are listed in section III of this report. Publications not previously been sent to AFOSR are included in this report.

Our work has resulted in forty-five conference presentations, which are listed in section IV of this report. Four additional invited talks are currently scheduled.

II. Summary of research work

1) Short pulse x-ray sources

Under this contract we proposed and demonstrated a novel source of pulsed x-rays which has an ultrashort pulse duration and high intensity. This source is based on x-ray emission from ultrashort, laser-heated solids. Applications of such a source include time resolved x-ray scattering (for the study of the temporal dynamics of structural changes in materials, phase transitions and chemical reactions) and pumping new types of x-ray lasers.

I believe that our pioneering work has led to a new field of high-intensity, short-pulse laser interaction with solids; in particular, a NSF workshop in this area was recently held at the University of Michigan. The major emphasis of our work is the development of the enhanced x-ray output from sub-wavelength, microstructured targets. We exploited the high absorption of short pulse laser energy by structured targets and measured the resulting enhancement of x-ray emission.

The most recent reports of this work are found in publications **#27 and 28**, listed in section III.

2) Subpicosecond electromagnetic pulses

We proposed and demonstrated a novel technique for the generation of high power, single cycle pulses at terahertz frequencies. This radiation may have applications as a new source for high frequency radar, or as a source for a new field of nonlinear far infrared optics. In particular it could excite molecules and solids in an impulsive manner, producing rapid conformational changes along highly nonadiabatic pathways. This source is based on the generation of intense pulsed fields at the focus of short pulse laser light in gases and solids. This emission, in the far-infrared, also serves as a diagnostic of high-intensity laser-matter interaction in our pulsed x-ray sources.

In this work, laser pulses with a power of 10^{12} W and a duration of 10^{-13} s are focused onto both gas and solid targets. Strong emission of pulsed radiation at terahertz frequencies is observed from the resulting plasmas. The most intense radiation is detected from solid density targets and is correlated with the emission of MeV x-rays and electrons. Results conclusively indicate that radiative processes in such plasmas are driven by laser induced space charge fields in excess of 10^8 V/cm. This work constitutes the first direct observation of a laser induced wakefield.

Detailed reports of this work is found in publication **#20 and 28**, listed in section III.

3) Propagation of intense laser pulses in plasmas

We have examined the propagation of high intensity (up to 10^{19} W/cm^2) ultrashort (100 fs) laser pulses in dense gases. This work has application to a variety of studies involving high power laser pulses such as harmonic generation, x-ray lasers, and laser wakefield accelerators. In particular we have searched for self channeling of the laser beam in plasmas; however, we observe a null result in the theoretically predicted regimes. However, we do observe an increase in the Rayleigh range of the focused laser, by a factor of 3, in a novel configuration that uses a spatially shaped intensity profile but lower than expected laser power. We conclude that in much of the parameter space for short-pulse, very high-power laser interaction with plasmas, channeling will not occur and plasma-refraction-induced beam break-up will dominate the interaction physics. More complex solutions to the beam propagation problem are required than simple self channeling.

A detailed report of this work has been submitted; it is publication **#30,** listed in section III.

4) X-ray laser development

We studied two schemes for new x-ray lasers. They involve:

(1) rapid photoionization of k-shell electrons (pumped by intense, short pulse x-ray sources) followed by lasing on k-α x-ray transitions and

(2) rapid recombination of highly ionized atoms (produced by multiphoton ionization) followed by lasing on Ly-α x-ray transitions.

Scheme (1) has been addressed in publication **#17** listed in section III; the result is that the demonstration of such systems awaits the development of higher power pump lasers. For scheme (2), we know that high intensity, short pulse lasers can produce highly ionized gas phase plasmas with extremely cold electrons which have essentially tunneled out of the atoms at low energy. Predictions of the rapid recombination of such a non-equilibrium system, with associated population inversions and lasing between energy states spaced by x-ray transitions, are well known in the field. We have modeled and performed experimental tests of this type of system by measuring the temperature of dense, multiphoton ionized gases. The slope of the continuum -

recombination spectrum indicates the electron temperature as a function of time; this technique has not been applied to this problem previously and measures the temperature of such plasmas at early times. We have combined our picosecond x-ray camera with a high resolution imaging x-ray spectrometer to determine the time resolved emission from such systems. Our new results indicate that electrons in plasmas formed under such conditions are indeed cold due to the rapid thermal conduction found in the filamentary geometry of focused laser beams. It is published in publication **# 25.**

In an exciting new experiment we are attempting to see gain in a recombination-pumped, triply ionized lithium x-ray laser system at 13.5 nm (Lα resonance line of H-like Li). We have observed laser gain in this system and preliminary results have been reported at conferences **# 44 and 45.**

This work has produced a broad view of emission from intense laser-gas interactions, including high order harmonic generation and continuum emission. This work is found in publications **#15 and 19** in section III.

5) High-intensity, short pulse lasers

We have developed the highest energy, sub-100 femtosecond laser ever reported. The preliminary version of this laser was described in reference **#8** of the publication list of this report. More recent improvements have generated higher beam quality and the laser has been operating at a multiterawatt level for the experiments described above for the past year. Commercial versions of our laser system are now available; in particular, we believe that our work encouraged the development of a similar commercial system by Spectra Physics Lasers.

6) Diagnosis of multiphoton ionized plasmas

We have developed a new Thomson scattering technique using multiple, ultrashort laser pulses. The studies were done in multiphoton ionized plasmas of interest to the construction of new x-ray lasers and complements the work discussed in (4), above. In summary, we confirmed for the first time that the tunneling model is appropriate to the analysis of electron energies in dense plasmas produced by high-intensity, sub-picosecond lasers. Our measurements were performed with femtosecond temporal resolution. This work has been submitted to Physical Review Letters, and is publication **# 31**, in section III.

III. Publications acknowledging AFOSR support

(* denotes papers enclosed with this report)

1. M.M. Murnane, H.C. Kapteyn, R.W. Falcone, "X-Ray Streak Camera with 2 ps Response," Appl. Phys. Lett. **56**, 1948 (1990).

2. H.C. Kapteyn, A. Sullivan, H. Hamster, R.W. Falcone, "Multiterawatt Femtosecond Laser Based on Ti:Sapphire," in *Femtosecond to Nanosecond High Intensity Lasers and Applications*, E. M. Campbell, ed. (SPIE, Bellingham, 1990) Vol. 1229, pp. 75-81.

3. H. Hamster, R.W. Falcone, "Proposed Source of Sub-picosecond Far Infrared Radiation," *Ultrafast Phenomena VII*, C.B. Harris, E.P. Ippen, G. A. Mourou, A. H. Zewail, eds. (Springer-Verlag, Berlin, 1990) pp. 122-124.

4. H.C. Kapteyn, M.M. Murnane, A. Szoke, A. Hawryluk, R.W. Falcone, "Enhanced Absorption and ASE Pedestal Suppression in the Generation of Ultrashort-pulse Solid-density Plasmas," *Ultrafast Phenomena VII*, C.B. Harris, E.P. Ippen, G. A. Mourou, A. H. Zewail, eds. (Springer-Verlag, Berlin, 1990) pp. 125-127.

5. Margaret M. Murnane, Henry C. Kapteyn, Mordecai D. Rosen, Roger W. Falcone, "Ultrafast X-Ray Pulses From Laser-Produced Plasmas," Science **251**, 531 (1991).

6. Henry C. Kapteyn, Margaret M. Murnane, Abraham Szoke, Roger W. Falcone, "Prepulse Energy Suppression For High-Energy Ultrashort Pulses Using Self-Induced Plasma Shuttering," Opt. Lett. **16**, 490 (1991).

7. R.W. Falcone, M.M. Murnane, H.C. Kapteyn, "High Intensity, Ultrashort Pulse Laser Heated Solids," *Laser Optics of Condensed Matter Volume 2: The Physics of Optical Phenomena and Their Use as Probes of Matter,"* E. Garmire, A.A. Maradudin, K.K. Rebane, eds. (Plenum Press, New York, 1991) pp. 83-86.

8. A. Sullivan, H. Hamster, H.C. Kapteyn, S. Gordon, W. White, H. Nathel, R.J. Blair, R.W. Falcone, "Multi-Terawatt, 100 Femtosecond Laser," Opt. Lett. **16**, 1406 (1991).

9. M. Murnane, H. Kapteyn, S. Gordon, S. Verghese, J. Bokor, W. Mansfield, R. Gnall, E. Glytsis, T. Gaylord, R.W. Falcone, "Efficient Coupling of High-Intensity Sub-Picosecond Laser Pulses into Dilute Solid Targets," *OSA Proceedings on Short Wavelength Coherent Radiation*, P.H. Bucksbaum and N.M. Ceglio, eds. (Optical Society of America, Washington, DC, 1991) Vol. 11, pp. 281-284.

10. A. Sullivan, H. Hamster, H.C. Kapteyn, S. Gordon, W. White, H. Nathel, R.J. Blair, R.W. Falcone, "Multiterawatt Laser System based on Ti:Al_2O_3," *OSA Proceedings on Short Wavelength Coherent Radiation*, P.H. Bucksbaum and N.M. Ceglio, eds. (Optical Society of America, Washington, DC, 1991) Vol. 11, pp. 181-183.

11. Margaret M. Murnane, Henry C. Kapteyn, Roger W. Falcone, "Generation of Efficient Ultrafast Laser Plasma X-Ray Sources," Phys. Fluids B **3**, 2409 (1991).

12. H.C. Kapteyn, M.M. Murnane, "Relativistic Pulse Compression," J. Opt. Soc. Am. B **8**, 1657 (1991).

13. R.W. Falcone, M.M. Murnane, H.C. Kapteyn, "Rapid Heating of Solids by Ultra-Short Pulse Lasers," in *Research Trends in Physics: Nonlinear and Relativistic Effects in Plasmas*, V. Stefan, ed. (AIP, New York, 1992) pp. 311-313.

14. H. C. Kapteyn, L.B. Da Silva, R.W. Falcone, "Short-Wavelength Lasers," Proc. IEEE **80**, 342 (1992).

15. J.K. Crane, M.D. Perry, S. Herman, R.W. Falcone, "High Field Harmonic Generation in Helium," Opt. Let. **17**, 1256 (1992).

16. R.W. Falcone, "Experiments with High-Intensity, Ultrashort-Pulse Lasers: Interactions with Solids and Gases," in *X-Ray Lasers 1992*, E.E. Fill, ed. (Institute of Physics, Bristol, England, 1992) Vol. 125, pp. 213-218.

17. H.C. Kapteyn, "Photoionization-Pumped X-Ray Lasers using Ultrashort-Pulse Excitation," Appl. Opt. **31**, 4931 (1992).

18. M.M. Murnane, H.C. Kapteyn, S.P. Gordon, J. Bokor, E.N. Glytsis, R.W. Falcone, "Efficient Coupling of High-Intensity Subpicosecond Laser Pulses into Solids," Appl. Phys. Lett. **62**, 1068 (1993).

19. John K. Crane, Michael D. Perry, Donna Strickland, Steve Herman, Roger W. Falcone, "Coherent and Incoherent XUV Emission in Helium and Neon, Laser-Driven Plasmas," IEEE Trans. Plasma Sci. **21**, 82 (1993).

20. H. Hamster, A. Sullivan, S. Gordon, W. White, R.W. Falcone, "Subpicosecond, Electromagnetic Pulses from Intense Laser-Plasma Interaction," Phys. Rev. Lett. **71**, 2725 (1993).

***21.** R.W. Falcone, S.P Gordon, H. Hamster, A. Sullivan, "X-Rays from High-Intensity, Short-Pulse Laser Interaction with Solids," in *Laser Ablation: Mechanisms and Applications II*, J.C. Miller and D. B. Geohegan, eds. (AIP, New York, 1994) pp. 529-533.

22. S.P. Gordon, R. Sheppard, T. Donnelly, D. Price, B. White, A. Osterheld, H. Hamster, A. Sullivan, R.W. Falcone, "Short Pulse X-Rays from Porous Targets," in *Shortwavelength V: Physics with Intense Laser Pulses*, M.D. Perry and P.B. Corkum, eds. (OSA, Washington, DC, 1993) pp. 203-205.

23. A. Sullivan, S. Gordon, H. Hamster, H. Nathel, R.W. Falcone, "Propagation of Intense, Ultrashort Laser Pulses in Plasmas," in *Shortwavelength V: Physics with Intense Laser Pulses*, M.D. Perry and P.B. Corkum, eds. (OSA, Washington, DC, 1993) pp. 40-44.

24. H. Hamster, A. Sullivan, S. Gordon, B. White, R.W. Falcone, "Subpicosecond, Far-Infrared Emission from High-Intensity Laser Plasmas," in *Shortwavelength V: Physics with Intense Laser Pulses*, M.D. Perry and P.B. Corkum, eds. (OSA, Washington, DC, 1993) pp. 62-65.

25. T.E. Glover, J.K. Crane, M.D. Perry, R.W. Falcone, "Electron Energy Distributions in Plasmas Produced By Intense Short Pulse Lasers," in *Shortwavelength V: Physics with Intense Laser Pulses*, M.D. Perry and P.B. Corkum, eds. (OSA, Washington, DC, 1993) pp. 189-191.

***26.** R.W. Falcone, S.P. Gordon, H. Hamster, A. Sullivan, an T. Donnelly, "X-Ray Radiation by Ultrashort Pulse Lasers," in *Ultrashort Wavelength Lasers II*, S. Suckewer, ed. (SPIE, Bellingham, 1994) Vol. 2012, pp. 242-245.

To be published

*27. M.M. Murnane, H.C. Kapteyn, S.P. Gordon, R.W. Falcone, "Ultrashort X-Ray Pulses," (in Appl. Phys. B)

*28. H. Hamster, A. Sullivan, S. Gordon, R.W. Falcone, "Short-Pulse Terahertz Radiation from High-Intensity Laser-Produced Plasmas," (in Phys. Rev. E)

*29. S.P. Gordon, T. Donnelly, A. Sullivan, H. Hamster, R.W. Falcone, "X-Rays from Microstructured Targets Heated by Femtosecond Lasers," (in Opt. Lett.)

Submitted for publication

*30. A. Sullivan, H. Hamster, S.P. Gordon, H. Nathel, R.W. Falcone, "Propagation of Intense, Ultrashort Laser Pulses in Plasmas," (submitted to PRL)

*31. T. E. Glover, T.D. Donnelly, E.A. Lipman, A. Sullivan, R.W. Falcone, "Sub-Picosecond Thomson Scattering Measurements of Optically Ionized Helium Plasmas," (submitted to PRL)

IV. Invited and contributed talks on work supported by AFOSR

1. Optical Society of America Topical Meeting on High Energy Density Physics with Sub-Picosecond Lasers, September 1989, Snowbird, Utah, "Ultrashort Pulse Laser Heating of Solids," R.W. Falcone. (invited talk)

2. Lawrence Berkeley Laboratory Center for X-Ray Optics, October 1989, Berkeley, California, "Generation and Applications of Sub-Picosecond X-Ray Pulses," R.W. Falcone. (invited talk)

3. USA-USSR Binational Symposium on the Physics of Optical Phenomena and Their Uses as Probes of Matter, January 1990, Irvine, California, "High Intensity, Ultrashort Laser Heated Solids," R.W. Falcone. (invited talk)

4. La Jolla Institute Topical Conference on Research Trends in Nonlinear and Relativistic Effects in Plasmas, February 1990, La Jolla, California, "Rapid Heating of Solids by Ultrashort Pulse Lasers," R.W. Falcone, et al. (invited talk)

5. Xth Vavilov Conference on Nonlinear Optics, May 1990, Novosibirsk, USSR, "Solid Density Plasmas heated by Ultrafast Laser Pulses," R.W. Falcone. (invited talk)

6. Physics Department Condensed Matter Seminar, University of California at Berkeley, September 1990, "High Temperature Laser Heated Solids," R.W. Falcone. (invited talk)

7. Optical Society of America Annual Meeting, November 1990, Boston, Massachusetts, "Ultrashort Pulse X-rays From Laser Heated Solids," R.W. Falcone, et al. (invited talk)

8. Harvard University, Division of Applied Science, November 1990, Boston, Massachusetts, "Ultrashort Pulse X-rays From Laser Heated Solids," R.W. Falcone. (invited talk)

9. University of Toronto Summer School on Ultra-Fast and Super-Intense Laser Technology, Science and Applications, May 1991, Toronto, Canada, "Ultrafast Bursts of X-Rays from Femtosecond Laser-Matter Interaction," R.W. Falcone. (invited talk)

10 CLEO Conference, May 1991, Baltimore, Maryland, "Terawatt, TiAl2O3 Laser System," A. Sullivan, et al. (postdeadline paper)

11. Macquarie University, New South Wales, Australia, September 1991, "Laser Induced Emission at Short Wavelengths from Gases and Solids," R.W. Falcone. (invited talk)

12. Australian Conference on Optics, Lasers and Spectroscopy, September 1991, Canberra, Australia,"Laser Induced Emission at Short Wavelengths from Gases and Solids," R.W. Falcone. (invited talk)

13. Lawrence Livermore National Laboratory, October 1991, Livermore, California, "High-Intensity, Short-Pulse Laser Interactions with Matter," R.W. Falcone. (invited talk)

14. Lawrence Livermore National Laboratory, February 1992, Livermore, California, "New Experiments in High Intensity Laser Matter Interaction using Ultrashort Pulse Lasers," R.W. Falcone. (invited talk)

15. IBM Almaden Research Center, February 1992, San Jose, California, "X-Rays and Other Emissions from Short-Pulse, High-Intensity, Laser-Matter Interaction," R.W. Falcone. (invited talk)

16. Rice University, March 1992, Houston, Texas, "Experiments with High-Intensity, Ultrashort-Pulse Lasers: Interactions with Solids and Gases," R.W. Falcone. (invited talk)

17. Third International Colloquium on X-Ray Lasers, May 1992, Schliersee, Germany, "Experiments with High-Intensity, Ultrashort-Pulse Lasers: Interactions with Solids and Gases," R.W. Falcone. (invited talk)

18. Optical Society of America Topical Meeting on Nonlinear Optics, August 1992, Maui, Hawaii, "Interaction of High Intensity, Ultrashort Pulse Lasers with Solids and Gases," R.W. Falcone. (invited talk)

19. Washington State University Physics Department Colloquim, October 1992, Pullman, Washington, "High Intensity Laser Interactions," R.W. Falcone. (invited talk)

20. University of Michigan NSF Center for Ultrafast Optical Science Seminar, November 1992, Ann Arbor, Michigan "High Intensity Laser Interactions," R.W. Falcone. (invited talk)

21. IEEE Lasers and Electro-Optics Society Annual Meeting, November 1992, Boston, Massachusetts, "high Intensity Short-Pulse Lasers and Applications to High Field Physics," R.W. Falcone. (invited talk)

22. Ultrafast Electronics and Optoelectronics Conference, January 1993, San Francisco, California, "Subpicosecond, Far-Infrared Emission from High-Intensity Laser Plasmas," H. Hamster, et al. (postdeadline paper)

23. Stanford University Quantum Electronics Seminar, February 1993, Stanford, California, "Short-Pulse, High-Intensity Laser Interaction With Solids and Gases," R.W. Falcone. (invited talk)

24. Japanese Science and Technology Agency Symposium, February 1993, Tokyo, Japan, "Short-Pulse, High-Intensity Laser Interaction With Solids and Gases," R.W. Falcone. (invited talk)

25. Osaka University, February 1993, Osaka, Japan, "Short-Pulse, High-Intensity Laser Interaction With Solids and Gases," R.W. Falcone. (invited talk)

26. Electrotechnical Laboratory, February 1993, Tsukuba, Japan, "Short-Pulse, High-Intensity Laser Interaction With Solids and Gases," R.W. Falcone. (invited talk)

27. OSA Conference on Short Wavelengths: Physics with Intense Laser Pulses, March 1993, San Diego, California, "Short Pulse X-Rays from Porous Targets," S.P. Gordon, et al. (contributed paper)

28. OSA Conference on Short Wavelengths: Physics with Intense Laser Pulses, March 1993, San Diego, California, "Propagation of Intense, Utrashort Laser Pulses in Plasmas," A. Sullivan, et al. (contributed paper)

29. OSA Conference on Short Wavelengths: Physics with Intense Laser Pulses, March 1993, San Diego, California, "Subpicosecond, Far-Infrared Emission from High-Intensity Laser Plasmas," H. Hamster, et al.(contributed paper)

30. OSA Conference on Short Wavelengths: Physics with Intense Laser Pulses, March 1993, San Diego, California, "Electron Energy Distributions in Plasmas Produced By Intense Short Pulse Lasers" T.E. Glover, et al. (contributed paper)

31. University of Michigan Workshop at the NSF Center for Ultrafast Optical Science, April 1993, Ann Arbor, Michigan "Laser Interactions with Solids," R.W. Falcone. (invited talk)

32. International Conference on Laser Ablation, April 1993, Knoxville, Tennessee, "X-Rays from High-Intensity, Short-Pulse Laser Interaction with Solids," R.W. Falcone. (invited talk)

33. QELS Conference, May 1993, Baltimore, Maryland, "Short Pulse X-Rays from Porous Targets," S.P. Gordon, et al. (contributed paper)

34. QELS Conference, May 1993, Baltimore, Maryland, "Propagation of Intense, Utrashort Laser Pulses in Plasmas," A. Sullivan, et al. (contributed paper)

35. QELS Conference, May 1993, Baltimore, Maryland, "Subpicosecond, Far-Infrared Emission from High-Intensity Laser Plasmas," H. Hamster, et al. (contributed paper)

36. QELS Conference, May 1993, Baltimore, Maryland, "Electron Energy Distributions in Plasmas Produced By Intense Short Pulse Lasers," T.E. Glover, et al. (contributed paper)

37. CLEO Conference, May 1993, Baltimore, Maryland, "Experiments with High Intensity, Ultrashort-Pulse Lasers," R.W. Falcone. (invited talk)

38. University of Central Florida CREOL, May 1993, Orlando, Florida, "Experiments with High Intensity, Ultrashort-Pulse Lasers," R.W. Falcone. (invited talk)

39. Canadian Association of Physicists Workshop, June 1993, Vancouver, BC, Canada, "Experiments with High Intensity, Ultrashort-Pulse Lasers," R.W. Falcone. (invited talk)

40. SPIE Meeting, July 1993, Los Angeles, California, "X-Ray Radiation by Ultrashort Pulse Lasers," R.W. Falcone. (invited talk)

41. Gordon Research Conference on Nonlinear Optics and Lasers, August 1993, Wolfeboro, New Hampshire, "Terahertz Through X-Ray Generation from High-Intensity Lasers Interactions with Gases and Solids," R.W. Falcone. (invited talk)

42. Optical Society of America Annual Meeting, October 1993, Toronto, Canada, "High-Intensity Laser Interactions with Solids and Gases," R.W. Falcone. (invited talk)

43. Symposium on Coherent Radiation Sources, Lawrence Berkeley Laboratory, Berkeley, California, December 1993, Berkeley, California, "Terahertz to X-Ray Generation Using High-Power, Ultrashort-Pulse Lasers," R.W. Falcone. (invited talk)

44. 24th Winter Colloquim on Quantum Electronics, Snowbird, Utah, January 1994, "Characterization of Plasmas Produced by Intense, Short-Pulse Lasers," R.W. Falcone. (invited talk)

45. SPIE Meeting, January 1994, Los Angeles, California, "Thomson Scattering and X-Ray Lasers from Multiphoton Ionized Plasmas," T. Donnelly and R.W. Falcone. (invited talk)

Curriculum Vitae

Roger Wirth Falcone

Physics Department
University of California at Berkeley
Berkeley, California 94720

TEL (510) 642-8916 FAX (510) 643-8497 EMAIL rwf@physics.berkeley.edu

PROFESSIONAL EXPERIENCE

Professor, Physics Department
University of California at Berkeley (1991-present)

Associate Professor, Physics Department
University of California at Berkeley (1988-91)

Assistant Professor, Physics Department
University of California at Berkeley (1983-88)

Marvin Chodorow Fellow, Applied Physics Department
Stanford University (1980-83)

EDUCATION

Ph.D. Electrical Engineering Stanford University (1979)

M.S. Electrical Engineering Stanford University (1976)

A.B. Physics Princeton University (1974)

HONORS

Fellow of the American Physical Society (1992)

Distinguished Traveling Lecturer of the American Physical Society Laser Science Topical Group (1992-93)

Fellow of the Optical Society of America (1988)

Presidential Young Investigator Award
of the National Science Foundation (1984-89)

PROFESSIONAL ACTIVITIES

Topical Editor for *Optics Letters*

Consultant to Lawrence Livermore National Laboratory

American Physical Society Representative to the
Joint Council on Quantum Electronics

BIRTHDATE AND PLACE

June 27, 1952
New York City

PUBLICATIONS AND TALKS

see attached

Bibliography

Roger Wirth Falcone

1. D.B. Lidow, R.W. Falcone, J.F. Young, S.E. Harris, "Inelastic Collision Induced by Intense Optical Radiation," Phys. Rev. Lett. **36**, 462 (1976). [erratum: Phys. Rev. Lett. **37**, 1590 (1976)]

2. S.E. Harris, R.W. Falcone, W.R. Green, D.B. Lidow, J.C. White, J.F. Young, "Laser Induced Collisions," in *Tunable Lasers and Applications*, A. Mooradian, T. Jaeger and P. Stokseth, eds. (Springer-Verlag, New York, 1976) pp. 193-206.

3. R.W. Falcone, W.R. Green, J.C. White, J.F. Young, S.E. Harris, "Observation of Laser Induced Inelastic Collisions," Phys. Rev. A **15**, 1333 (1977).

4. W.R. Green, R.W. Falcone, "Inversion of the Resonance Line of Sr^+ Produced by Optically Pumping Sr Atoms," Optics Lett. **2**, 115 (1978).

5. R.W. Falcone, J.R. Willison, J.F. Young, S.E. Harris, "Measurement of the He 1s2s $^1S_0$ Isotopic Shift Using a Tunable VUV Anti-Stokes Light Source," Optics Lett. **3**, 162 (1978)

6. R.W. Falcone, "Inversion of Atoms and Molecules to the Ground State by Optical Pumping," Appl. Phys. Lett. **34**, 150 (1979).

7. S.E. Harris, J.F. Young, W.R. Green, R.W. Falcone, J. Lukasik, J.C. White, J.R. Willison, M.D. Wright, G.A. Zdasiuk, "Laser Induced Collisional and Radiative Energy Transfer," in *Laser Spectroscopy IV*, H. Walther and K.W. Rothe, eds. (Springer-Verlag, New York, 1979) pp. 349-359.

8. R.W. Falcone, G.A. Zdasiuk, "Pair Absorption Pumped Barium Laser," Optics Lett. **5**, 155 (1980).

9. J.R. Willison, R.W. Falcone, J.C. Wang, J.F. Young, S.E. Harris, "Emission Spectra of Core Excited Even Parity ^2P States of Neutral Lithium," Phys. Rev. Lett. **44**, 1125 (1980).

10. R.W. Falcone, G.A. Zdasiuk, "Radiative Collisional Fluorescence Observed From Thermally Excited Atoms," Optics Lett. **5**, 365 (1980).

11. S.E. Harris, J.F. Young, R.W. Falcone, W.R. Green, D.B. Lidow, J. Lukasik, J.C. White, M.D. Wright, G.A. Zdasiuk, "Laser Induced Collisional Energy Transfer," in *Atomic Physics 7*, D. Kleppner and F.M. Pipkin, eds. (Plenum Press, New York, 1981) pp. 407-428.

12. S.E. Harris, R.W. Falcone, M. Gross, R. Normandin, K.D. Pedrotti, J.E. Rothenberg, J.C. Wang, J.R. Willison, J.F. Young, "Anti-Stokes Scattering as an XUV Radiation Source," in *Laser Spectroscopy V*, A.R.W. McKellar, T. Oka and B.P. Stoicheff, eds. (Springer Verlag, New York, 1981) pp. 437-445.

13. J.R. Willison, R.W. Falcone, J.F. Young and S.E. Harris, "Laser Spectroscopy of Metastable Extreme-Ultraviolet Levels in Lithium Atoms and Ions," Phys. Rev. Lett. **47**, 1827 (1981).

14. R.W. Falcone, K.D. Pedrotti, "Pulsed Hollow Cathode Discharge for XUV Lasers and Radiation Sources," Optics Lett. **7**, 74 (1982).

15. S.E. Harris, R.W. Falcone, D.M. O'Brien, "Proposal for High Power Radiative Collisional Lasers," Optics Lett. **7**, 397 (1982).

16. S.E. Harris, J.F. Young, R.W. Falcone, J.E. Rothenberg, J.R. Willison, J.C. Wang, "Anti-Stokes Scattering as an XUV Radiation Source and Flashlamp," in *Laser Techniques for Extreme Ultraviolet Spectroscopy*, T.J. McIlrath and R.R. Freeman, eds. (American Institute of Physics, New York, 1982) pp. 137-152.

17. R.W. Falcone, D.E. Holmgren, K.D. Pedrotti, "Hollow Cathode Discharge for XUV Lasers and Radiation Sources," in *Laser Techniques for Extreme Ultraviolet Spectroscopy*, T.J. McIlrath and R.R. Freeman, eds. (American Institute of Physics, New York, 1982) pp. 287-295.

18. S.E. Harris, J.F. Young, R.W. Falcone, J.E. Rothenberg, J.R. Willison, "Laser Techniques for Spectroscopy of Core Excited Atomic Levels," in *Atomic and Molecular Physics Close to Ionization Thresholds in High Fields*, J.P. Connerade, J.C. Gay and S. Liberman, eds. (Les Editions de Physique, France, 1982) pp. 243-254.

19. R.G. Caro, J.C. Wang, R.W. Falcone, J.F. Young, S.E. Harris, "Soft X-Ray Pumping of Metastable Levels of Li^{+}," Appl. Phys. Lett. **42**, 9 (1983).

20. R.W. Falcone, J. Bokor, "Dichroic Beamsplitter for Extreme Ultraviolet and Visible Radiation," Optics Lett. **8**, 21 (1983).

21. S.E. Harris. J.F. Young, R.G. Caro, R.W. Falcone, D.E. Holmgren, D.J. Walker, J.C. Wang, J.E. Rothenberg, J.R. Willison, "Laser Techniques for Extreme Ultraviolet Spectroscopy," in *Laser Spectroscopy VI*, H.P. Weber and W. Luthy, eds. (Springer-Verlag, New York, 1983) pp. 376-381.

22. D.E. Holmgren, R.W. Falcone, D.J. Walker, S.E. Harris, "Measurement of Lithium and Sodium Metastable Quartet Atoms in a Hollow Cathode Discharge," Optics Lett. **9**, 85 (1984).

23. S.E. Harris, R.G. Caro, R.W. Falcone, D.E. Holmgren, J.E. Rothenberg, D.J. Walker, J.C. Wang, J.R. Willison, J.F. Young, "Metastabiltiy in the XUV: Lasers and Spectroscopy," in *Atomic Physics 9*, R.S. Van Dyck, Jr. and E.N. Fortson, eds. (World Scientific Publishing Co, Singapore, 1985) pp. 462-479.

24. K.D. Pedrotti, A.J. Mendelsohn, R.W. Falcone, J.F. Young, S.E. Harris, "Extreme Ultraviolet Emission Spectra of Core-Excited Levels in Sodium and Magnesium," J. Opt. Soc. Am. B **2**, 1942 (1985).

25. R.W. Falcone, M.Murnane, "Proposal for a Femtosecond X-Ray Light Source," in *Short Wavelength Coherent Radiation: Generation and Applications*, D.T. Attwood and J. Bokor, eds. (American Institute of Physics, New York, 1986) Vol. 147, pp. 81-85.

26. H.C. Kapteyn, R.W. Lee, R.W. Falcone, "Observation of a Short Wavelength Laser Pumped by Auger Decay," Phys. Rev. Lett. **57**, 2939 (1986).

27. H.C. Kapteyn, M.M. Murnane, R.W. Falcone, G. Kolbe, R.W. Lee, "Measurements on a Proposed Short Wavelength Laser System in Xenon III," in *Multilayer Structures and Laboratory X-Ray Laser Research*, N.M. Ceglio and P. Dhez, eds. (SPIE, Bellingham, 1986) Vol. 688, pp. 54-60.

28. H.C. Kapteyn, M.M. Murnane, R.W. Falcone, "Time Resolved Measurements of Short Wavelength Fluorescence from X-Ray Excited Ions," Optics Lett. **12**, 663 (1987).

29. A. Zigler, J.H. Underwood, J. Zhu, R.W. Falcone, "Rapid Lattice Expansion and Increased X-Ray Reflectivity of a Multilayer Structure due to Pulsed Laser Heating," Appl. Phys. Lett. **51**, 1873 (1987).

30. H.C. Kapteyn, W.W. Craig, G.D. Power, J. Schachter, R.W. Falcone, "A Soft X-Ray Streak Camera Using a Microchannel Plate Photocathode," in *High Speed Photography, Videography and Photonics*, H.C. Johnson and G.L. Stradling, eds. (SPIE, Bellingham, 1988) Vol. 832, pp. 376-378.

31. H.C. Kapteyn, R.W. Falcone, "Auger Pumped Short Wavelength Laser Studies in Xenon and Krypton," Phys. Rev. A **37**, 2033 (1988).

32. R.W. Falcone, H.C. Kapteyn, "Photopumped Short Wavelength Lasers," Nucl. Instrum. & Methods B **31**, 321 (1988).

33. H.C. Kapteyn, R.W. Falcone, "Photopumped Short Wavelength Lasers in Xenon and Krypton," in *Proceedings of the International Conference on Lasers 1987*, F.J. Duarte, ed. (STS Press, McLean, VA, 1988) pp. 66-72.

34. A. Zigler, J.H. Underwood, R.W. Falcone, "X-Ray Reflectivity of a Rapidly Heated Multilayer Structure," in *High Intensity Laser-Matter Interactions*, E. Michael Campbell and H. Baldis, eds. (SPIE, Bellingham, 1988) Vol. 913, pp. 80-81.

35. M.M. Murnane, R.W. Falcone, "Short Pulse Laser Interaction with Solids," in *High Intensity Laser-Matter Interactions*, E. Michael Campbell and H. Baldis, eds. (SPIE, Bellingham, 1988) Vol. 913, pp. 5-8.

36. M.M. Murnane, R.W. Falcone, "High Power Femtosecond Dye Laser System," J. Opt. Soc. Am. B **5**, 1573 (1988).

37. M.M. Murnane, R.W. Falcone, "Plasmas Produced by Short Pulse Lasers," in *Atomic Processes in Plasmas*, A. Hauer and A.L. Merts, eds. (American Institute of Physics, New York, 1988) Vol. 168, pp. 25-32.

38. S.M. Kahn, W. Craig, J. Schachter, B. Wargelin, H. Kapteyn, R.W. Falcone, M.C. Hettrick, R.A. London, R.W. Lee, "Laboratory Astrophysics Experiments in X-Ray Transfer Physics Relevant to Cosmic Accretion-Powered Sources," Jour. de Physique **49** (colloque C1), 67 (1988).

39. M.M. Murnane, H.C. Kapteyn, R.W. Falcone, "X-Ray Emission Studies of Sub-Picosecond Laser Produced Plasmas," in *Short Wavelength Coherent Radiation: Generation and Applications*, R.W. Falcone and J. Kirz, eds. (Optical Society of America,Washington DC, 1988) Vol. 2, pp. 189-193.

40. R.M. More, Z. Zinamon, K.H. Warren, R. Falcone, M. Murnane, "Heating of Solids with Ultra-short Laser Pulses," Jour. de Physique **49** (colloque C7) 43 (1988).

41. M.M. Murnane, H.C. Kapteyn, R.W. Falcone, "High Density Plasmas Produced By Ultrafast Laser Pulses," Phys. Rev. Lett. **62**, 155 (1989).

42. M.M. Murnane, H.C. Kapteyn, R.W. Falcone, "reply to comment on 'High Density Plasmas Produced By Ultrafast Laser Pulses," Phys. Rev. Lett. **63**, 339 (1989).

43. M.M. Murnane, H.C. Kapteyn, R.W. Falcone, "Sub-Picosecond Laser Produced Plasmas," Nucl. Instrum. & Methods **B43**, 463 (1989).

44. M.M. Murnane, H.C. Kapteyn, R.W. Falcone,"Generation and Application of Ultrafast X-Ray Sources," IEEE J. Quantum Electron. **25**, 2417 (1989).

45. R.W. Falcone, M.M. Murnane, H.C. Kapteyn, "Picosecond X-Ray Sources," in *Laser Spectroscopy XI*, M.S. Feld, J.E. Thomas and A. Mooradian, eds. (Academic Press, San Diego, 1989) pp. 262-264.

46. M.M. Murnane, H.C. Kapteyn, R.W. Falcone, "Picosecond Streak Camera Measurements of Short X-Ray Pulses," in *Ultrahigh Speed and High Speed Photography, Photonics and Videography*, G.L. Stradling and D.E. Caudle, eds. (SPIE, Bellingham, 1989) Vol. 1155, pp. 563-568.

47. M.M. Murnane, H.C. Kapteyn, R.W. Falcone, "X-Ray Streak Camera with 2 ps Response," Appl. Phys. Lett. **56**, 1948 (1990).

48. H.C. Kapteyn, A. Sullivan, H. Hamster, R.W. Falcone, "Multi-terawatt Femtosecond Laser Based on Ti:Sapphire," in *Femtosecond to Nanosecond High Intensity Lasers and Applications*, E. M. Campbell, ed. (SPIE, Bellingham, 1990) Vol. 1229, pp. 75-81.

49. H. Hamster, R.W. Falcone, "Proposed Source of Sub-picosecond Far Infrared Radiation," *Ultrafast Phenomena VII*, C.B. Harris, E.P. Ippen, G. A. Mourou, A. H. Zewail, eds. (Springer-Verlag, Berlin, 1990) pp. 122-124.

50. H.C. Kapteyn, M.M. Murnane, A. Szoke, A. Hawryluk, R.W. Falcone, "Enhanced Absorption and ASE Pedestal Suppression in the Generation of Ultrashort-pulse Solid-density Plasmas," *Ultrafast Phenomena VII*, C.B. Harris, E.P. Ippen, G. A. Mourou, A. H. Zewail, eds. (Springer-Verlag, Berlin, 1990) pp. 125-127.

51. Margaret M. Murnane, Henry C. Kapteyn, Mordecai D. Rosen, Roger W. Falcone, "Ultrafast X-Ray Pulses From Laser-Produced Plasmas," Science **251**, 531 (1991).

52. Henry C. Kapteyn, Margaret M. Murnane, Abraham Szoke, Roger W. Falcone, "Prepulse Energy Suppression For High-Energy Ultrashort Pulses Using Self-Induced Plasma Shuttering," Opt. Lett. **16**, 490 (1991).

53. R.W. Falcone, M.M. Murnane, H.C. Kapteyn, "High Intensity, Ultrashort Pulse Laser Heated Solids," *Laser Optics of Condensed Matter Volume 2: The Physics of Optical Phenomena and Their Use as Probes of Matter,"* E. Garmire, A.A. Maradudin, K.K. Rebane, eds. (Plenum Press, New York, 1991) pp. 83-86.

54. L.B. Da Silva, M.H. Muendel, R.W. Falcone, D.J. Fields, J.B. Kortright, B.J. MacGowan, D.L. Matthews, S. Mrowka, G.M. Shimkaveg, J.E. Trebes, "Nonlinear Optics With Focused X-Ray Lasers," *X-Ray Lasers 1990*, G.J. Tallents, ed. (Institute of Physics, Bristol, England, 1991) Vol. 116, pp. 177-180.

55. A. Sullivan, H. Hamster, H.C. Kapteyn, S. Gordon, W. White, H. Nathel, R.J. Blair, R.W. Falcone, "Multi-Terawatt, 100 Femtosecond Laser," Opt. Lett. **16**, 1406 (1991).

56. M. Murnane, H. Kapteyn, S. Gordon, S. Verghese, J. Bokor, W. Mansfield, R. Gnall, E. Glytsis, T. Gaylord, R.W. Falcone, "Efficient Coupling of High-Intensity Sub-Picosecond Laser Pulses into Dilute Solid Targets," in *Short Wavelength Coherent Radiation*, P.H. Bucksbaum and N.M. Ceglio, eds. (Optical Society of America, Washington, DC, 1991) Vol. 11, pp. 281-284.

57. A. Sullivan, H. Hamster, H.C. Kapteyn, S. Gordon, W. White, H. Nathel, R.J. Blair, R.W. Falcone, "Multi-Terawatt Laser System based on Ti:Al_2O_3," in *Short Wavelength Coherent Radiation*, P.H. Bucksbaum and N.M. Ceglio, eds. (Optical Society of America, Washington, DC, 1991) Vol. 11, pp. 181-183.

58. Margaret M. Murnane, Henry C. Kapteyn, Roger W. Falcone, "Generation of Efficient Ultrafast Laser Plasma X-Ray Sources," Phys. Fluids B **3**, 2409 (1991).

59. R.W. Falcone, M.M. Murnane, H.C. Kapteyn, "Rapid Heating of Solids by Ultra-Short Pulse Lasers," in *Research Trends in Physics: Nonlinear and Relativistic Effects in Plasmas*, V. Stefan, ed. (AIP, New York, 1992) pp. 311-313.

60. H. C. Kapteyn, L.B. Da Silva, R.W. Falcone, "Short-Wavelength Lasers," Proc. IEEE **80**, 342 (1992).

61. J.K. Crane, M.D. Perry, S. Herman, R.W. Falcone, "High Field Harmonic Generation in Helium," Opt. Lett. **17**, 1256 (1992).

62. R.W. Falcone, "Experiments with High-Intensity, Ultrashort-Pulse Lasers: Interactions with Solids and Gases," in *X-Ray Lasers 1992*, E.E. Fill, ed. (Institute of Physics, Bristol, England, 1992) Vol. 125, pp. 213-218.

63. M.M. Murnane, H.C. Kapteyn, S.P. Gordon, J. Bokor, E.N. Glytsis, R.W. Falcone, "Efficient Coupling of High-Intensity Subpicosecond Laser Pulses into Solids," Appl. Phys. Lett. **62**, 1068 (1993).

64. G.L. Strobel, D.C. Eder, R.A. London, M.D. Rosen, R.W. Falcone, S.P. Gordon, "Inner-Shell Photo-Ionized X-Ray Laser Schemes," in *Short-Pulse High-Intensity Lasrs and Applications II*, Hector A. Baldis, ed. (SPIE, Bellingham, 1993) Vol. 1860, pp. 157-166.

65. A.C. Abare, C.J. Keane, J.K. Crane, L.B. DaSilva, R.W. Lee, M.D. Perry, R.W. Falcone, "Analysis of Neon Soft X-ray Spectra from Short-Pulse Laser-Produced Plasmas," in *Short-Pulse High-Intensity Lasrs and Applications II*, Hector A. Baldis, ed. (SPIE, Bellingham, 1993) Vol. 1860, pp. 178-188.

66. John K. Crane, Michael D. Perry, Donna Strickland, Steve Herman, Roger W. Falcone, "Coherent and Incoherent XUV Emission in Helium and Neon, Laser-Driven Plasmas," IEEE Trans. Plasma Sci. **21**, 82 (1993).

67. H. Hamster, A. Sullivan, S. Gordon, W. White, R.W. Falcone, "Subpicosecond, Electromagnetic Pulses from Intense Laser-Plasma Interaction," Phys. Rev. Lett. **71**, 2725 (1993).

68. R.W. Falcone, S.P Gordon, H. Hamster, A. Sullivan, "X-Rays from High-Intensity, Short-Pulse Laser Interaction with Solids," in *Laser Ablation: Mechanisms and Applications II*, J.C. Miller and D. B. Geohegan, eds. (AIP, New York, 1994) pp. 529-533.

69. S.P. Gordon, R. Sheppard, T. Donnelly, D. Price, B. White, A. Osterheld, H. Hamster, A. Sullivan, R.W. Falcone, "Short Pulse X-Rays from Porous Targets," in *Shortwavelength V: Physics with Intense Laser Pulses*, M.D. Perry and P.B. Corkum, eds. (OSA, Washington, DC, 1993) pp. 203-205.

70. A. Sullivan, S. Gordon, H. Hamster, H. Nathel, R.W. Falcone, "Propagation of Intense, Ultrashort Laser Pulses in Plasmas," in *Shortwavelength V: Physics with Intense Laser Pulses*, M.D. Perry and P.B. Corkum, eds. (OSA, Washington, DC, 1993) pp. 40-44.

71. H. Hamster, A. Sullivan, S. Gordon, B. White, R.W. Falcone, "Subpicosecond, Far-Infrared Emission from High-Intensity Laser Plasmas," in *Shortwavelength V: Physics with Intense Laser Pulses*, M.D. Perry and P.B. Corkum, eds. (OSA, Washington, DC, 1993) pp. 62-65.

72. T.E. Glover, J.K. Crane, M.D. Perry, R.W. Falcone, "Electron Energy Distributions in Plasmas Produced By Intense Short Pulse Lasers," in *Shortwavelength V: Physics with Intense Laser Pulses*, M.D. Perry and P.B. Corkum, eds. (OSA, Washington, DC, 1993) pp. 189-191.

73. D.C. Eder, G.L. Strobel, R.A. London, M.D. Rosen, R.W. Falcone, S.P. Gordon, "Photo-Ionized Inner-Shell X-Ray Lasers," in *Shortwavelength V: Physics with Intense Laser Pulses*, M.D. Perry and P.B. Corkum, eds. (OSA, Washington, DC, 1993) pp. 220-222.

74. R.W. Falcone, S.P. Gordon, H. Hamster, A. Sullivan, an T. Donnelly, "X-Ray Radiation by Ultrashort Pulse Lasers," in *Ultrashort Wavelength Lasers II*, S. Suckewer, ed. (SPIE, Bellingham, 1994) Vol. 2012, pp. 242-245.

To be published

M.M. Murnane, H.C. Kapteyn, S.P. Gordon, R.W. Falcone, "Ultrashort X-Ray Pulses," (in Appl. Phys. B)

H. Hamster, A. Sullivan, S. Gordon, R.W. Falcone, "Short-Pulse Terahertz Radiation from High-Intensity Laser-Produced Plasmas," (in Phys. Rev. E)

S.P. Gordon, T. Donnelly, A. Sullivan, H. Hamster, R.W. Falcone, "X-Rays from Microstructured Targets Heated by Femtosecond Lasers," (in Opt. Lett.)

D.C. Eder, P. Amendt, L.B. DaSilva, R.A. London, B.J. MacGowan, D.L. Matthews, B.M. Penetrante, M.D. Rosen, S.C. Wilks, T.D. Donnelly, R.W. Falcone, G.L. Strobel, "Table-Top X-Ray Lasers," (in Physics of Plasmas)

Submitted for publication

A. Sullivan, H. Hamster, S.P. Gordon, H. Nathel, R.W. Falcone, "Propagation of Intense, Ultrashort Laser Pulses in Plasmas," (submitted)

Conference Presentations

Roger Wirth Falcone

1. Gordon Research Conference on Non-Linear Optics and Lasers, July 1985, Wolfboro, New Hampshire, "Spectroscopy of an VUV Laser System in Xe III," R.W. Falcone. (post deadline paper)

2. Gaseous Electronics Conference, October 1985, Monterey, California, "Progress Towards a VUV Laser in Xe III," R.W. Falcone. (invited talk)

3. Lawrence Livermore National Laboratory, October 1985, Livermore, California, "Progress Towards a XUV Laser in Xe III," R.W. Falcone. (invited talk)

4. Du Pont Research Laboratories, February 1986, Wilmington, Delaware, "Extreme Ultraviolet Spectroscopy," R.W. Falcone. (invited talk)

5. Lawrence Livermore National Laboratories, April 1986, Livermore, California, "Ultrafast Laser Produced Plasmas," R.W. Falcone. (invited talk)

6. Optical Society of America Meeting on Short Wavelength Coherent Radiation, March 1986, Monterey, California, "Proposal for a Femtosecond X-Ray Light Source," R.W. Falcone and M.M. Murnane. (post deadline paper)

7. Optical Society of America Meeting, October 1986, Seattle, Washington, "Demonstration of a Short Wavelength Laser Pumped by Auger Decay," R.W. Falcone, H.C. Kapteyn and R.W. Lee. (post deadline paper)

8. International Conference on Lasers, November 1986, Orlando, Florida, "Demonstration of a Short Wavelength Laser Pumped by Auger Decay," R.W. Falcone. (invited talk)

9. International Quantum Electronics Conference, April 1987, Baltimore, Maryland, "Short Wavelength Lasers Pumped by Auger Decay," R.W. Falcone and H.C. Kapteyn. (invited talk)

10. IEEE International Conference on Plasma Science, June 1987, Arlington, Virginia, "Short Wavelength Lasing Pumped by Auger Decay," R.W. Falcone and H.C. Kapteyn. (invited talk)

11. Gordon Research Conference on Non-Linear Optics and Lasers, July 1987, Wolfboro, New Hampshire, "Short Wavelength Lasers," R.W. Falcone. (invited talk)

12. Symposium on Atomic Spectroscopy and Highly Ionized Atoms, August 1987, Lisle, Illinois, "Photopumped Short Wavelength Lasers," R.W. Falcone. (invited talk)

13. University of Toronto, September 1987, Toronto, Canada, "Ultraviolet Lasers: Physics, Applications and Prospects," R.W. Falcone. (invited talk)

14. APS Conference on Atomic Processes in High Temperature Plasmas, September 1987, Santa Fe, New Mexico, "Plasmas Produced by Short Pulse Lasers," R.W. Falcone and M.M. Murnane. (invited talk)

15. Princeton University, October 1987, Princeton, New Jersey, "New Short Wavelength Light Sources," October 1987, R.W. Falcone. (invited talk)

16. SPIE Conference on High Intensity Laser-Matter Interactions, January 1988, Los Angeles, California, "Short Pulse Laser Interaction with Solids," R.W. Falcone. (invited talk)

17. American Physical Society Meeting, April 1988, Baltimore, Maryland, "Spectroscopy of Short Pulse Laser Produced Plasmas," R.W. Falcone. (invited talk)

18. Los Alamos National Laboratory, May 1988, Los Alamos, New Mexico, "Generation and Applications of Ultrashort X-Ray Pulses," May 1988, R.W. Falcone. (invited talk)

19. National Bureau of Standards, July 1988, Gaithersburg, Maryland, "New Short Pulse X-Ray Sources form Laser Heated Solids," R.W. Falcone. (invited talk)

20. International Laser Science Conference, October 1988, Atlanta, Georgia, "New Short Pulse X-Ray Sources from Laser Heated Solids," R.W. Falcone. (invited talk)

21. Sandia National Laboratories, December 1988, Albuquerque, New Mexico, "Solid Density Plasmas Produced by Intense Ultrafast Laser Pulses," R.W. Falcone. (invited talk)

22. Nineteenth Winter Colloquium on Quantum Electronics, January 1989, Snowbird, Utah, "X-Ray Pulses Produced by Femtosecond Lasers," R.W. Falcone. (invited talk)

23. Quantum Electronics and Laser Science Conference, April 1989, Baltimore, Maryland, "Generation and Application of Ultrafast X-Ray Pulses," R.W. Falcone. (invited talk)

24. Ninth International Conference on Laser Spectroscopy, June 1989, Bretton Woods, NH, "Picosecond X-Ray Sources," R.W. Falcone, M.M. Murnane and H.C. Kapteyn. (invited talk)

25. Optical Society of America Topical Meeting on High Energy Density Physics with Sub-Picosecond Lasers, September 1989, Snowbird, Utah, "Ultrashort Pulse Laser Heating of Solids," R.W. Falcone. (invited talk)

26. Lawrence Berkeley Laboratory Center for X-Ray Optics, October 1989, Berkeley, California, "Generation and Applications of Sub-Picosecond X-Ray Pulses," R.W. Falcone. (invited talk)

27. USA-USSR Binational Symposium on the Physics of Optical Phenomena and Their Uses as Probes of Matter, January 1990, Irvine, California, "High Intensity, Ultrashort Laser Heated Solids," R.W. Falcone. (invited talk)

28. La Jolla Institute Topical Conference on Research Trends in Nonlinear and Relativistic Effects in Plasmas, February 1990, La Jolla, California, "Rapid Heating of Solids by Ultrashort Pulse Lasers," R.W. Falcone, et al. (invited talk)

29. Xth Vavilov Conference on Nonlinear Optics, May 1990, Novosibirsk, USSR, "Solid Density Plasmas heated by Ultrafast Laser Pulses," R.W. Falcone. (invited talk)

30. Physics Department Condensed Matter Seminar, University of California at Berkeley, September 1990, "High Temperature Laser Heated Solids," R.W. Falcone. (invited talk)

31. Optical Society of America Annual Meeting, November 1990, Boston, Massachusetts, "Ultrashort Pulse X-rays From Laser Heated Solids," R.W. Falcone, et al. (invited talk)

32. Harvard University, Division of Applied Science, November 1990, Boston, Massachusetts, "Ultrashort Pulse X-rays From Laser Heated Solids," R.W. Falcone. (invited talk)

33. University of Toronto Summer School on Ultra-Fast and Super-Intense Laser Technology, Science and Applications, May 1991, Toronto, Canada, "Ultrafast Bursts of X-Rays from Femtosecond Laser-Matter Interaction," R.W. Falcone. (invited talk)

34. Macquarie University, New South Wales, Australia, September 1991, "Laser Induced Emission at Short Wavelengths from Gases and S. ' ds," R.W. Falcone. (invited talk)

35. Australian Conference on Optics, Lasers and Spectroscopy, September 1991, Canberra, Australia,"Laser Induced Emission at Short Wavelengths from Gases and Solids," R.W. Falcone. (invited talk)

36. Lawrence Livermore National Laboratory, October 1991, Livermore, California, "High-Intensity, Short-Pulse Laser Interactions with Matter," R.W. Falcone. (invited talk)

37. Lawrence Livermore National Laboratory, February 1992, Livermore, California, "New Experiments in High Intensity Laser Matter Interaction using Ultrashort Pulse Lasers," R.W. Falcone. (invited talk)

38. IBM Almaden Research Center, February 1992, San Jose, California, "X-Rays and Other Emissions from Short-Pulse, High-Intensity, Laser-Matter Interaction," R.W. Falcone. (invited talk)

39. Rice University, March 1992, Houston, Texas, "Experiments with High-Intensity, Ultrashort-Pulse Lasers: Interactions with Solids and Gases," R.W. Falcone. (invited talk)

40. Third International Colloquium on X-Ray Lasers, May 1992, Schliersee, Germany, "Experiments with High-Intensity, Ultrashort-Pulse Lasers: Interactions with Solids and Gases," R.W. Falcone. (invited talk)

41. Optical Society of America Topical Meeting on Nonlinear Optics, August 1992, Maui, Hawaii, "Interaction of High Intensity, Ultrashort Pulse Lasers with Solids and Gases," R.W. Falcone. (invited talk)

42. Washington State University Physics Department Colloquim, October 1992, Pullman, Washington, "High Intensity Laser Interactions," R.W. Falcone. (invited talk)

43. University of Michigan NSF Center for Ultrafast Optical Science Seminar, November 1992, Ann Arbor, Michigan "High Intensity Laser Interactions," R.W. Falcone. (invited talk)

44. IEEE Lasers and Electro-Optics Society Annual Meeting, November 1992, Boston, Massachusetts, "high Intensity Short-Pulse Lasers and Applications to High Field Physics," R.W. Falcone. (invited talk)

45. Stanford University Quantum Electronics Seminar, February 1993, Stanford, California, "Short-Pulse, High-Intensity Laser Interaction With Solids and Gases," R.W. Falcone. (invited talk)

46. Lawrence Berkeley Laboratory Center for Beam Physics Seminar, February 1993, "Short-Pulse, High-Intensity Laser Interaction With Solids and Gases," R.W. Falcone. (invited talk)

47. Japanese Science and Technology Agency Symposium, February 1993, Tokyo, Japan, "Short-Pulse, High-Intensity Laser Interaction With Solids and Gases," R.W. Falcone (invited talk)

48. Osaka University, February 1993, Osaka, Japan, "Short-Pulse, High-Intensity Laser Interaction With Solids and Gases," R.W. Falcone. (invited talk)

49. Electrotechnical Laboratory, February 1993, Tsukuba, Japan, "Short-Pulse, High-Intensity Laser Interaction With Solids and Gases," R.W. Falcone. (invited talk)

50. University of Michigan Workshop at the NSF Center for Ultrafast Optical Science, April 1993, Ann Arbor, Michigan "Laser Interactions with Solids," R.W. Falcone. (invited talk)

51. International Conference on Laser Ablation, April 1993, Knoxville, Tennessee, "X-Rays from High-Intensity, Short-Pulse Laser Interaction with Solids," R.W. Falcone. (invited talk)

52. CLEO Conference, May 1993, Baltimore, Maryland, "Experiments with High Intensity, Ultrashort-Pulse Lasers," R.W. Falcone. (invited talk)

53. University of Central Florida CREOL, May 1993, Orlando, Florida, "Experiments with High Intensity, Ultrashort-Pulse Lasers," R.W. Falcone. (invited talk)

54. Canadian Association of Physicists Workshop, June 1993, Vancouver, BC, Canada, "Experiments with High Intensity, Ultrashort-Pulse Lasers," R.W. Falcone. (invited talk)

55. SPIE Meeting, July 1993, Los Angeles, California, "X-Ray Radiation by Ultrashort Pulse Lasers," R.W. Falcone. (invited talk)

56. Gordon Research Conference on Nonlinear Optics and Lasers, August 1993, Wolfeboro, New Hampshire, "Terahertz Through X-Ray Generation from High-Intensity Lasers Interactions with Gases and Solids," R.W. Falcone. (invited talk)

57. Optical Society of America Annual Meeting, October 1993, Toronto, Canada, "High-Intensity Laser Interactions with Solids and Gases," R.W. Falcone. (invited talk)

58. Symposium on Coherent Radiation Sources, Lawrence Berkeley Laboratory, Berkeley, California, December 1993, Berkeley, California, "Terahertz to X-Ray Generation Using High-Power, Ultrashort-Pulse Lasers," R.W. Falcone. (invited talk)

59. 24th Winter Colloquim on Quantum Electronics, Snowbird, Utah, January 1994, "Characterization of Plasmas Produced by Intense, Short-Pulse Lasers," R.W. Falcone. (invited talk)

#21

X-RAYS FROM HIGH-INTENSITY, SHORT-PULSE LASER INTERACTION WITH SOLIDS

R.W. Falcone, S.P. Gordon, H. Hamster and A. Sullivan
Physics Department
University of California at Berkeley
Berkeley, CA 94720

ABSTRACT

Laser pulses with high intensity (up to 10^{18} W/cm^2) and short duration (100 fs) were focused on solids. The result was highly ionized material and hot electrons, along with the emission of short pulse x-rays and unicycle electromagnetic pulses with subpicosecond duration.

Ultrafast x-ray pulses have applications as sources for time-resolved x-ray scattering experiments and as flashlamps for photoionization-pumped x-ray lasers.[1] Such pulses can be generated by focusing ultrashort laser pulses [2] at high intensity onto solid targets. This results in a new type of x-ray tube in which instead of using an electron beam, we heat electrons inside the target by a laser field; x-rays are then generated as in a conventional x-ray target. Radiation mechanisms include innershell ionization followed by line emission, Bremsstrahlung, and recombination radiation from highly ionized material. However, such schemes, which typically employ flat, solid density targets, tend to be inefficient because of the high reflectivity of the target surface and because the hot electron plasma loses energy rapidly by thermal transport of energy away from the target surface and into the bulk of the material. Solid targets have an abrupt interface with the vacuum, which results in mirror-like reflectivity and a waste of laser energy. Prepulsing the target in order to generate a somewhat lower density plasma in front of the solid results in a more efficient source because more energy is absorbed, but also tends to cause the emission of hard x-rays (which may be damaging in some applications) and longer pulse x-rays (which is contrary to the short duration requirement).

We recently demonstrated that plasmas created in microstructured media emit x-rays more efficiently than flat targets.[3] We employ two types of targets: first, porous metals (for example, gold black) that have an average density of < 1% of solid

density and are made up of 10 nm solid metal spheres, and second, subwavelength scale grating structures. Porous metals and gratings with sufficient depth efficiently absorb almost all of the incident laser energy.

In our experiment we focused laser pulses with an energy up to 200 mJ, a duration of 120 fs, and intensity up to 10^{18} W/cm^2 on gold black targets. As shown in Fig. 1, we measured > 1 mJ of x-rays and a conversion efficiency of about 1%.

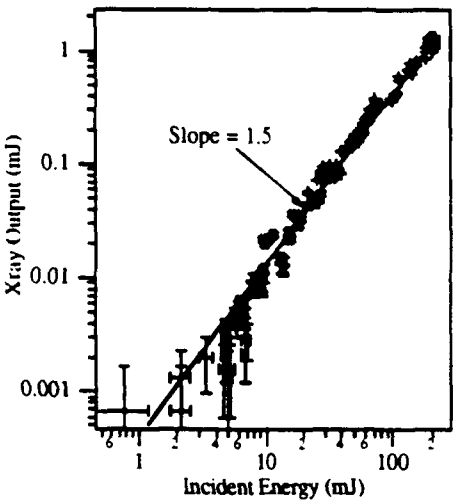

Fig. 1. X-ray emission > 1 keV from porous Au versus incident laser energy.

Solid Au, for comparison, provided a conversion efficiency of 0.01%. A filtered diode measurement of the radiated spectrum revealed that most of this radiation was emitted at roughly 1 keV by the N-shell of Au. The x-ray output of the porous Au target followed a power law dependence with an exponent of about 1.5.

We also measured the K-shell emission spectra from porous aluminum. As seen in Fig. 2, this was likewise shown to be much more efficient than the emission from a flat aluminum target. Conversion efficiencies in porous Al were found to be nearly as high as in porous Au.

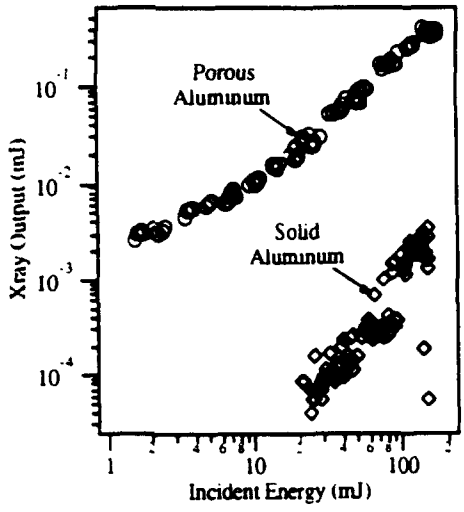

Fig. 2. X-ray emission > 1 keV from porous and solid Al versus laser energy.

The spectrum from aluminum targets is dominated by He-like Al emission. With porous Al, ten times fewer shots were required to expose film in a Von Hamos spectrometer than with a traditional flat target. Some 'cold' K-shell emission and H-like emission were present, as shown in Fig. 3.

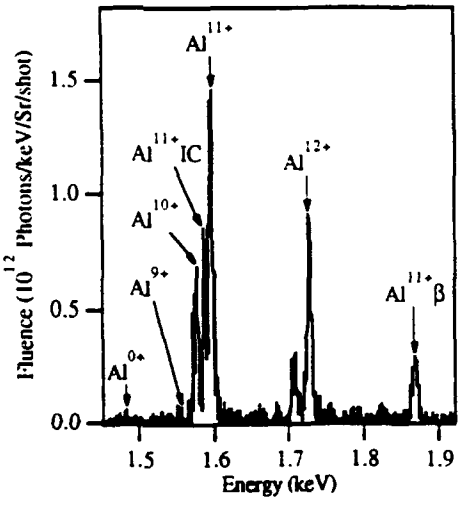

Fig. 3. K-shell emission spectrum of porous Al.

The advantages of microstructured targets can be summarized as follows:

(1) Absorption of the incident laser is greater. There is a local field enhancement at sharp edges in the microstructures and this leads to increased energy deposition per unit volume of material. Absorption may also be enhanced by collisions of the electrons at surfaces since there is much larger surface area in the microstructured targets compared to the solid targets.

(2) Thermal transport is reduced. The thermal gradient which drives energy away from absorption regions during the laser pulse is reduced in microstructured targets, since the stopping length for the laser radiation is about 2 μm of material, compared to < 10 nm for a solid metal. This reduction in thermal conduction results in higher temperature material and brighter x-ray emission.

(3) Expansion cooling following the laser pulse is enhanced. The structures expand in three dimensions, rather than two dimensions for a flat target. This rapidly cools the target and results in short pulse x-rays.

(4) There appear to be reduced superthermal electrons compared to prepulsed targets. We observe both a lower yield of hard x-rays and a lack of x-rays from solid material that underlies the microstructure.

In additional experiments, we showed that ponderomotive forces generated at the focus of an intense laser pulse in a plasma are sufficient to create a very large density difference between ionic and electronic charges.[4] This results in a powerful, radiated electromagnetic transient at terahertz frequencies, in the far-infrared (FIR). In the experiment we focused 100 fs laser pulses with intensities > 10^{18} W/cm^2 on dense gas and solid targets. A liquid helium cooled bolometer was used in conjunction with a Fourier transform spectrometer to characterize the emitted FIR. We observed a strong resonant enhancement of the emitted FIR when the plasma frequency was close to the inverse pulse length of the laser. At these plasma densities, the emission extends over several cycles of a plasma oscillation. At the highest densities we observed emission of an approximately half cycle electromagnetic pulse with a frequency centered around 1.5 THz, as shown below.

AIP CONFERENCE PROCEEDINGS 288

LASER ABLATION: MECHANISMS AND APPLICATIONS–II

SECOND INTERNATIONAL CONFERENCE

KNOXVILLE, TN APRIL 1993

EDITORS:

JOHN C. MILLER

DAVID B. GEOHEGAN

SOLID STATE DIVISION

OAK RIDGE NATIONAL LABORATORY

AIP PRESS

American Institute of Physics **New York**

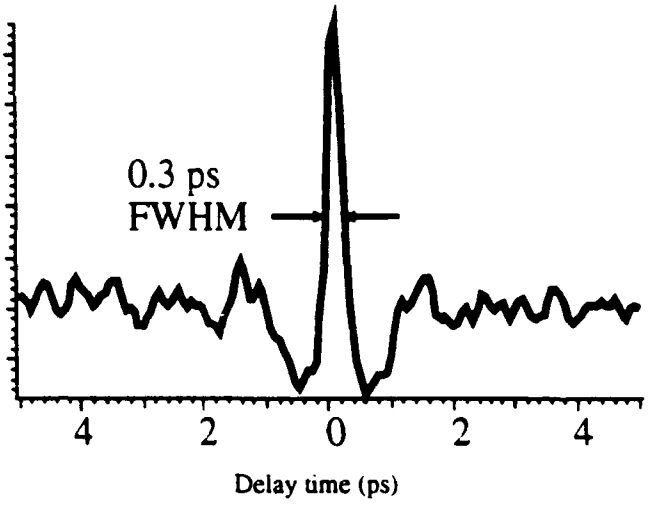

Fig. 4 Autocorrelation of a unicycle pulse from high-intensity laser-matter interaction.

The strongest FIR signal was observed from a near solid density plasma formed at the surface of a solid target. We found correlations between the intensity of the FIR signal and the emitted hot electrons and hard x-rays. We developed a linearized hydrodynamic model which accounts for the motion of a plasma driven by the strong ponderomotive forces present in the laser focus; the measured emissions indicate the existence of laser induced fields in the plasma in excess of 10^8 V/cm, in agreement with our predictions.

This work was supported by the U.S. Air Force Office of Scientific Research and the Department of Energy through a collaboration with Lawrence Livermore National Laboratory under contract W-7405-ENG-48.

REFERENCES

1. M.M. Murnane, et. al., Science **251**, 531 (1991).
2. A. Sullivan, et. al., Opt. Lett. **16**, 1406 (1991).
3. M.M. Murnane, et. al., Appl. Phys. Lett. **62**, 1068 (1993).
4. H. Hamster, R.W. Falcone, in Ultrafast Phenomena VII, C.B. Harris, et. al., eds. (Springer-Verlag, Berlin, 1990) pp. 122-124; H. Hamster, et. al. (to be published).

#26

X-Ray Radiation by Ultrashort Pulse Lasers

R.W. Falcone, S.P. Gordon, H. Hamster and A. Sullivan, T. Donnelly
Physics Department
University of California at Berkeley
Berkeley, CA 94720

ABSTRACT

Laser pulses with high intensity (up to 10^{18} W/cm^2) and short duration (100 fs) were focused on gases and solids. The result was ionized material, and emission of short pulse x-rays and unicycle electromagnetic pulses with subpicosecond duration.

Ultrafast x-ray pulses have applications as sources for time-resolved x-ray scattering experiments and as flashlamps for photoionization-pumped x-ray lasers.[1] Such pulses can be generated by focusing ultrashort laser pulses [2] at high intensity onto solid targets. This results in a new type of x-ray tube in which instead of using an electron beam, we heat electrons inside the target by a laser field; x-rays are then generated as in a conventional x-ray target. Radiation mechanisms include innershell ionization followed by line emission, Bremsstrahlung, and recombination radiation from highly ionized material.

We recently demonstrated that plasmas created in microstructured media emit x-rays more efficiently than flat targets.[3] We employ two types of targets; first, porous metals (for example, gold black) that have an average density of < 1% of solid density and are made up of 10 nm solid metal spheres, and second, subwavelength scale grating structures. Porous metals and gratings with sufficient depth efficiently absorb almost all of the incident laser energy.

In our experiment we focused laser pulses with an energy up to 200 mJ, a duration of 120 fs, and intensity up to 10^{18} W/cm^2 on targets. As shown in Fig. 1, we measured the K-shell emission spectra from porous Al. This emission was observed to be more efficient than emission from a flat Al target.

0-8194-1261-9/94/$6.00

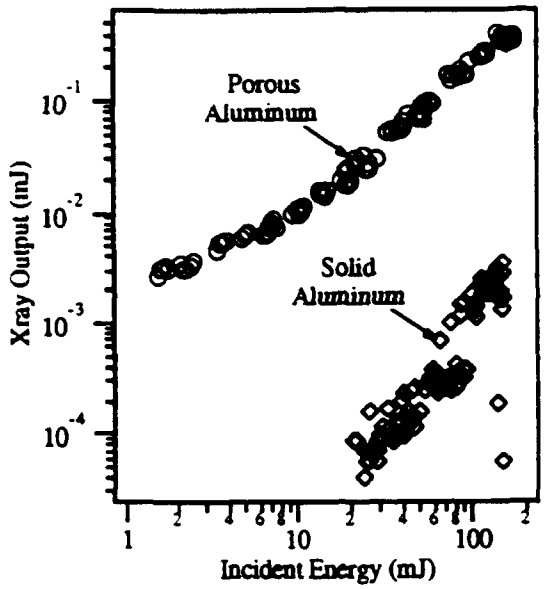

Fig. 1. X-ray emission > 1 keV from porous and solid Al versus laser energy.

The spectrum from aluminum targets is dominated by He-like Al lines. With porous Al, ten times fewer shots were required to expose film in a Von Hamos spectrometer than with a traditional flat target. Some 'cold' K-shell emission and H-like emission were present, as shown in Fig. 2.

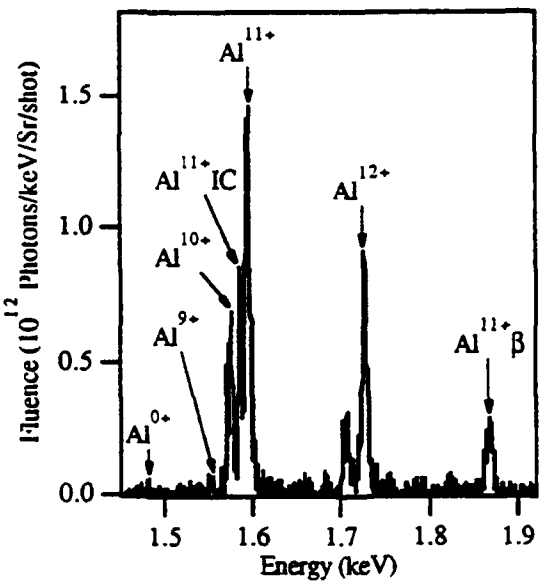

Fig. 2. K-shell emission spectrum of porous Al.

The advantages of microstructured targets can be summarized as follows:

(1) Absorption of the incident laser is greater. There is a local field enhancement at sharp edges in the microstructures and this leads to increased energy deposition per unit volume of material. Absorption may also be enhanced by collisions of the electrons at surfaces since there is much larger surface area in the microstructured targets compared to the solid targets.

(2) Thermal transport is reduced. The thermal gradient which drives energy away from absorption regions during the laser pulse is reduced in microstructured targets, since the stopping length for the laser radiation is about 2 mm of material, compared to < 10 nm for a solid metal. This reduction in thermal conduction results in higher temperature material and brighter x-ray emission.

(3) Expansion cooling following the laser pulse is enhanced. The structures expand in three dimensions, rather than two dimensions for a flat target. This rapidly cools the target and results in short pulse x-rays.

(4) There appear to be reduced superthermal electrons compared to prepulsed targets. We observe both a lower yield of hard x-rays and a lack of x-rays from solid material that underlies the microstructure.

In additional experiments, we showed that ponderomotive forces generated at the focus of an intense laser pulse in a plasma are sufficient to create a very large density difference between ionic and electronic charges.[4] This results in a powerful, radiated electromagnetic transient at terahertz frequencies, in the far-infrared (FIR). In the experiment we focused 100 fs laser pulses with intensities > 10^{18} W/cm^2 on gas and solid targets. A liquid He cooled bolometer was used in conjunction with a Fourier transform spectrometer to characterize the emitted FIR. We observed strong resonant enhancement of the emitted FIR when the plasma frequency was close to the inverse pulse length of the laser. At these plasma densities, the emission extends over several cycles of a plasma oscillation. At the highest densities we observed emission of an approximately half cycle electromagnetic pulse with a frequency centered around 1.5 THz, as shown below.

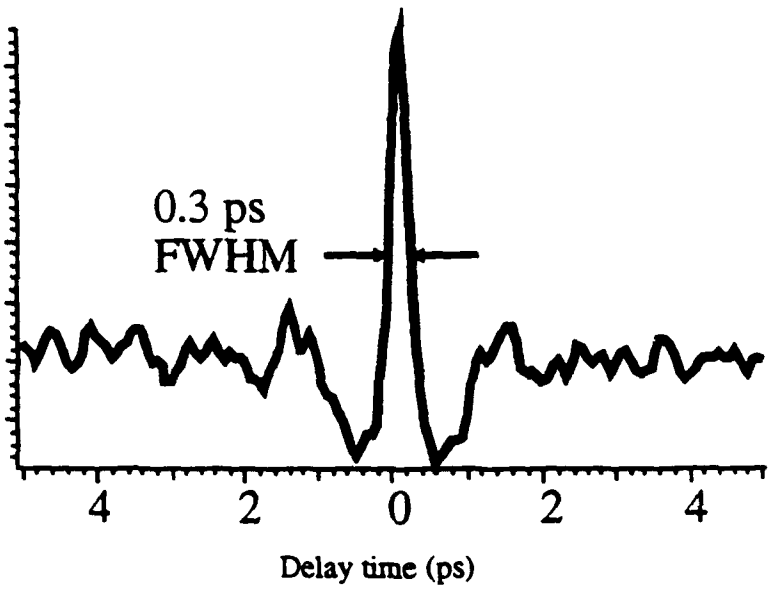

Fig. 3 Autocorrelation of a unicycle pulse from high-intensity laser-matter interaction.

The strongest FIR signal was observed from a near solid density plasma formed at the surface of a solid target. We found correlations between the intensity of the FIR signal and the emitted hot electrons and hard x-rays. We developed a linearized hydrodynamic model which accounts for the motion of a plasma driven by the strong ponderomotive forces present in the laser focus; the measured emissions indicate the existence of laser induced fields in the plasma in excess of 10^8 V/cm, in agreement with our predictions.

This work was supported by the U.S. Air Force Office of Scientific Research and the Department of Energy through a collaboration with Lawrence Livermore National Laboratory under contract W-7405-ENG-48.

REFERENCES

1. M.M. Murnane, et. al., Science **251**, 531 (1991).
2. A. Sullivan, et. al., Opt. Lett. **16**, 1406 (1991).
3. M.M. Murnane, et. al., Appl. Phys. Lett. **62**, 1068 (1993).
4. H. Hamster, R.W. Falcone, in Ultrafast Phenomena VII, C.B. Harris, et. al., eds. (Springer-Verlag, Berlin, 1990) pp. 122-124.

#27

Ultrashort X-Ray Pulses

M.M. Murnane, H.C. Kapteyn,

Department of Physics, Washington State University, Pullman, WA 99164-2814

S.P. Gordon and R.W. Falcone

Department of Physics, University of California at Berkeley, Berkeley, CA 94720

Abstract

In this paper, we discuss recent advances in ultrashort-pulse x-ray technology. Femtosecond laser-plasma-based x-ray sources can now generate sub-picosecond soft x-ray pulses, with photon energies from ~10 eV to ~10^6 eV, and with a high conversion efficiency of incident laser light to broadband x-rays. Recent advances in high-speed x-ray detectors and soft x-ray optics make it practical to use such sources as experimental tools for time-resolved x-ray science. Other possible generation techniques, such as laser-electron beam scattering, promise to further expand the our experimental capabilities in this area.

Introduction

The past seven years have marked the emergence of the new field of ultrafast x-ray science. This field was made possible by the development of x-ray sources and detectors that operate on picosecond, and even sub-picosecond, time scales.[1,2] In particular, a variety of x-ray source technologies, involving laser-produced plasmas,[1,2] synchrotrons,[3] Compton scattering,[4,5] x-ray lasers[6,7] and harmonic generation,[8-10] have been extended to shorter time scales. Much of this ultrafast x-ray technology has been driven by dramatic advances in ultrashort-pulse laser technology. Femtosecond lasers today are easier to use, generate pulses with shorter duration, and have much high peak power than were available

in the 1980's.[11,12] In addition to the advances in x-ray source development, ultrafast x-ray detectors have also been demonstrated.[13] These advances, when combined with the development of high efficiency soft x-ray optics,[3] now make it possible to extend x-ray science to sub-picosecond time resolution.

Experimental efforts in this field have concentrated on source development and, consequently, few applications have been demonstrated to date.[14-16] However, there is potential for this technology to make an important contribution to our understanding of nature. Since x-ray scattering and diffraction are sensitive to the position of atoms and the composition of materials, and have long been used to elucidate the structure of molecules, surfaces and solids, the availability of ultrashort duration x-ray sources and detectors will allow researchers to obtain such information from systems undergoing changes on the time scale relevant to the motion of individual atoms. Thus, this technology should lead to an understanding of dynamic processes with atomic size resolution and sub-picosecond temporal resolution.

Laser-Produced-Plasma Sources

High-density plasmas generated by intense, femtosecond lasers have recently been demonstrated to be sources of sub-picosecond x-ray pulses in the soft x-ray region.[1,17,18] X-rays from these sources are incoherent, but have a high brightness as a result of the small size, short lifetime and high temperature of the radiating plasma. The demonstration of ultrashort x-ray pulses using laser plasmas was made possible in the late 1980's by the development of high-power femtosecond lasers,[19,20] and by improvements in the time-resolution of x-ray detectors.[13]

When a solid is illuminated by an intense laser pulse, electrons in the material absorb energy. These hot electrons will ionize and heat the atoms, forming a high-temperature plasma spark on the surface of the material. The plasma explodes at approximately the sound speed, while maintaining charge neutrality.[21]

A distinction can be made between plasmas created by long-pulse and short-pulse lasers, which depends on whether the laser energy is coupled into the material before or after the explosion. When a solid is excited by a short laser pulse with a rapid risetime, a fraction of the laser energy couples into a high-density material,[18,22,23] penetrating to approximately an optical skin depth of ≈ 100Å. The remainder of the energy is reflected. The solid is ionized and heated on a time scale comparable to the exciting laser pulse. X-rays result from line emission, recombination radiation, and bremsstrahlung radiation. Short x-ray pulses are generated because the high-density plasma cools rapidly due to high thermal and pressure gradients, on both sides of the thin heated layer. Electron energy loss is due to thermal conduction,[24] plasma expansion,[25] and collisions with ions.[26] The effect of thermal conduction and expansion is to increase the plasma volume, which leads to a rapid drop in temperature and density following the laser pulse; x-ray emission is therefore rapidly terminated. Expansion is negligible provided the leading edge of the short laser pulse rises rapidly. In addition, as recent experiments at the University of Michigan[27] have shown, when the average electron quiver energy in the expanding plasma becomes comparable to the electron thermal energy, the ponderomotive force of the high-intensity laser will slow the plasma expansion.

In the case of a long laser pulse, or even a short laser pulse that has a slowly rising leading edge or prepulse, plasma ablates from the surface of the solid during the early part of the laser excitation. A density gradient forms in front of the target,[22,28] and the bulk of the laser energy is coupled into a lower-density plasma. Coupling is maximum at a density such that the electron plasma frequency equals the laser frequency; this density is typically a few orders of magnitude below that of solid. The long scale-length of the heated region, combined its relatively low density, results in a slow cooling time and relatively long-pulse x-ray emission.[18] However, the highest-temperature components of this plasma can also cool rapidly and may lead to short pulse x-ray emission near the extreme high energy portion of the plasma emission spectrum.

Laser-produced plasma based x-ray sources are especially efficient sources of sub-picosecond pulses in the sub-kilovolt or soft x-ray region of the spectrum. These sources can be qualitatively described as blackbodies in certain spectral regions, with effective temperatures of a few hundred electron volts. Our initial experiments with these high-density plasmas were performed using an amplified dye laser system,[20] which supplied pulses with an energy of 5 mJ, pulse length of 160 fs, and a clean (prepulse-free) rising edge. The laser was focused onto a raster-scanned target by an off-axis parabolic reflector inside the vacuum chamber. This system allowed us to irradiate a target with intensities of up to 10^{16} W cm^{-2}. At this intensity, we estimate a peak plasma temperature of $\approx$ 400 eV.

We used a modified, commercial x-ray streak camera to measure the x-ray pulse duration in these experiments.[13] The output phosphor screen of the streak camera was imaged onto a CCD camera, and streaked images were transferred to a computer for data analysis and storage. We obtained the highest temporal resolution with the streak camera by using an x-ray photocathode with a narrow secondary electron distribution, a high electric field to accelerate the electrons, and a fast, well calibrated sweep speed. Typical results showing sub-kilovolt x-ray emissions from a silicon target is shown in Fig. 1. The 2 ps x-ray pulse is bracketed by two ultraviolet (uv) timing fiducials which were used to estimate the instrument response and to calibrate the sweep speed. The estimated streak camera impulse, both from first principles and from the uv measurement, was 1.7 ps. Deconvolution of the impulse response from the x-ray pulse width measurement yields an upper bound on the x-ray pulse of 1.1 $\pm$ 1 ps. This measurement is likely to be instrument-limited; the predicted x-ray pulse width from the plasma was between 300 and 800 fs,[1,29] depending on the target material. Higher time-resolution instruments are currently under development.[30]

An alternative technique for sub-picosecond x-ray pulse measurements has been demonstrated by a group at AT&T and the University of Maryland.[31] In this work, an intense 200 fs laser was used to rapidly modify the transmission of an x-ray absorbing

medium. This allowed the researchers to measure the cross-correlation of the visible laser pulse and plasma emissions near 90 eV. This experiment measured a relatively long 22 ps x-ray pulse width, probably because the plasma was created at a relatively low density and the plasma emission was at relatively long wavelength.

Increased Efficiency

Although laser plasma-based x-ray sources as discussed above are capable of generating ultrashort x-ray pulses, a major limitation to their general use has been the relatively low laser-energy to x-ray-energy conversion efficiency observed in many experiments using flat targets (< 1%). This low efficiency is a result of inefficient coupling of the laser energy into the solid, and also of the relatively low plasma temperatures produced.

Inefficient laser-to-solid coupling in the case of a flat target can be understood using a simple model.[18,23,32] When a flat solid surface is illuminated with a high-intensity ultrashort laser pulse, the solid rapidly evolves into a high-conductivity plasma. The complex refractive index in Si at 300 eV is calculated to be approximately $N = n + i\,k \approx 4.5 + i\,10.5$. The normal incidence reflectivity, R, is given by $|(N - 1)/(N + 1)|^2$. For these high values of n and k the reflectivity is therefore 90%, and most of the laser light is reflected from the mirror-like plasma surface.

In an attempt to increase absorption of the laser by solid density material, we studied two types of microstructured targets which exhibited low reflectivity.[32-34] The first was a grating structure and the second consisted of a low average density matrix of solid metal clusters. The grating targets had low periodicity (less than the 6200 Å laser wavelength) to avoid energy loss in a diffracted beam, and groove widths sufficiently wide (≥ 1000 Å) so that they did not fill with low-density blow-off vapor during the laser pulse. The gratings were fabricated using either electron-beam lithography or holographic exposure techniques and were used at normal incidence.

For groove depths greater than ≈ 1000 Å, laser light polarized perpendicular to the grating grooves was mostly absorbed. In contrast, for laser light polarized parallel to the grooves, the reflectivity was always ≥ 50%. Absorption was relatively independent of target composition, laser intensity, fill factor and groove width, and depends mainly on the groove depth, increasing with increasing depth. We calculate that the absorption per unit surface area increases by approximately a factor of 3 in these targets compared to flat targets. Figure 2 shows a plot of reflectivity as a function of incident laser intensity, for both a grating and flat target (Si wafer); in contrast to flat targets which become more reflective as they are heated and ionized, grating targets continue to absorb most of the laser light even at high incident laser intensities.

The grating structure can be qualitatively modeled as a set of parallel, lossy waveguides.[35] For radiation polarized *parallel* to the grooves, the guide is cut off and the structure is reflective. For radiation polarized *perpendicular* to the grooves, only a fraction of the incident radiation is reflected from the top surface[36] and most of the radiation is coupled into a propagating TE mode in the grooves.[37,38] The confinement of the radiation causes field enhancement, which can lead to increased absorption. In addition, absorption mechanisms such as resonance absorption can become effective in this geometry since the electric field is perpendicular to the plasma surface.

A group at Ecole Polytechnique recently demonstrated that a small prepulse, incident on a flat target at just above the melting fluence, can induce a periodic surface deformation on the target.[39] The main femtosecond laser pulse is then more efficiently coupled into the target and the x-ray emission is enhanced.

A second type of target which exhibits low reflectivity is made up of a low-density matrix of gold clusters. This is usually made with gold and called gold smoke or gold black. This matrix consists of chains of clusters of ≈ 50 Å particle size, which form a low-average-density structure (typically ≈ 0.3% of solid density), but a high local density. Gold black is fabricated by evaporating gold in background of several torr of a gas (rare

gas or nitrogen) which causes the gold to cluster and form a microscopic fractal structure.[40-42] It is strongly absorbing throughout the visible region,[43-45] and may be absorbing in the infrared depending on the preparation conditions.[45]

By considering Mie scattering[46] from metal particles, we can qualitatively understand why metal blacks strongly absorb radiation. For spherical, metal particle with diameter d much smaller than a wavelength, the absorption cross section is proportional to d^3 whereas the scattering cross section is proportional to d^6. Therefore, for small metal particles, absorption can dominate the interaction of such particles with light. In addition, gold clusters typically have absorption resonances between 2 eV and 1.6 eV, resulting in near-resonant excitation by the laser.[42,47,48] Radiation penetrates easily into the structure and is subsequently absorbed. Typically, a depth of 10 microns is required to absorb visible radiation near resonance. Finally, interactions between the metal particles can further enhance the local fields and local absorption within the clusters.

During the laser heating process, the structure will begin to homogenize due to expansion. This process will begin on 50 fs time scales, as neighboring particles merge into each other. However, homogenization will not be complete until the largest pores in the structure are filled; these are typically a micron in size; thus up to 10 ps are required for the structure to completely disappear. It is unlikely that our structures fill in completely during the excitation pulse, but some modification of the smallest structures is expected. Substantial cooling due to expansion in three dimensions is possible, which may lower the temperature by a factor of ≈20 during the initial picosecond after excitation.[25] Thereafter, cooling will be slower due to reduced gradients. However, because of the significantly reduced thermal conduction heat loss and laser energy reflectance loss in the laser-heated microstructures, the peak temperatures of the heated material can be higher than those attained using flat targets.

From the predicted scaling of plasma temperature and x-ray yield with absorbed laser energy, we estimate an increase in both the temperature (≈ 2) and the total x-ray yield

(≈ 10) for the grating and cluster targets compared to the flat targets. Absolute x-ray yields from both target types were experimentally measured using a filtered x-ray diode. For gold black, we measured a laser-to-x-ray total conversion efficiency approaching 25% (for x-rays above 30 eV), with ≈ 1% of the x-rays at energies above 1 keV. For gold coated gratings, we observed a total conversion efficiency of ≈ 12%, with ≈ 0.6% above 1 keV. For a flat gold target, the measured conversion efficiency was ≈ 0.9% for x-rays above 30 eV.

In recent experiments which use a Ti:sapphire-based laser system at intensities up to 10^{18} W/cm^2, we have found that a layer of gold black ≈ 1μm deep was sufficient to obtain the maximum x-ray output. This absorption depth corresponds to an absorptivity of 30 or 40% over the entire surface area of the fractal structure. With 175 mJ on target, black gold emitted > 1 mJ of x-rays above a kilovolt (filtered through 25 μm of Be); this corresponds to a conversion efficiency of nearly 1%. Under similar conditions, solid gold provided only 10 μJ of x-rays.[49,50]

The same porous structure can be produced from a variety of different materials. We also measured the emission from porous aluminum. It generated x-rays above a kilovolt almost as efficiently as the gold, and was likewise seen to be much more efficient than a flat aluminum target. With 150 mJ on target, porous aluminum emitted over 0.5 mJ of x-rays, compared to 3 μJ from solid aluminum. Figure 3 shows the dependence of output x-ray energy versus incident laser energy for a 140 fs pulse at 800 nm focused to an 8 micron spot size. This radiation is primarily aluminum k-shell emission, and therefore spectra of porous aluminum emission were studied with a von Hamos geometry, KAP spectrometer. As shown in Fig. 4, the dominant emission lines were He-like (Al^{11+}), with some H-like (Al^{12+}) emission also present. The almost complete lack of Kα radiation from un-ionized material emission implies the absence of hot electrons which penetrate into the target's unionized underlayer.

Hard X-Rays

In recent work by several groups, a pre-pulse was used to pre-ionize and ablate the target prior to arrival of the main short pulse.[2,51-54] The prepulse creates an optimal density gradient for laser light absorption and hot electron generation. Energetic electrons can penetrate relatively long distances into the solid target; hard x-rays can be generated as a result of inner-shell ionization of atoms deep in the target or inverse bremsstrahlung. Researchers at Los Alamos, Stanford, Ecole Polytechnique, and Livermore have used this scheme to generate x-rays in the keV region. At Stanford, a 0.5 TW, 120 fs laser[55] was used to produce radiation above 1 MeV. In contrast to the generation of ultrashort soft x-ray pulses from plasmas, the efficient generation of very hard x-rays (> 1MeV) requires the presence of a prepulse. This latter source can be compared to a conventional x-ray tube source operating with a 10 kA sub-picosecond current pulse.[2]

Hard x-ray pulse widths from such plasmas are expected to be sub-picosecond, because the radiation comes from high energy electrons which cool rapidly. However, no measurement of the hard x-ray pulsewidth has been made to date. Soft x-ray pulses from these plasmas are not expected to be short due to slow cooling of the low-density plasma.

Scaling to Larger Systems

The recent revolution in femtosecond laser technology should make it possible to produce pulse energies of several joules with a modestly sized laser system.[56,57] Using these lasers, it will be possible to generate an x-ray flux sufficiently intense to be used for applications. For example, including conversion efficiency, mirror reflectivity and spectrometer throughput, a 1-joule laser system should generate a monochromatic soft x-ray beam with up to 3×10^8 photons per pulse, in a 0.1% bandwidth, covering a wavelength range between 20 Å and 500 Å. In the hard x-ray region, a 1 joule laser system should generate > 10 μJ of keV x-rays per pulse, in narrow-bandwidth line emission. This flux is ample for pump-probe experiments, and will be ideally suited for transient or excited-state measurements, and for single-shot x-ray diffraction experiments.

Synchrotron Sources

Synchrotron radiation sources emit x-ray radiation at high repetition rate (up to 1 GHz) with sub-nanosecond pulses. Researchers have recently begun to use the time resolution available with this source. For example, Larson and co-workers at the CHESS synchrotron source examined the recrystalization of silicon that was melted with a pulsed laser, using 150 ps-duration x-ray pulses mechanically gated to reduce the repetition rate to match the pump laser.[14]

The current generation of synchrotrons, including the Advanced Light Source (ALS) at Berkeley and the Advanced Photon Source (APS) at Argonne, will not approach laser-plasma sources in terms of pulse-duration. The ALS will have a pulse width of approximately 40 ps and a flux of 3×10^6 photons per pulse per 0.1% bandwidth in the 20 - 50Å range.[3] The much higher average power of these sources (100 mW), together with improved electronic synchronization techniques, make likely an expanding number of time-resolved synchrotron radiation experiments. High-speed streak cameras may make sub-picosecond time-resolution possible using longer-duration x-ray pulses.

Future sources

An important source of radiation in the XUV range is harmonic conversion of intense laser pulses.[8-10] When atoms are driven by a very strong laser field ($> 10^{15}$ W cm^{-2}), they can produce coherent harmonic radiation beyond the 100th harmonic of near visible laser wavelengths, corresponding to wavelengths < 100 Å. Using femtosecond laser pulses, harmonic radiation should have short pulse duration, perhaps even shorter than the driving laser pulse.[8] The efficiency of conversion into the higher harmonics in the soft x-ray region appears to be low, between 10^{-6} and 10^{-11}; however, the emitted radiation is coherent and highly directional.

A number of new techniques, both laser-based, synchrotron-based, and a combination thereof, have been proposed as sources of intense, coherent, ultrashort-pulse x-rays. Because the duration of a synchrotron x-ray pulse depends on the spatial extent of an

electron bunch (which is limited by space charge effects), further direct reductions in pulse duration from synchrotrons will be difficult.

One synchrotron-based approach would use a rapidly-rotating grazing-incidence mirror and a diffraction grating to compress x-ray pulses by a factor of ~100.[58] Another promising approach for generating short-duration x-ray pulses combines laser and accelerator techniques.[4,5] Light scattered from relativistic electrons will be emitted in the direction of the electron motion, and will be up-shifted into the x-ray region of the spectrum. Since electron-photon scattering cross-sections are quite small, such a technique requires both an intense electron beam and laser beam. Sprangle and co-workers propose that, by using a 50-250 MeV, 200A, 1 ps electron beam, and a 20 J, 2 ps laser, they can generate x-rays of 50-1200 keV with $>10^9$ photons/pulse, and with a pulse duration ~1 ps.[5] Kim and co-workers suggest that the pulse duration can be shortened by crossing the electron and photon beams at 90 degrees to limit the interaction distance between the two. Using readily achievable electron beam and laser parameters, they predict that they can generate x-ray pulses of $>10^5$ photons at ≈ 0.3 Å wavelength.[4]

Another potential source of ultrashort x-ray pulses are x-ray lasers. Because of the high power requirements for an x-ray laser, a number of schemes have been proposed which use high-power ultrashort laser pulses as pump sources. For example, a short, intense laser pulse can be used tc ionize a gas to create a cold plasma. Recombination in this plasma can result in population inversion.[7] In some of these schemes, an inversion with respect to the ground state is predicted.[59] Since such an inversion is self-terminating, it is expected that soft x-ray pulses of ps or sub-ps duration should be produced. Recent experimental data suggests that laser gain may have been demonstrated in a transition in Lithium @ 13.4 nm.[60]

Another x-ray laser approach is to use the incoherent x-ray burst from a laser-produced plasma as a "flashlamp" excitation source. Kapteyn recently suggested that the inner-shell photoionization scheme originally proposed by Duguay and Rentzepis[61] should be practical

using a 20 TW, 50 fs laser. The predicted output of this x-ray laser source is a 5-50 fs duration pulse at 1.5 nm, with $>10^{10}$ photons/pulse.[6]

Conclusion

Sub-picosecond x-ray pulses from a variety of different sources and covering a wavelength range from the soft x-ray to the MeV region are now available. Recent improvements in source technology, detectors, and optics will allow scientists to use these ultrashort x-ray pulses to probe fast reactions in atoms, materials and in living cells. Coherent versions of such x-ray sources could also be used for time-resolved x-ray holography and for x-ray nonlinear optics.

Acknowledgments

This work was supported by the National Science Foundation, the U.S. Air Force Office of Scientific Research and the Department of Energy through a collaboration with Lawrence Livermore National Laboratory. M. Murnane acknowledges support from a Sloan Foundation Fellowship.

References

1. M. M. Murnane, H. C. Kapteyn, M. D. Rosen, R. W. Falcone, Science **251**, 531 (1991).
2. J. D. Kmetec, C. L. Gordon III, J. J. Macklin, B. E. Lemoff, G. S. Brown, S. E. Harris, Phys. Rev. Lett. **68**, 1527 (1992).
3. D. T. Attwood, Phys. Today **45**, 24 (1992).
4. K. J. Kim, S. Chattopadhyay, C. V. Shank, at the*Eighth International Conference on Ultrafast Phenomena* (Antibes, France, 1992).
5. P. Sprangle, A. Ting, E. Esarey, A. Fisher, J. Appl. Phys. **72**, 5032 (1992).
6. H. C. Kapteyn, Appl. Opt. **31**, 4931 (1992).
7. N. H. Burnett, P. B. Corkum, J. Opt. Soc. Am. B **6**, 1195 (1989).
8. A. L'Huillier, P. Balcou, Phys. Rev. Lett. **70**, 774 (1993).
9. J. J. Macklin, J. D. Kmetec, C. L. Gordon III, Phys. Rev. Lett. **70**, 766 (1993).
10. J. K. Krane, M. D. Perry, S. Herman, R. W. Falcone, Opt. Lett. **17**, 1256 (1992).
11. A. Sullivan, H. Hamster, H. C. Kapteyn, S. Gordon, W. White, H. Nathel, R. J. Blair, R. W. Falcone, Opt. Lett. **16**, 1406 (1991).
12. M. T. Asaki, C. P. Huang, D. Garvey, J. Zhou, H. C. Kapteyn, M. M. Murnane, Opt. Lett. **18**, 977 (1993).
13. M. M. Murnane, H. C. Kapteyn, R. W. Falcone, Appl. Phys. Lett. **56**, 1948 (1990).
14. B. C. Larson, J. Z. Tischler, D. M. Mills, Materials Research Society Symposium Proceedings vol. 100, p. 513 (1988).
15. J. S. Wark, in *X-Ray Microscopy III*, A. G. Michette, G. R. Morrison, C. J. Buckley, Eds., Springer Series in Optical Sciences vol. 67, p. 455 (Springer-Verlag, Berlin, 1992).
16. A. Beswick, Eds.,*Synchrotron Radiation and Dynamic Phenomena*, AIP Conference Proceedings vol. 258 (AIP, New York, 1991).

17. R. W. Falcone, M. M. Murnane, in *Short Wavelength Coherent Radiation: Generation and Applications*, D. T. Attwood. J. Bokor, Eds., AIP Conference Proceedings vol. 147, p. 81 (AIP, New York, 1986).

18. M. M. Murnane, H. C. Kapteyn, R. W. Falcone, Phys. Rev. Lett. **62**, 155 (1989).

19. R. L. Fork, C. V. Shank, R. T. Yen, Appl. Phys. Lett. **41**, 223 (1982).

20. M. M. Murnane, R. W. Falcone, J. Opt. Soc. Am. B **5**, 1573 (1988).

21. W. L. Kruer, *The Physics of Laser Plasma Interactions* (Addison-Wesley, Redwood City, CA, 1988).

22. H. M. Milchberg, R. R. Freeman, J. Opt. Soc. Am. B **6**, 1351 (1989).

23. H. M. Milchberg, R. R. Freeman, S. C. Davey, R. M. More, Phys. Rev. Lett. **61**, 2364 (1988).

24. L. Spitzer, *Physics of Fully Ionized Gases* (Interscience, New York, 1962).

25. D. J. Bradley, A. G. Roddie, W. Sibbett, M. H. Key, M. J. Lamb, C. L. S. Lewis, P. Sachsenmaier, Opt. Comm. **15**, 231 (1975).

26. S. E. Harris, J. D. Kmetec, Phys. Rev. Lett. **61**, 62 (1988).

27. X. Liu, D. Umstadter, Phys. Rev. Lett. **69**, 1935 (1992).

28. O. L. Landen, D. G. Stearns, E. M. Campbell, Phys. Rev. Lett. **63**, 1475 (1989).

29. M. D. Rosen, in *Femtosecond to Nanosecond High-Intensity Lasers and Applications*, E. M. Campbell, Eds., Proceedings of the SPIE vol. 1229, p. 160 (SPIE, Bellingham, WA, 1990).

30. R. Shepherd, personal communication (1993).

31. M. H. Sher, U. Mohideen, H. W. K. Tom, O. R. Wood, G. D. Aumiller, R. R. Freeman, Opt. Lett. **18**, 646 (1993).

32. M. M. Murnane, H. C. Kapteyn, S. P. Gordon, J. Bokor, E. N. Glytsis, R. W. Falcone, Appl. Phys. Lett. **62**, 1068 (1993).

33. H. C. Kapteyn, M. M. Murnane, A. Szoke, A. Hawryluk, R. W. Falcone, in *Ultrafast Phenomena VII*, C. B. Harris, E. P. Ippen, G. A. Mourou, A. H. Zewail,

Eds., Springer Series in Chemical Physics vol. 53, p. 122 (Springer-Verlag, Berlin, 1990).

34. M. Murnane, H. Kapteyn, S. Gordon, S. Verghese, J. Bokor, W. Mansfield, R. Gnall, E. Glytsis, T. Gaylord, R. Falcone, in *Short-Wavelength Coherent Radiation: Generation and Application*, P. H. Bucksbaum, N. M. Ceglio, Eds., OSA Conference Proceedings vol. 11, (Optical Society of America, Washington DC, 1991).
35. S. Ramo, J. R. Whinnery, *Fields and Waves in Modern Radio* (Wiley, New York, 1944).
36. J. P. Auton, Appl. Opt. **6**, 1023 (1967).
37. T. K. Gaylord, E. N. Glytsis, M. G. Moharam, Appl. Opt. **26**, 3123 (1987).
38. N. F. Hartman, T. K. Gaylord, Appl. Opt. **27**, 3738 (1988).
39. J. C. Gauthier, A. Rousse, F. Fallies, J. P. Geindre, P. Audebert, A. Mysyrowicz, G. Grillon, J. P. Chambaret, A. Antonetti, at the*NATO Advanced Study Institute* (Corsica, 1992), to be published, Plenum Press.
40. C. Doland, P. O'Neill, A. Ignatiev, J. Vac. Sci. Tech. **14**, 259 (1977).
41. V. A. Markel, L. S. Muratov, M. I. Stockman, T. F. George, Phys. Rev. B **43**, 8183 (1991).
42. J. Perenboom, P. Wyder, F. Meier, Phys. Rep. **78**, 174 (1981).
43. L. Harris, J. Opt. Soc. Am. **51**, 80 (1961).
44. L. Harris, J. K. Beasley, J. Opt. Soc. Am. **42**, 134 (1952).
45. S. Verghese, P. L. Richards, IEEE Trans. Magn. **27**, 3077 (1991).
46. G. Mie, Ann. Phys. **25**, 377 (1908).
47. C. G. Granqvist, O. Hunderi, Phys. Rev. B **16**, 3513 (1977).
48. U. Kriebig, L. Genzel, Surf. Sci. **156**, 678 (1985).
49. R. Shepherd, D. Price, B. White, S. Gordon, A. Osterheld, R. Walling, D. Slaughter, S. Stewart, in *Ultrafast Phenomena VIII*, J. L. Martin, A. Migus, G.

Mourou, A. Zewail, Eds., Springer Series on Chemical Physics vol. 55, p. 275 (Springer-Verlag, Berlin, 1992).

50. S. P. Gordon, R. Sheppard, T. Donnelly, D. Price, B. White, A. Osterheld, H. Hamster, A. Sullivan, R. W. Falcone, in *Short Wavelength Coherent Radiation: Generation and Applications*, M. Perry, P. Corkum, Eds., OSA Conference Proceedings vol. TBP, (Optical Society of America, Washington, DC, 1993).
51. J. A. Cobble, G. T. Schappert, L. A. Jones, A. J. Taylor, G. A. Kyrala, R. D. Fulton, J. Appl. Phys. **69**, 3369 (1991).
52. J. A. Cobble, G. A. Kyrala, A. A. Hauer, A. J. Taylor, C. C. Gomez, N. D. Delamater, G. T. Schappert, Phys. Rev. A **39**, 454 (1989).
53. P. Audebert, J. P. Geindre, J. C. Gauthier, A. Mysyrowicz, J. P. Chambaret, A. Antonetti, Europhys. Lett. **19**, 189 (1992).
54. D. V. d. Linde, H. Schuler, H. Schulz, T. Engers, in *Ultrafast Phenomena VIII*, J. L. Martin, A. Migus, G. A. Mourou, A. Zewail, Eds., Springer Series in Chemical Physics vol. 55, p. 280 (Springer-Verlag, Berlin, 1992).
55. J. D. Kmetec, J. J. Macklin, J. F. Young, Opt. Lett. **16**, 1001 (1991).
56. O. E. Martinez, IEEE J. Quant. Elec. **QE-23**, 59 (1987).
57. P. Maine, D. Strickland, P. Bado, M. Pessot, G. Mourou, IEEE J Quan. Electon. **24**, 398 (1988).
58. P. L. Csonka, J. Appl. Phys. **64**, 967 (1988).
59. D. C. Eder, P. Amendt, S. C. Wilks, Phys. Rev. A **45**, 6761 (1992).
60. K. Midorikawa, Y. Nagata, M. Obara, H. Tashiro, K. Toyoda, at the*Quantum Electronics Laser Science Conference* Paper QPD4 (Baltimore, MD, 1993).
61. M. A. Duguay, P. M. Rentzepis, Appl . Phys. Lett. **10**, 350 (1967).

Figures

Figure 1: Single shot streak camera trace of the sub-kilovolt x-ray emission from a silicon target. The x-ray pulse is in the center, bracketed by 2 ultraviolet pulses for timing calibration.

Figure 2: Reflectivity of a solid target as a function of increasing incident laser energy. (a): flat silicon target ; (b): grating target with the laser polarization parallel to the grooves; (c): grating target with the laser polarization perpendicular to the grooves.

Figure 3: X-rays transmitted through a 25 μm Be filter from solid and porous aluminum. The peak incident energy corresponds to an intensity of 10^{18} W/cm^2.

Figure 4: K-Shell spectrum of porous aluminum.

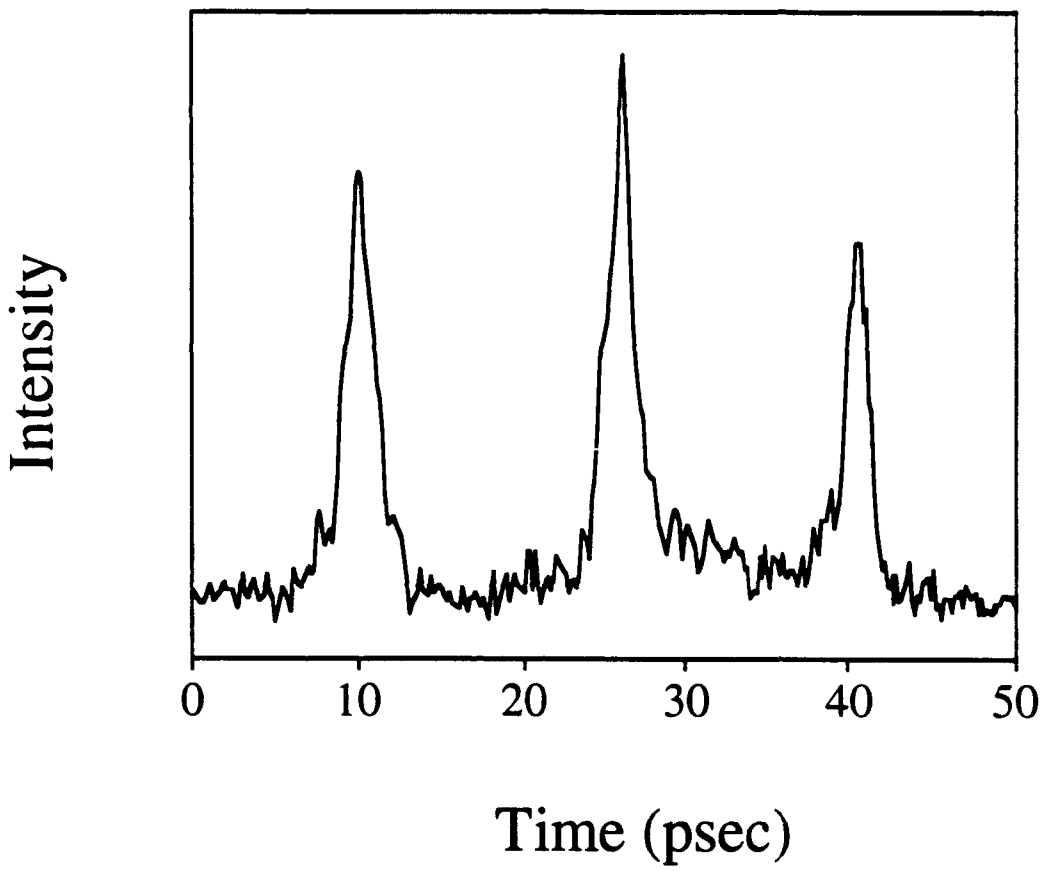

FIGURE 1

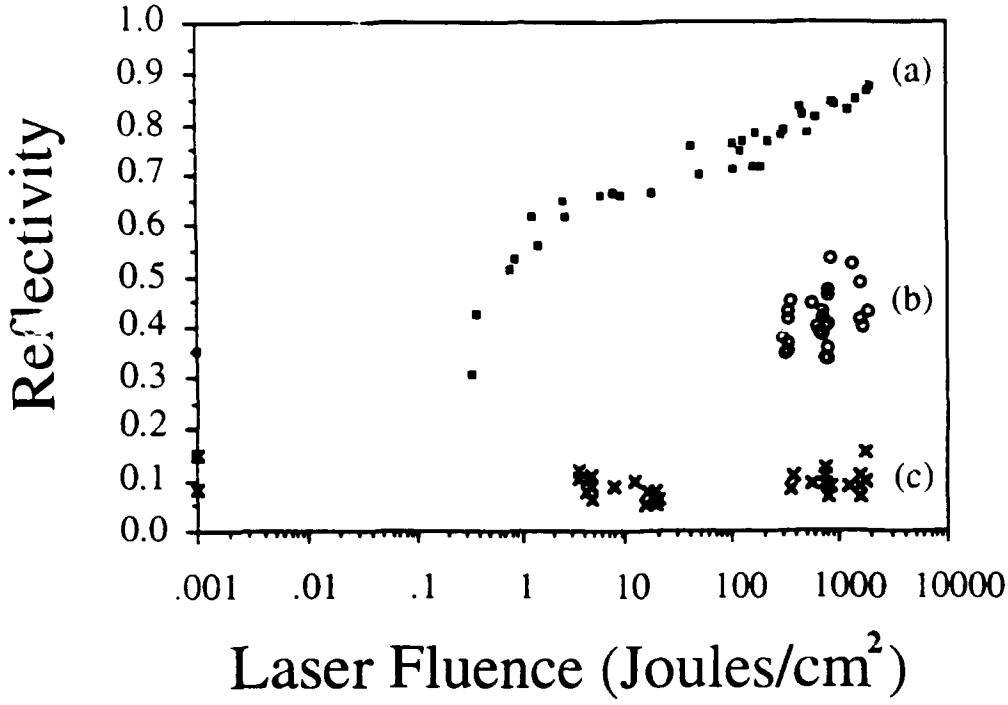
Reflectivity
1.0
0.9
0.8
0.7
0.6
0.5
0.4
0.3
0.2
0.1
0.0
(a)
(b)
(c)
.001
.01
.1
1
10
100
1000
10000
Laser Fluence (Joules/cm²)

FIGURE 2

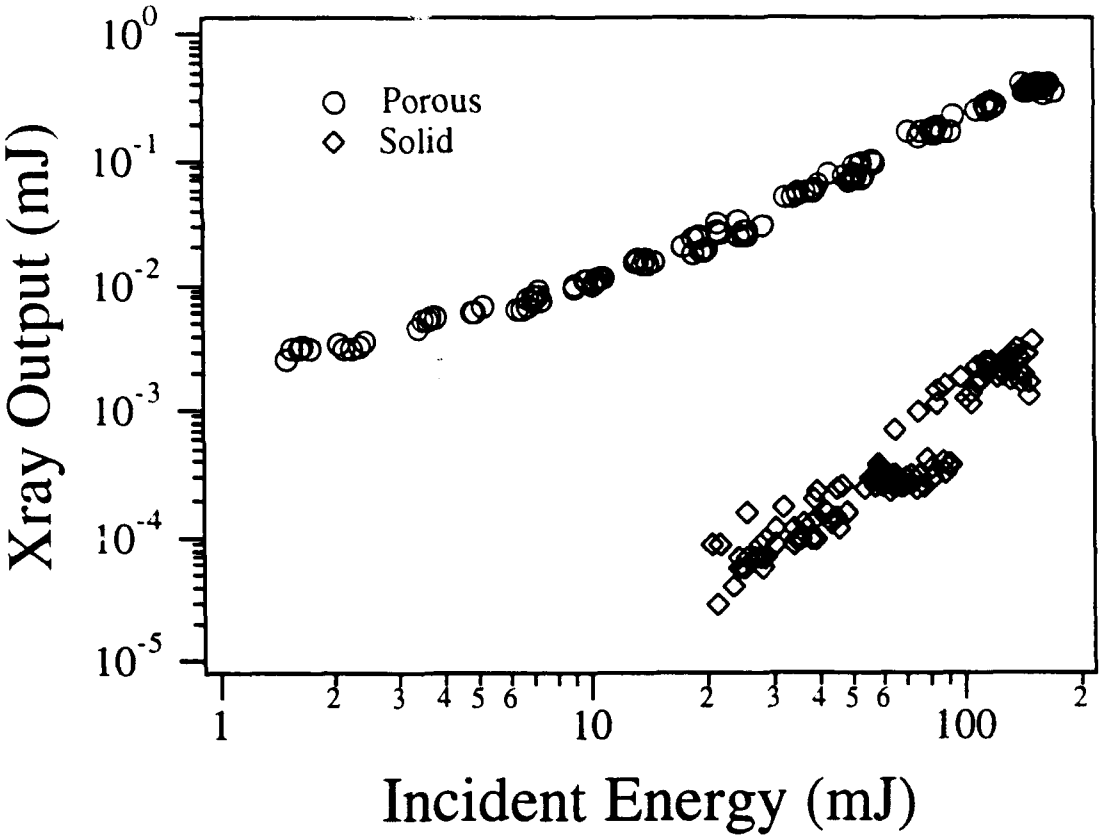
Xray Output (mJ)
10^0
10^{-1}
10^{-2}
10^{-3}
10^{-4}
10^{-5}
Porous
Solid
1
2
3
4
5
6
10
2
3
4
5
6
100
2
Incident Energy (mJ)

FIGURE 3

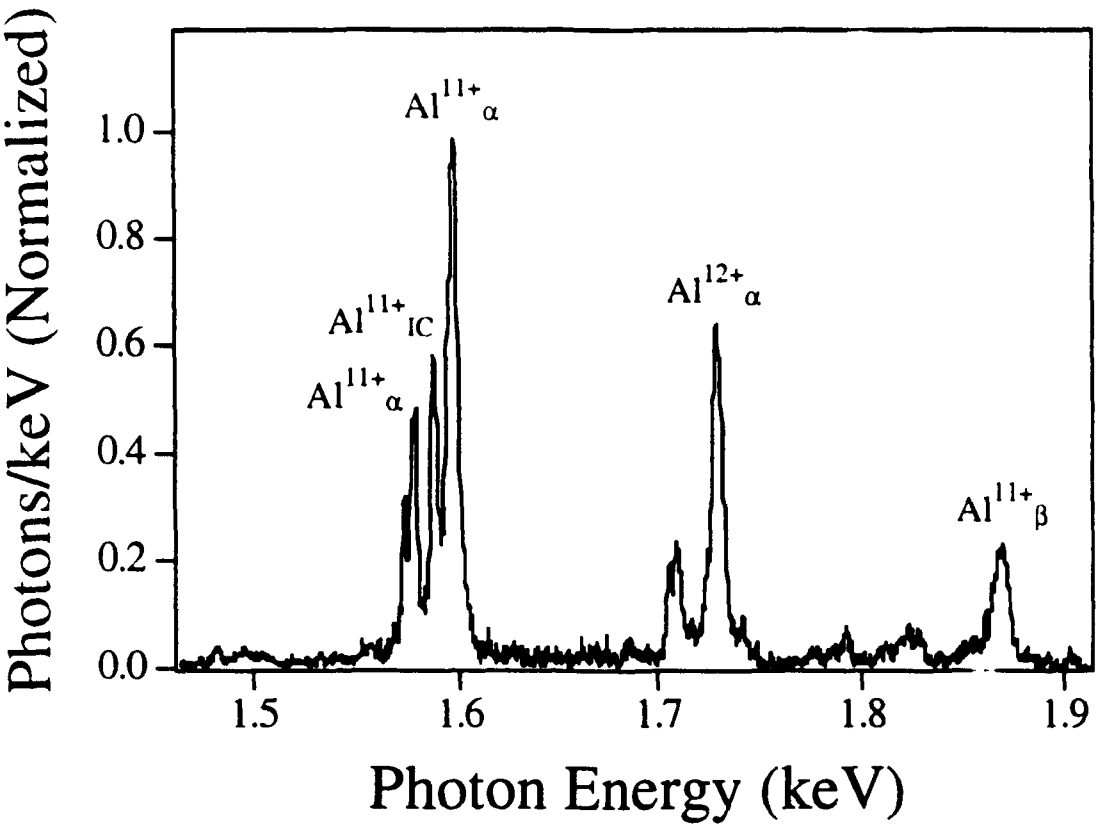
Photons/keV (Normalized)
1.0
0.8
0.6
0.4
0.2
0.0
1.5
1.6
1.7
1.8
1.9
Photon Energy (keV)
Al11+α
Al11+IC
Al11+α
Al12+α
Al11+β

FIGURE 4

Short-Pulse Terahertz Radiation from High-Intensity Laser Produced Plasmas

H. Hamster, A. Sullivan, S. Gordon and R.W. Falcone

Department of Physics

University of California at Berkeley

Berkeley, CA 94720

Abstract

The interaction between high-intensity, ultrashort laser pulses and plasmas leads to the emission of coherent, short-pulse radiation at terahertz frequencies. In this work we discuss a model for this effect and its experimental realization. Our measurements constitute the direct observation of laser-induced wake fields. From gas density targets, resonant enhancement of the terahertz emission is observed if the plasma frequency is close to the inverse pulse length of the exciting laser pulse. At higher plasma densities, the emission of sub-picosecond, unipolar electromagnetic pulses is observed. With the use of solid density targets, emission of more than 0.5 μJ of FIR energy was measured. Simultaneous emission of MeV x-rays and 0.6 MeV electrons was observed and correlated with the terahertz emission. This indicates that the radiative processes in such plasmas are driven by ponderomotively induced space charge fields in excess of 10^8 V/cm.

PACS numbers: 52.40.Nk, 42.65.Re, 52.25.Rv, 52.35 Mw

The interaction of intense laser light with plasmas is a complex process which requires a sophisticated theoretical treatment [1-6]. Novel experimental observations are of great importance to enhance our understanding of these phenomena. In this paper we report the observation of electromagnetic transients that result from such interactions. The interpretation of these measurements allows a better understanding of the underlying plasma dynamics. Our research illuminates the mechanism which leads to the generation of wake fields, energetic electrons, x-rays and terahertz radiation from laser produced plasmas.

Plasmas created by high-intensity laser pulses with sub-picosecond duration have received considerable attention as sources of radiation. The observed emission includes radiation at very high harmonics of the laser frequency [7, 8], x-ray bursts of sub-picosecond duration [9] and the generation of hard x-rays with energies of greater than one MeV [10]. At the low energy end of the electromagnetic spectrum, a strong emission of coherent far infrared radiation (FIR) at terahertz frequencies has been predicted [11]. This radiation arises from the rapid development of space charge fields in such plasmas. We have recently reported the first observation of this effect [12] and in this paper we give a more detailed account of those measurements.

The generation of strong electric and magnetic fields by laser induced plasmas has been considered before. The creation of magnetic fields with megagauss strength in the focus of sub-nanosecond laser pulses has been observed in the 1970's [13, 14]. Electrical fields greater than 10^8 V/cm have been predicted in the context of plasma-wave accelerators [2] and for the interaction of high-intensity short pulse lasers with plasmas [3]. Magnetic fields up to 10^9 G were calculated for the interaction of intense short pulse lasers with solid density plasmas [4, 5]. Electric fields of up to 10^7 V/cm have been measured in experiments involving plasma wave accelerators [15]. Our experiments allow a comparison with this previous work by measuring the time derivative of these fields in the far-field.

Terahertz radiation results from the interaction of femtosecond laser pulses with matter through a variety of different mechanisms. These employ electro-optic crystals [16], photoconductive switches and antennas [17, 18] or large-area semiconductor wafers [19, 20]. Pulse energies of up to 0.8 μJ have been demonstrated by using a biased GaAs wafer [21].

In our experiment the mechanism of pulse generation involves ponderomotive forces generated in the focus of an intense femtosecond laser pulse. These forces create a large density difference between ionic and electronic charges if the pulse length is short enough to inertially confine the ions [3, 6]. This results in a powerful electromagnetic transient. Using Poisson's equation and Larmor's formula we estimate that the emitted FIR power P (in MW) is given by [11, 22]

$$P \approx \frac{1}{7}\left(\frac{W}{R_0}\right)^2\left(\frac{\lambda}{\tau}\right)^4, \qquad (1)$$

where W is the laser energy in J, R_0 is the $1/e^2$-radius of the focused beam in μm, λ is the laser wavelength in μm and τ is the pulse length in ps. For a pulse energy of 1 J, 1 μm beam radius, 0.1 ps pulse length and 1 μm laser wavelength we expect peak powers in excess of 1 GW.

In order to estimate the F.F. emission in a more rigorous fashion, we have employed a linearized hydrodynamic model for the plasma dynamics. By calculating the spatial and temporal dependence of the charge density and acceleration within the focal region we are able to compute the far-field radiation pattern. In particular we require the electron density n(r, z, t) and acceleration $\vec{a}(r, z, t)$ as a function of time t and cylindrical coordinates r and z. We assume radial symmetry around the direction of propagation $\hat{z}$ and model the electron fluid as cold, i.e., the thermal pressure $p=n\,k_B\,T_e$ is assumed to be small compared to the ponderomotive pressure $n\,U_{pon}$. k_B is the Boltzmann constant and T_e the electron temperature; the ponderomotive energy U_{pon} is defined in Ref. [23]. The cold fluid approximation is justified since plasmas produced by short pulse lasers tend to

have temperatures below 10^3 eV [24, 25] while the ponderomotive energies for our experimental conditions are on the order of 10^5 eV. Under these conditions, the dynamical equations of motion for the electron fluid [26] may be linearized and decoupled to yield simple harmonic oscillator equations for the density n, velocity $\bar{v}$ and a low frequency electric field $\bar{E}$ which arises from charge separation [27]. We solved this system of harmonic oscillator equations for a realistic beam profile by using the method of variation of constants. We choose a temporally and spatially gaussian pulse envelope while considering the natural divergence of the gaussian mode. The ponderomotive potential used is given by

$$U_{pon}(r,z,t) = U_0 \times \frac{R_0^2}{R_0^2 + z^2\kappa^2} \times \exp(-\frac{r^2}{R_0^2 + z^2\kappa^2}) \times \exp(-\frac{(z/v_g - t)^2}{\tau_0^2}). \qquad (2)$$

Here U_0 is the ponderomotive energy at the peak intensity of the laser, v_g is the group velocity of the pulse in the plasma, $\kappa = \lambda/(\sqrt{2}\pi R_0)$ is a constant relating to the divergence of the beam and the time τ_0 is the $1/e^2$ half-width of the pulse. The model can be solved in a closed form and the resulting analytical expressions for n, $\bar{v}$ and $\bar{E}$ are given in terms of the error-function with a complex argument [22]. The time derivative of the resulting current is summed numerically over the excitation volume at retarded times in order to calculate the far-field radiation pattern. Note that we employ an expression which contains all orders in a multipole expansion [26].

The terahertz radiation will experience losses while propagating out of the laser-produced plasma since the plasma is overcritical to electromagnetic waves with frequencies below the plasma frequency ω_p. Due to the small spatial extent of the plasma these losses are estimated to be small and are therefore not further considered.

Figure 1 gives examples of our calculations. The emitted FIR power is shown versus view angle and time. The results of these calculations may be summarized as follows. The peak of the emission is in forward direction with respect to the beam propagation. A strong resonant enhancement of the signal is observed for $\omega_p\tau_0=2$. In this

density regime ($n \approx 2 \times 10^{17}$ cm^{-3} for $\tau_0 \approx 0.1$ ps) one expects the emission of radiation over many cycles of the plasma oscillation. This is shown in Fig. 1 (a) for a plasma frequency $\omega_p/2\pi$ of 4.6 THz. We note that the damping of the plasma oscillations on a time scale of a few picoseconds due to electron-ion collision can be ruled out; a dephasing time of less than 2 ps requires a plasma temperature below 0.5 eV [28]. This seems too low for this type of laser produced plasma [24, 25].

Figure 1 (b) shows the case of nonresonant excitation of plasma at a density of 10^{19} cm^{-3}. The peak power remains relatively low while the pulse shape is essentially given by the derivative of the exciting optical pulse. Note that there is a dependence of the spatial emission pattern on the spot size of the focused laser beam. A smaller beam leads to a shift of the emission maximum in a direction perpendicular to the laser propagation.

The radiation discussed so far arises solely from a *time averaged* driving force. There will be an additional radiative contribution which originates from the oscillation of the plasma at frequencies of $\omega \pm \Delta\omega$, where ω is the carrier frequency and $\Delta\omega$ is the bandwidth of the laser pulse. The frequencies components will mix if the plasma is inhomogeneous, i.e. $\vec{\nabla} n \neq 0$. This nonlinear current has been calculated before for the case of second harmonic generation in a plasma [29]. In a very similar fashion we estimate the leading contribution due to this effect to be given by [22]

$$\vec{J}^{NL}(\Delta\omega, \omega, -\omega) = \frac{4\pi e^3}{\omega^3 m_e{}^2 c}\left(\frac{1}{1-(\omega_p/\omega)^2}\right) I\,(\vec{\nabla} n \bullet \vec{e}_{pol})\,\vec{e}_{pol}\,. \qquad (3)$$

$\vec{e}_{pol}$ is the polarization vector of the exciting electromagnetic field, I is the laser intensity, and e and m_e are the electron charge and mass. Note that $\vec{J}^{NL}$ is proportional to I and will only implicitly depend on the ponderomotive force through $\vec{\nabla} n$. We compute the far-field radiation pattern by integrating $d\vec{J}^{NL}/dt$ over the excitation volume. $\vec{\nabla} n$ is obtained from the hydrodynamic model. The result of one such calculation is shown Fig. 1 (c) for $n=10^{19}$ cm^{-3} and $I=5\times10^{18}$ W/cm^2.

In order to measure these effects, we used a terawatt laser system [30] capable of producing intensities up to 10^{19} W/cm^2. We achieve a pulse length of typically 120 fs and an energy of up to 0.5 J at 0.8 μm wavelength. The beam was focused with a 5 cm focal length off-axis paraboloidal reflector to a size of approximately 3.5 μm × 2.5 μm. At a laser repetition rate of 10 Hz, experiments were performed with a pulse energy of 20 - 50 mJ. At higher energies the repetition rate was limited to several shots per minute.

The first series of experiments was performed in a chamber filled with gas of pressures up to 10^5 Pa. The emitted radiation was collected by using a short focal length off-axis paraboloidal mirror with f/0.5. A liquid helium cooled bolometer was used in conjunction with a Fourier transform spectrometer to characterize the emitted FIR [31]. Care was taken in order to ensure that the optical path leading into the detector was free of water vapor. Sheets of thin black polyethylene prevented laser light from reaching the detector.

Figure 2 (a) shows the detected terahertz signal as a function of pressure as well as our model calculation. The absolute energy scale on the right hand side of the graph is only accurate within a factor of 2 due to the uncertainty of the optical throughput of our detection system. As expected, we observe a strong resonant enhancement of the radiation if the plasma frequency is close to the inverse pulse length of the laser. However, our linearized model fails to predict accurately the behavior at high pressures. A nonperturbative treatment for the plasma response in this pressure regime appears to be necessary. Fig. 2 (b) indicates the different contributions to the calculated signal. We believe the plateau around 6000 Pa is due to an artifact of the calculation [22].

The interferograms reveal that the strong signal around 400 Pa is indeed due to the oscillation of the plasma at the plasma frequency. We observe several cycles of radiation extending over a period of about 2 ps (Fig. 3 (a)). Assuming that the damping of the waves is due to electron-ion collisions in a thermal plasma, we infer an unreasonably low temperature of only 0.5 eV. However, we estimate that the radiative damping is

considerable. Modeling the plasma as a column with a diameter of 5 μm and a length of ≈ 50 μm, and assuming the electron density in the column is lowered by 10^{17} cm^{-3} from its unperturbed value, we estimate the electrostatic self-energy to be several nJ. The measured radiative yield is around one nJ. In addition, other nonlinear damping mechanisms like wave breaking [32] will have to be considered.

The frequency of the emission of the resonant signal is both tunable with density and close to the bulk plasma frequency as shown in Fig. 4. This observation is interesting since the size and shape of plasma are expected to lead to a deviation from the bulk plasma frequency.

At the highest density a new peak in the spectrum appears which is centered around 1.5 THz. The location of the peak remains essentially unchanged for all densities above 10^{18} cm^{-3} (Fig. 5) and is also independent of the gas in which the experiment was carried out (He, Ar, N, Air). The autocorrelation signal of such a pulse is shown in Fig. 3 (b) and has a FWHM of 0.3 ps. It shows a pulse which is dominantly unipolar. The pulse shape resembles the temporal characteristics calculated in Fig. 1 (c), indicating that this signal may be due to $\vec{J}^{NL}$. The signal is p-polarized as expected from Eq. (3). The fact that we fail to predict the signal strength correctly at this pressure is likely due to the breakdown of the linearized model. We found that the strength of the nonresonant signal was dependent on the target gas. In Ar, the nonresonant emission peaks at a pressure of 6500 Pa and is twice as strong as the resonant signal observed at low pressures (Fig. 6). The polarization of the signal is also pressure dependent and changes direction at intermediate pressures. At very high pressures ($> 1.5 \times 10^4$ Pa) the signal becomes depolarized. This is probably caused by the severe beam distortion and break up that is observed at high densities [33]. We believe the high plasma density in case of the Ar-target is significant for an explanation of the observed differences with our experiments in He.

The first order autocorrelation trace obtained with a Michelson interferometer alone does not provide a measure of the pulse length. Interferograms similar to Fig. 3 (b) may be obtained from a broad band thermal source. However, we estimate the emission due to thermal Bremsstrahlung from the plasma to be several orders of magnitude smaller than the observed signal levels [22, 34]. In addition, we performed a direct measurement of the pulse in the time domain. The terahertz radiation was transmitted through a semi-insulating GaAs wafer which functioned as a transient mirror following illumination with femtosecond optical radiation [21, 35]. We confirmed that for the case of nonresonant excitation all of the FIR was contained in a time interval of less than 0.8 ps (10% - 90% points, Fig. 7). The resonant excitation signal was emitted over a period of 1.7 ps. The fall time of the nonresonant signal was independent of the target gas and constant over a wide pressure range. We were not able to distinguish individual cycles of radiation for the case of resonant emission. This indicates that our measurement of a 0.8 ps fall time was limited by the time resolution of the technique.

We confirmed qualitatively that the main peak of the terahertz emission was directed in forward direction, about 60° with respect to the direction of beam propagation. No radiation was detected in the backward direction. However we were not able to make a quantitative comparison with theory because of the large collection angle of the off-axis paraboloidal mirror.

In a second set of experiments we investigated the emission of terahertz radiation from a solid target. The p-polarized laser light was incident on the target at $\approx 60^{\circ}$ with respect to normal. Al-coated glass slides were used as targets. The target chamber was filled with dry nitrogen of $\approx$ 2500 Pa pressure in order to protect the focusing mirror from debris. This had no noticeable effect on the emission. Since the radiation is emitted from a spatially fixed interface and not from a moving focus, we expect the emission pattern to be different from the ones shown in Fig. 1. For the case of normal incidence, the main emission is calculated to be in the backward direction $\approx 50^{\circ}$ off normal [11, 22]. In the

experiment, we found the emission to be at a maximum in the direction of specular forward reflection. The radiation was found to be p-polarized. The signal in the direction opposite to the incident laser beam was two orders of magnitude smaller. By using a pyroelectric detector in conjunction with a collection cone and a light pipe, we observe 0.5 μJ of FIR emitted into a solid angle of 1.5 sr at an optical pulse energy of 200 mJ. Due to coupling looses and the insufficient absorption of the detector element we estimate the actual radiative yield to be a factor of 3 higher. Assuming a pulse length of 0.5 ps we infer a peak FIR power of greater than 1 MW.

We observe that each laser pulse must be proceeded by a small amount of amplified spontaneous emission (ASE) in order to optimize the emission of FIR. Our main pulse is accompanied by a 5 ns ASE pedestal with an energy contrast to the main pulse of 4×10^3. By using glass saturable absorber filters, we improved this contrast ratio to 4×10^5. However, the emitted FIR dropped by a factor of 10 when the saturable absorber was inserted. The total amount of emitted FIR scales linearly with the incident laser energy as shown in Fig. 8. We observe large fluctuations of the FIR signal on a shot-to-shot basis which are *not* correlated to fluctuations in the second harmonic of the laser from a KDP crystal. We were also not able to clearly relate these fluctuations to surface inhomogeneities or to vibrations of the target mount.

Along with the terahertz emission we observe a hard x-ray signal. The x-rays penetrate the 5 mm thick steel wall of the target chamber, which provides a low-energy cutoff of 0.1 MeV. They are detected with a 7.5 cm diameter NaI detector which is kept in 3 m distance and 70° off normal from the target. We observe the same signatures for the hard x-ray emission as reported previously [10], e.g., the strongest x-ray yield is observed when a strong scatter of light from the 3/2 harmonic of the laser occurs.

The x-ray and FIR emission occur simultaneously. Figure 9 (a) shows the x-ray signal on the NaI detector versus the FIR signal for 16, 000 shots. Both emissions are correlated on a shot-to-shot basis by a power law with an exponent of 0.7.

In addition we detected the emission of energetic electrons from the plasma. We used a 5 mm thick piece of BC408 scintillator plastic to detect the electrons. Before reaching the detector, the electrons had to penetrate a 0.2 mm thick sheet of black polyethylene which served as a vacuum window. By using a 5000 G Sm:Co magnet we verified that the signal was indeed due to electrons and not x-rays. The contrast ratio between electron and x-ray signal on the detector was determined to be greater than 10^3. Al-sheets of varying thickness were used to determine the electron energy since the stopping powers for energetic electrons in different materials are well documented [36]. We estimate that the bulk of the electrons had an energy of 0.6 MeV at a laser intensity of 1.6×10^{18} W/cm^2. This energy is ≈ 4 times larger than predicted by computer simulations [4]. The ponderomotive energy of the focused laser is 0.1 MeV, but we believe that the electrons originate close to the critical surface where the electric field is strongly enhanced [37]. This is supported by the observation that strong emission is detected only if the target is prepulsed with energy in excess of about 1 mJ. Simultaneously, we observe light at the 3/2 harmonic of the laser which comes from a region w th quarter critical density [1].

The electron signal is correlated to the terahertz emission as shown in Fig. 9 (b). We compute a power law with an exponent of 0.4. The electron emission is also related to the x-ray signal as shown in Fig. 9 (c). The x-ray yield goes as the 0.9-power of electronic signal.

One may try to understand these scalings in the following way. The simultaneous occurrence of strong x-ray, β- and FIR emissions indicates that the radiative processes are driven by ponderomotively induced space charge fields at the critical surface. The fields which give rise to the emission of terahertz radiation accelerate the electrons, which then in turn produce energetic x-rays via bremsstrahlung in the target substrate. The scaling for such a process is well known for x-ray tubes and is given by $P_x \propto W^2 \times I$ [38], where W is the electron energy, I the current and P_x the emitted x-ray power. However, we fail to

explain the observed power laws for the x-ray yield on the basis of this simple analogy. We may assume that the current I is constant since it will be determined by the total amount of excluded charges in the high intensity region. This number is directly related to the ponderomotive energy which fluctuates little as indicated by the reference signal from the KDP crystal. Since W will be proportional to the low frequency electric field E, and the emitted FIR power P_{FIR} will be proportional to E^2 we expect the x-ray yield to go linear with the FIR signal. We observe $P_x \propto (P_{FIR})^{0.7}$. The electronic signal P_e is proportional to $W \times I$, and hence we expect $P_x \propto (P_e)^{2.0}$ which contrasts the observed value of 0.9. However, the relation between FIR and electron signal is expected to be $P_e \propto (P_{FIR})^{0.5}$ which compares well to the experimentally observed exponent of 0.4.

It is also interesting to compare the radiative yields for all three types of radiation. Assuming that the electrons emitted from the plasma have an average energy of at 0.6 MeV and are isotropicaly distributed, we estimate that 2×10^9 electrons are emitted by the plasma per shot at a pulse energy of 20 mJ. The NaI detector was calibrated with a 100 μCi source of Cs^{137} in place of the laser focus. This allowed us to estimate the relative number of Compton events. Assuming a photon energy of 0.2 MeV, which is the average energy for a photon produced via Bremsstrahlung by a 0.6 MeV electron [39], we estimate that a total of 10^7 x-rays are produced per shot. The electron to x-ray energy conversion is thus 0.2 %. This compares well with calculated Bremsstrahlung yield of 0.4 % for 0.6 MeV electrons in glass [36].

We can make an estimate for the strength of the low frequency electric field in the focal region. Assuming that the electrons are accelerated over a distance of a few microns, we readily infer a field strength on the order of 10^9 V/cm from the observation 0.6 MeV electrons. At the same time we infer a field strength on the order of 10^8 V/cm from the observation of terahertz radiation with a peak power of several MW emerging from a spot a few microns in size. This corresponds to a strength of the magnetic field of the electromagnetic wave of $\approx 3 \times 10^5$ G. The discrepancy in field strength by a factor of

10 between both estimates may be reconciled by considering that there will be a coupling loss since the FIR has to penetrate a dense plasma which is overcritical for terahertz radiation. We note that key to inferring these high fields is the assumption that the radiation emerges from a spot of less than 10 μm in diameter. This is well justified since all length scales entering the problem, i.e. the beam diameter, the attenuation length of the laser field and the plasma scale length, are smaller than or equal to a few microns. We also note that the peak electric field of the laser is about 3×10^8 V/cm for a power density of 1×10^{18} W/cm^2.

In conclusion we demonstrated that short pulse laser produced plasmas are a novel and powerful source for the generation of short-pulse terahertz radiation; we demonstrated peak powers in excess of 1 MW. We also report the *direct* observation of laser induced wake fields. The measurement of electromagnetic pulses in laser-plasma interactions may contribute as a diagnostic tool to the realization of laser-based particle accelerators. Further, we have shown that the emission of FIR is strongly correlated with the production of x-rays and electrons of MeV energies. This may allow novel experiments with ultrafast time resolution, cross-correlating beams that span the electromagnetic spectrum from meV to MeV energies.

It is a pleasure to acknowledge help from and fruitful discussions with A. Belkacem, W. Holmes, W. Leemans, M. Nahum, S. Verghese and W. White. H.H. was supported by the Studienstiftung des deutschen Volkes. This work was supported by the U.S. Air Force Office of Scientific Research and through a collaboration with Lawrence Livermore National Laboratory under contract W-7405-ENG-48.

References

[1] W.L. Kruer, *The Physics of Laser Plasma Interaction* (Addison-Wesley, 1988).

[2] C. Joshi, *et al.*, Nature, **311**, 525 (1984).

[3] P. Sprangle, E. Esarey and A. Ting, Phys. Rev. Lett., **64**, 2011 (1990).

[4] S.C. Wilks, *et al.*, Phys. Rev. Lett., **69**, 1383 (1992).

[5] R.N. Sudan, Phys. Rev. Lett., **70**, 3075 (1993).

[6] G.Z. Sun, *et al.*, Phys. Fluids, **30**, 526 (1987).

[7] J.J. Macklin, J.D. Kmetec and C.L. Gordon, Phys. Rev. Lett., **70**, 766 (1993).

[8] A. L'Huillier and P. Balcou, Phys. Rev. Lett., **70**, 774 (1993).

[9] M.M. Murnane, *et al.*, Science, **251**, 531 (1991).

[10] J.D. Kmetec, *et al.*, Phys. Rev. Lett., **68**, 1527 (1992).

[11] H. Hamster and R.W. Falcone, in *Ultrafast Phenomena VII* edited by C.B. Harris, *et al.* (Springer, New York, 1990).

[12] H. Hamster, *et al.*, submitted to Phys. Rev. Lett., (1993).

[13] J.A. Stamper and B.H. Ripin, Phys. Rev. Lett., **34**, 138 (1975).

[14] J.A. Stamper, Laser and Particle Beams, **9**, 841 (1991).

[15] C.E. Clayton, *et al.*, Phys. Rev. Lett., **70**, 37 (1993).

[16] D.H. Auston and M.C. Nuss, IEEE J. Quantum Electron., **24**, 184 (1988).

[17] D. Grischkowsky, *et al.*, J. Opt. Soc. Am. B, **7**, 2006 (1990).

[18] P.R. Smith, D.H. Auston and M.C. Nuss, IEEE J. Quantum Electron., **24**, 255 (1988).

[19] X.C. Zhang, *et al.*, Appl. Phys. Lett., **56**, 1011 (1990).

[20] J.T. Darrow, *et al.*, Opt. Lett., **15**, 323 (1990).

[21] D. You, *et al.*, Opt. Lett., **18**, 290 (1993).

[22] H. Hamster, Ph.D. Thesis, University of California at Berkeley (1993).

[23] T.W.B. Kibble, Phys. Rev., **150**, 1060 (1966).

[24] T.E. Glover, *et al.*, *Electron Energy Distributions in Plasmas Produced by Intense Short-Pulse Lasers* in *OSA conference "Short Wavelength V: Physics with Intense Lasers"* (OSA, San Diego, 1993).

[25] B.M. Penetrante and J.N. Bardsley, Phys. Rev. A, **43**, 3100 (1991).

[26] J.D. Jackson, *Classical Electrodynamics* (J. Wiley & Sons, New York, 1975), 2nd Edition.

[27] R. Fedele, U. de Angelis and T. Katsouleas, Phys. Rev. A, **33**, 4412 (1986).

[28] L. Spitzer, *Physics of Fully Ionized Gases* (Wiley & Sons, New York, 1962).

[29] Y.R. Shen, *The Principles of Nonlinear Optics* (Wiley & Sons, New York, 1984).

[30] A. Sullivan, *et al.*, Optics Letters, **16**, 1406 (1991).

[31] B.I. Greene, *et al.*, Appl. Phys. Lett., **59**, 893 (1991).

[32] T. Katsouleas and W.B. Mori, Phys. Rev. Lett., **61**, 90 (1988) and references therein.

[33] A. Sullivan, *et al.*, *Propagation of Intense, Ultrashort Pulses in Plasmas* in *OSA conference "Short Wavelength V: Physics with Intense Lasers"* (OSA, San Diego, 1993).

[34] N.G. Basov, Sov. J. Quantum Electr., **1**, 2 (1971).

[35] G. Mourou, C.V. Stancampiano and D. Blumenthal, Appl. Phys. Lett., **38**, 470 (1981).

[36] M.J. Berger and S.M. Seltzer, *Stopping Powers and Ranges of Electrons and Positrons* (National Bureau of Standards, Washington, DC, 1982).

[37] R. Fedosejevs, *et al.*, Appl. Phys. B, **50**, 79 (1990).

[38] N.A. Dyson, *X-Rays in Atomic and Nuclear Physics* (Cambridge Univ. Press, Cambridge, 1990), 2nd Edition.

[39] W. Heitler, *The Quantum Theory of Radiation* (Clarendon Press, Oxford, 1954), 3rd Edition.

Figure captions

Figure 1. Calculated radiation pattern. The vertical axis denotes power (W/sr), the bottom axis are time (ps) and view angle (rad) with respect to the beam propagation direction. The calculations are for a pulse length of 120 fs FWHM, 50 mJ pulse energy and a beam diameter of 3 μm. (a) Resonant plasma response when the electron density is 2.5×10^{17} cm^{-3}. (b) Non-resonant response at a density of 10^{19} cm^{-3}. (c) FIR signal due to $\bar{J}^{NL}$ at a density of 10^{19} cm^{-3}.

Figure 2. (a) Observed FIR emission from He gas as a function of pressure in comparison with calculations assuming a 140 fs, 50 mJ laser pulse. (b) Calculation of different contributions to the FIR signal. Shown are the contributions due to the time averaged source term, due to $\bar{J}^{NL}$ and the sum of both signals.

Figure 3. Autocorrelation of FIR signal in He for a 120 fs, 50 mJ pulses. (a) Resonant excitation at an electron density of 7×10^{16} cm^{-3}. (b) Nonresonant excitation at a density of 2×10^{19} cm^{-3}.

Figure 4. Spectra for a resonant excitation of the plasma where $\omega_p \tau_0 \approx 2$. The arrows indicate the plasma frequency $\omega_p/2\pi$ at each density. Note the emerging nonresonant signal around 1.5 THz at the highest densities. Data is for a He-gas and 120 fs, 50 mJ laser pulses.

Figure 5. Spectra for nonresonant excitation of the plasma, i.e. $\omega_p \tau_0 \gg 2$. Data is for a He gas target and 120 fs, 50 mJ laser pulses.

Figure 6. Observed terahertz emission from an Ar plasma versus pressure for s- and p-polarization. The laser pulse length was 120 fs and the energy 50 mJ.

Figure 7. Transmission through an optically gated GaAs wafer. 10% - 90% fall times are 0.8 ps for the case of nonresonant excitation in Ar or He and 1.7 ps for the resonant signal from He at a pressure of 400 Pa.

Figure 8. Dependence of the terahertz emission from a solid target on the laser energy. Each point represents an average of 1000 laser shots. The laser pulse energy was attenuated with neutral density filters. A dependence between the laser energy and FIR yield by a power law with an exponent of 1.1 is derived from a least square fit.

Figure 9. Correlation between hot electron, x-ray and terahertz emission from a solid target. Each graph shows the signal for 16, 000 laser shots. The slopes are obtained from a least square fit. (a) FIR signal versus x-ray signal. (b) Electron signal versus FIR signal. (c) X-ray signal versus electron signal.

(a)

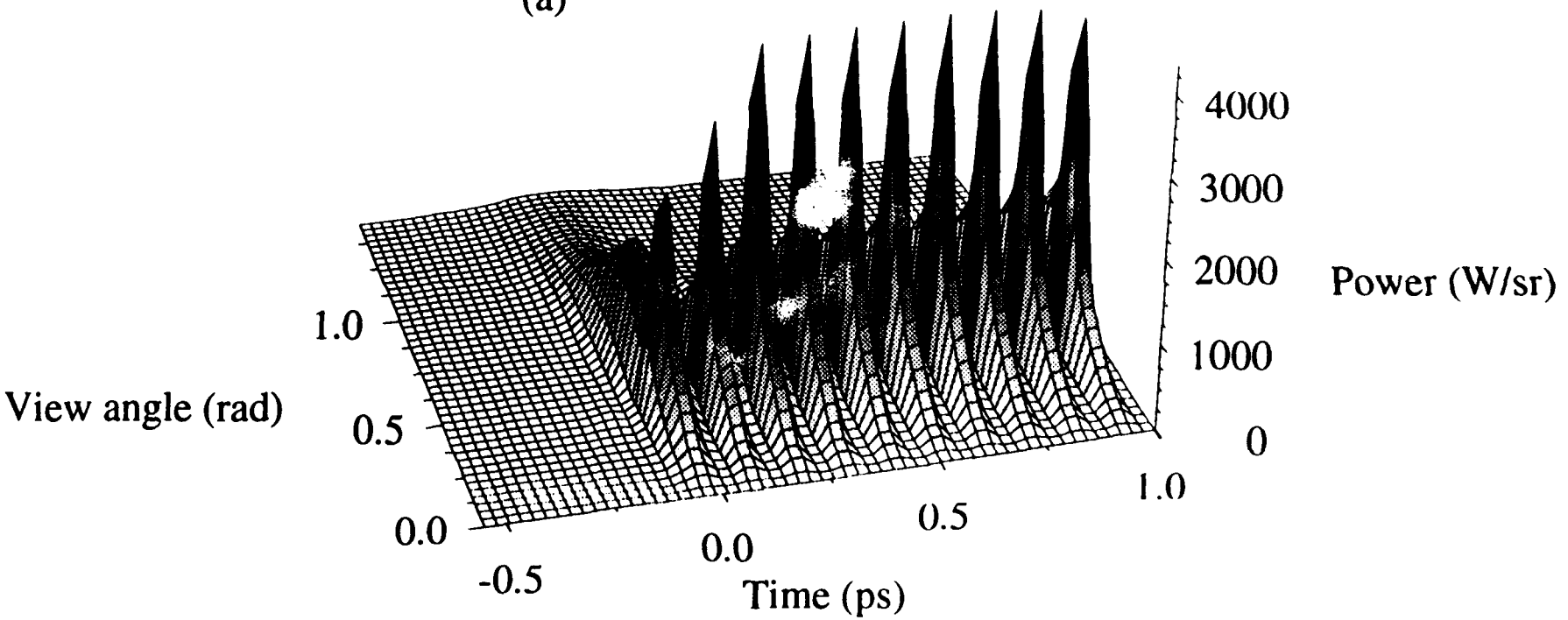

Power (W/sr) vs. (Time (ps), View angle (rad))

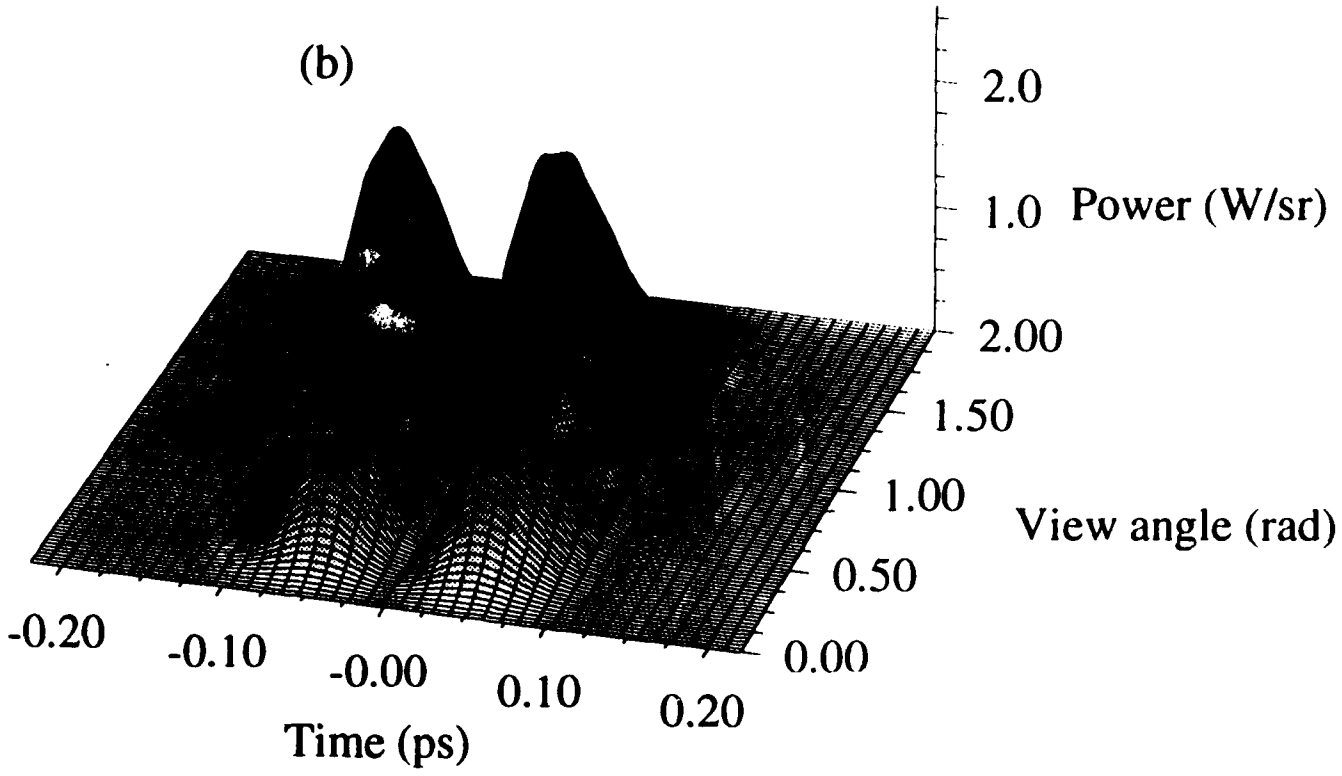

Power (W/sr) vs. (View angle (rad), Time (ps))

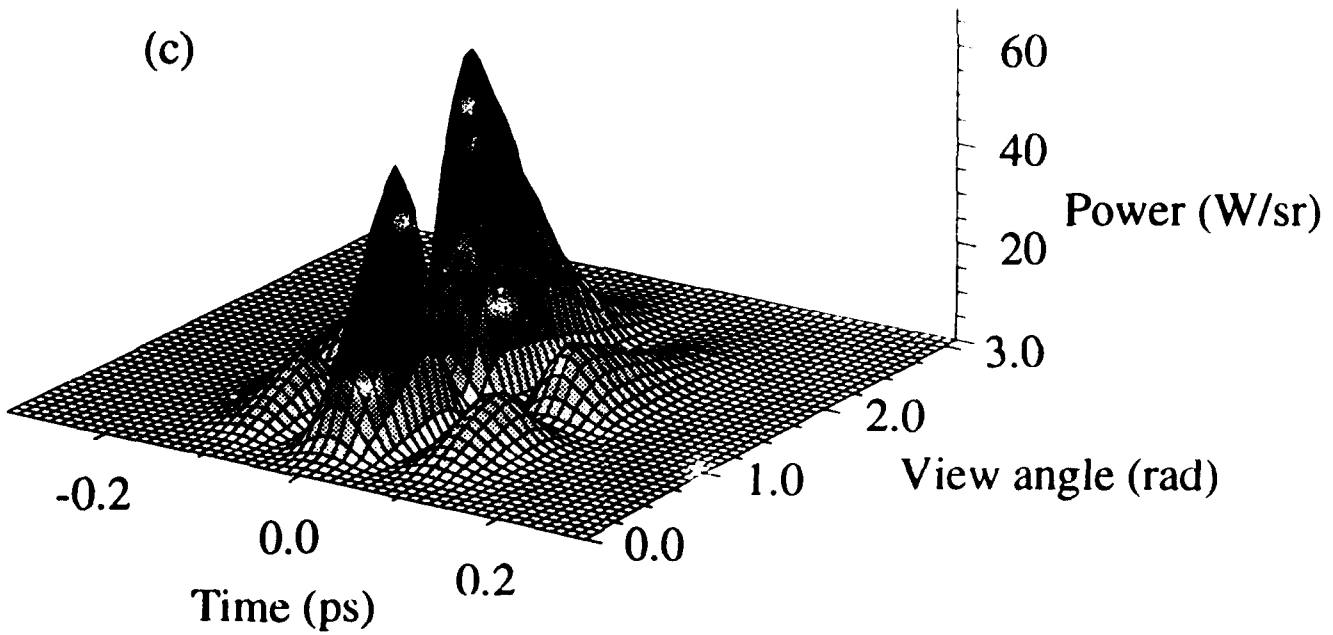

Power (W/sr) vs. (View angle (rad), Time (ps))

Fig 1c

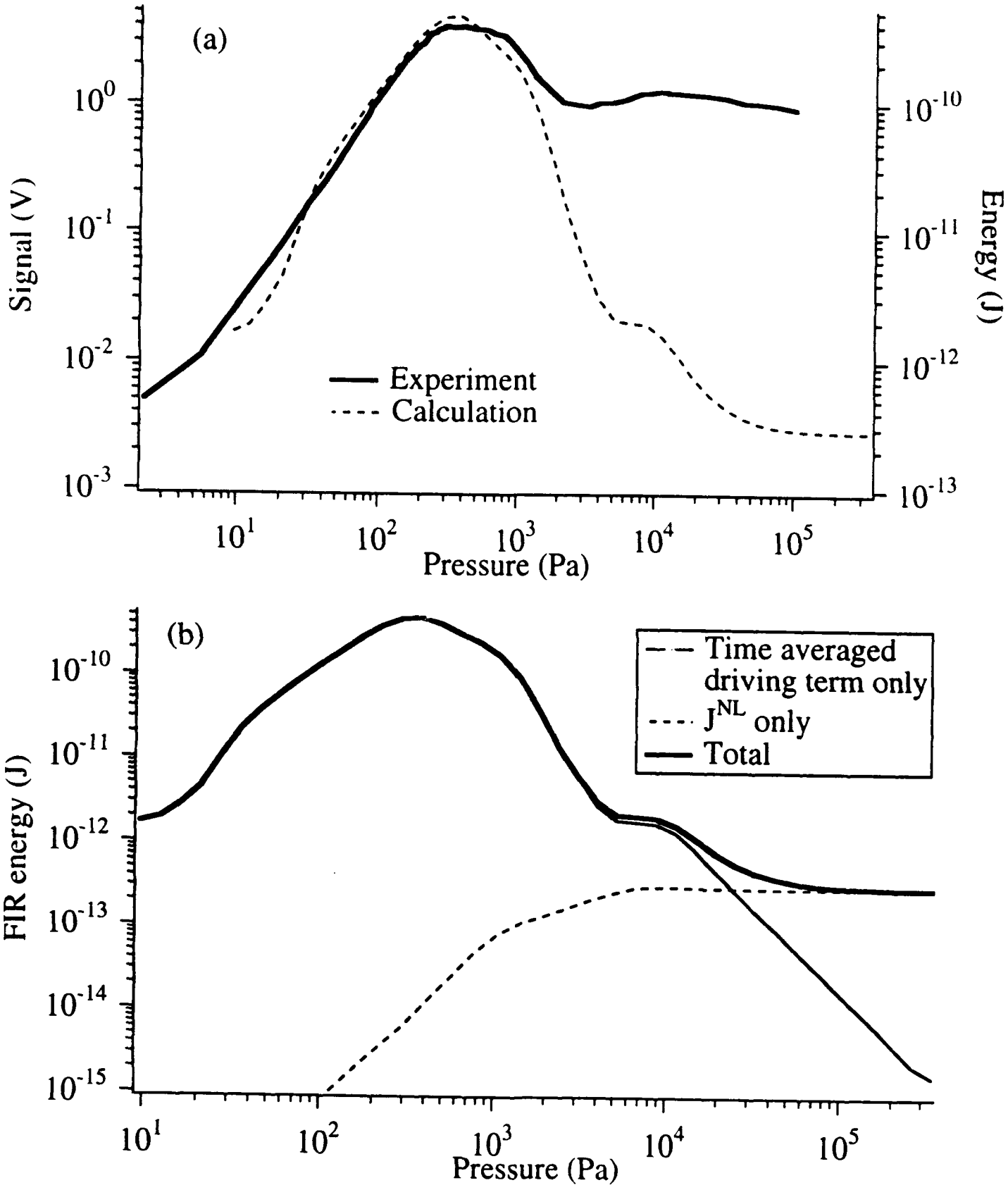
(a)
Signal (V)
Energy (J)
Experiment
Calculation
Pressure (Pa)
(b)
FIR energy (J)
Time averaged driving term only
J^NL only
Total
Pressure (Pa)

Figure 2

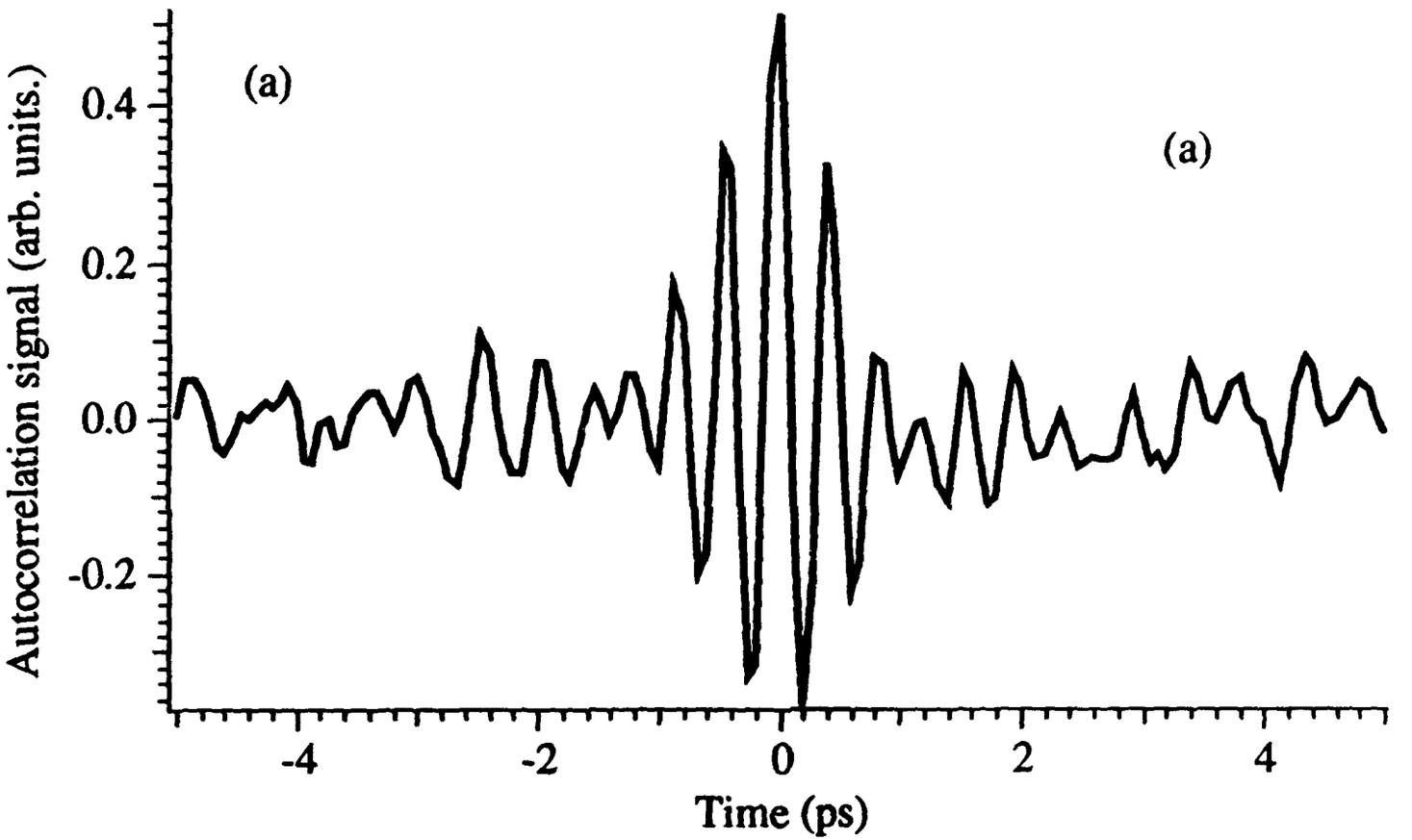
(a)
(a)
Autocorrelation signal (arb. units.)
0.4
0.2
0.0
-0.2
-4
-2
0
2
4
Time (ps)

Figure 3 (a)

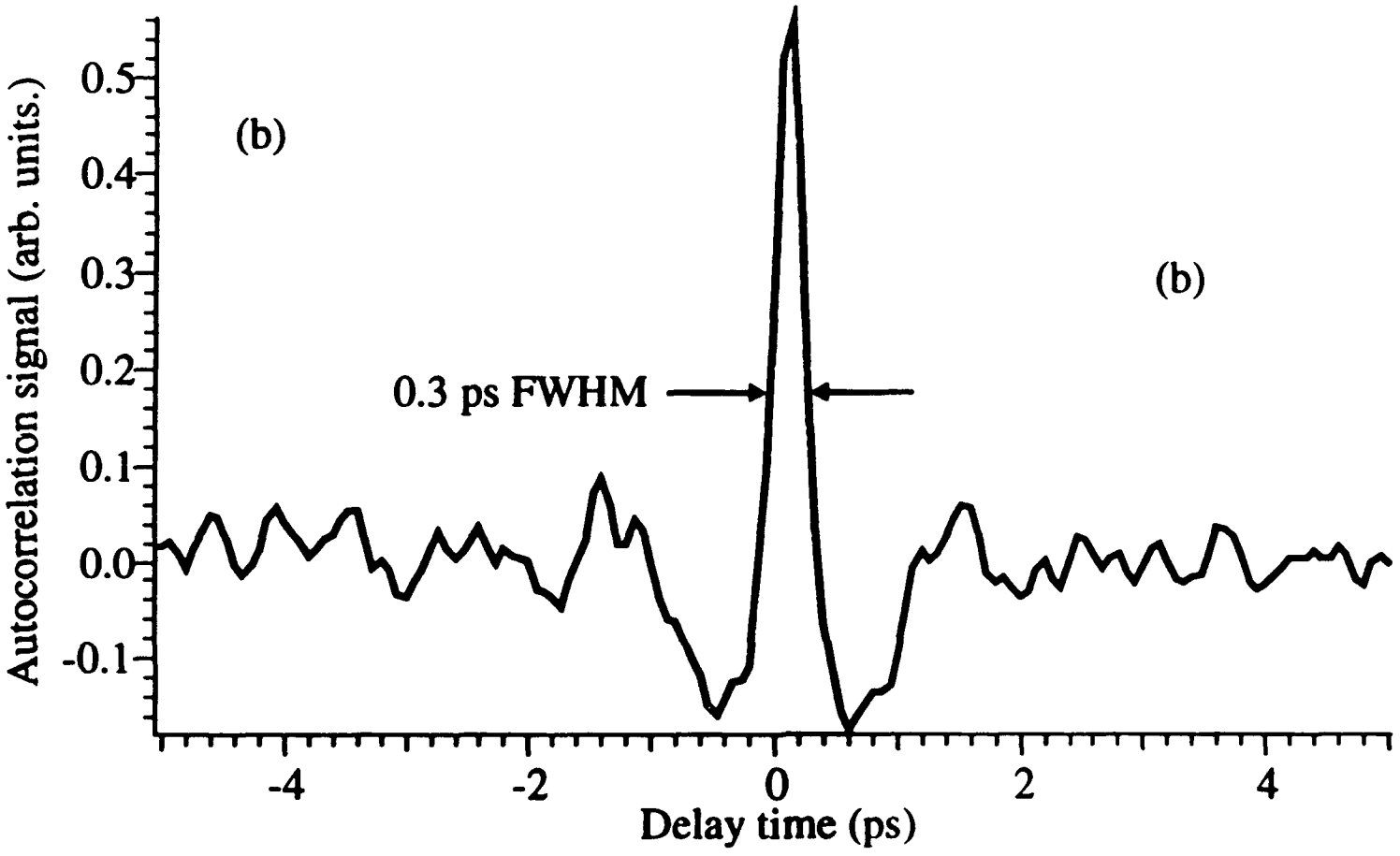
(b)
(b)
0.3 ps FWHM
Autocorrelation signal (arb. units.)
0.5
0.4
0.3
0.2
0.1
0.0
-0.1
-4
-2
0
2
4
Delay time (ps)

Figure 3 (b)

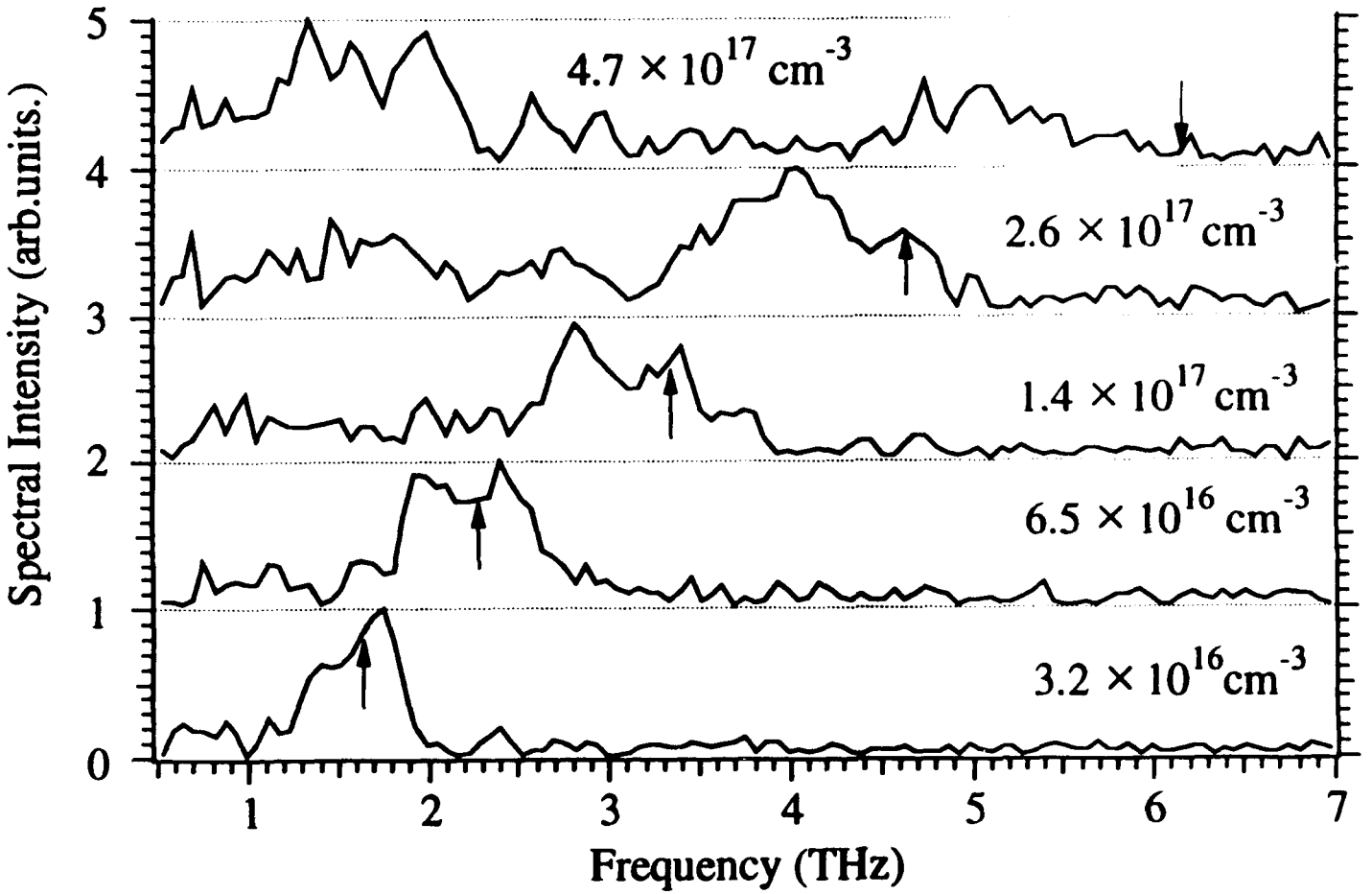
Spectral Intensity (arb.units.)
Frequency (THz)
4.7 × 10^17 cm^-3
2.6 × 10^17 cm^-3
1.4 × 10^17 cm^-3
6.5 × 10^16 cm^-3
3.2 × 10^16 cm^-3
0
1
2
3
4
5
1
2
3
4
5
6
7

Figure 4

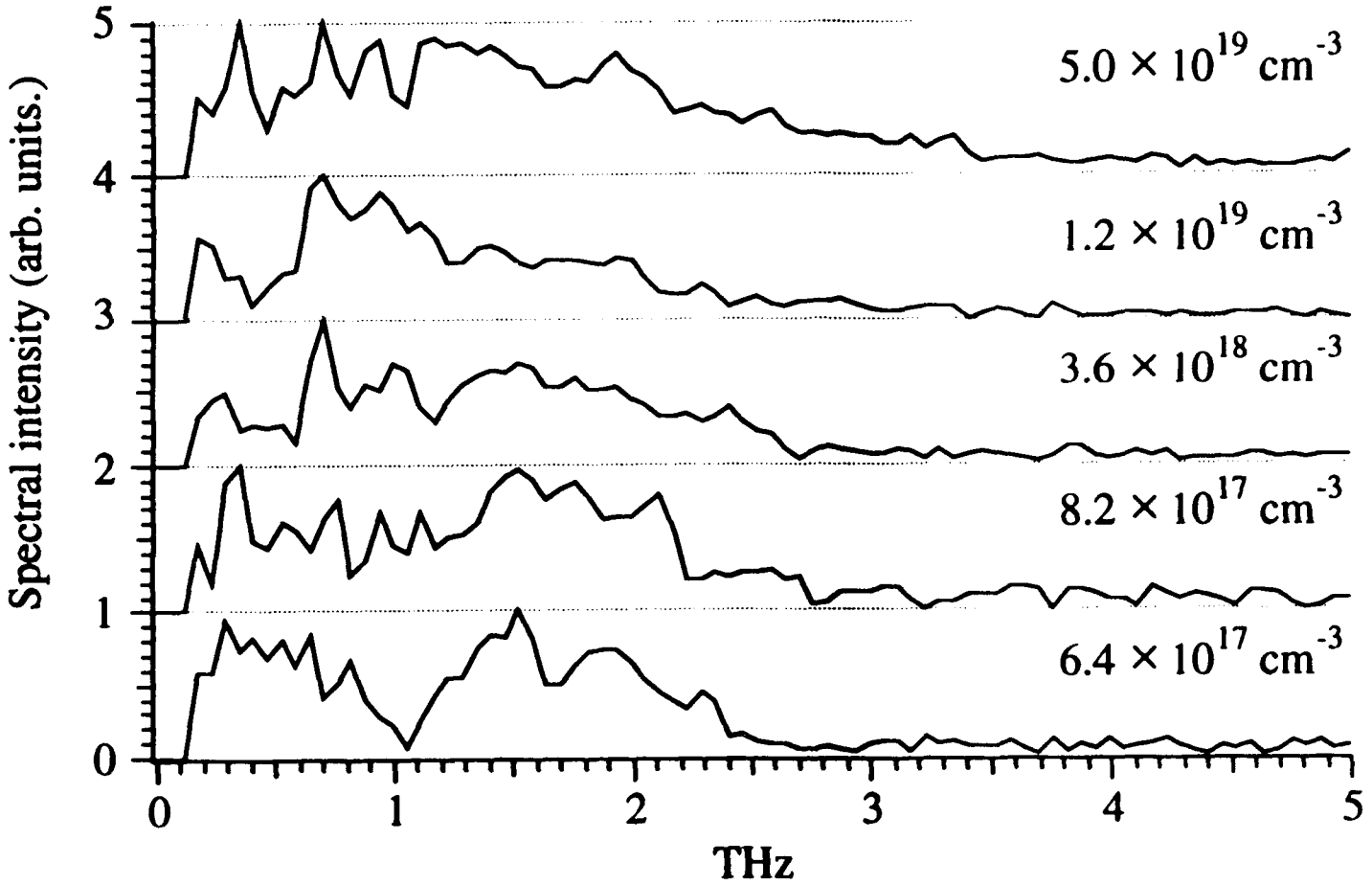
Spectral intensity (arb. units.)
5
4
3
2
1
0
0
1
2
3
4
5
THz
5.0 × 10^19 cm^-3
1.2 × 10^19 cm^-3
3.6 × 10^18 cm^-3
8.2 × 10^17 cm^-3
6.4 × 10^17 cm^-3

Figure 5

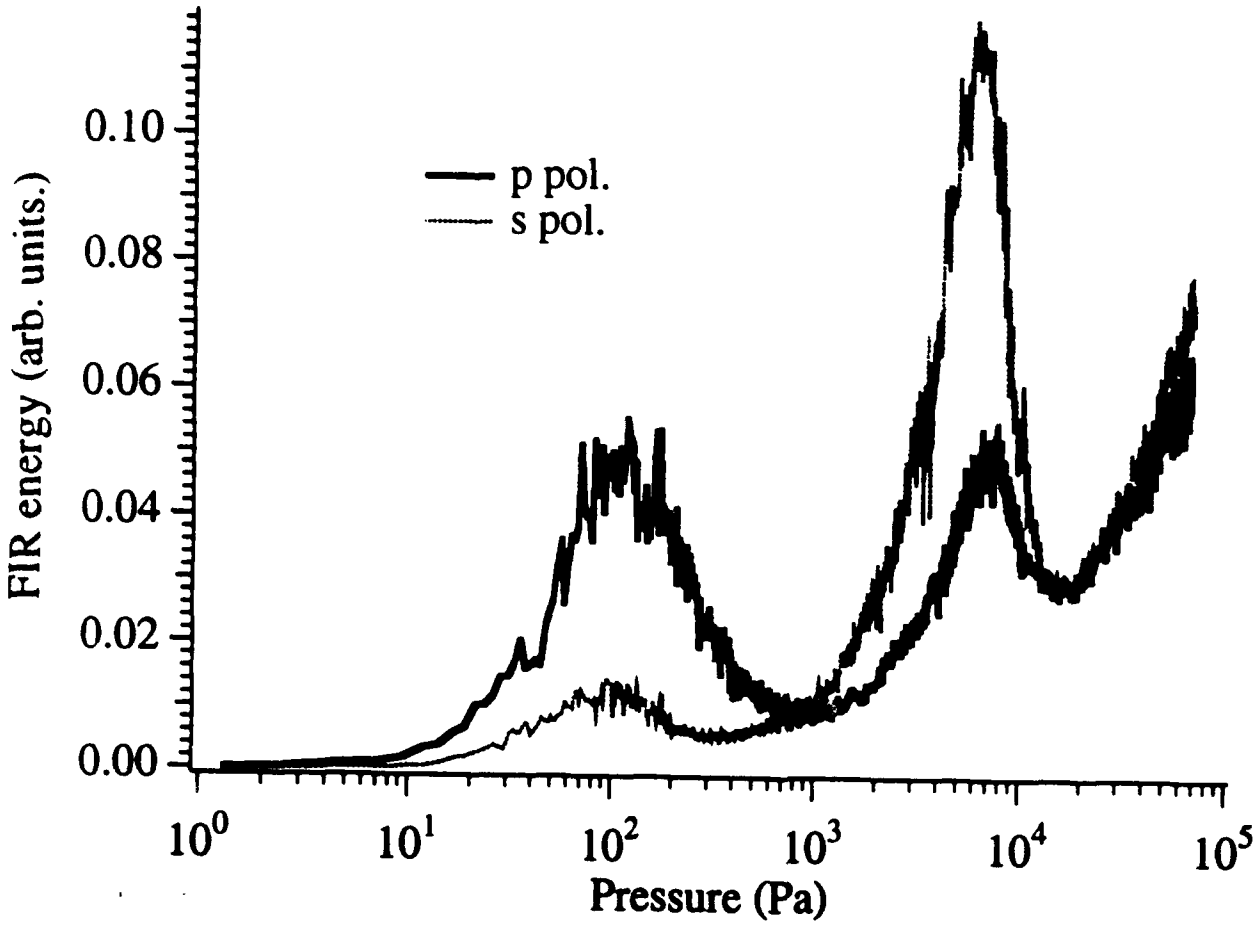
FIR energy (arb. units.)
0.10
0.08
0.06
0.04
0.02
0.00
p pol.
s pol.
10^0
10^1
10^2
10^3
10^4
10^5
Pressure (Pa)

Fig 6

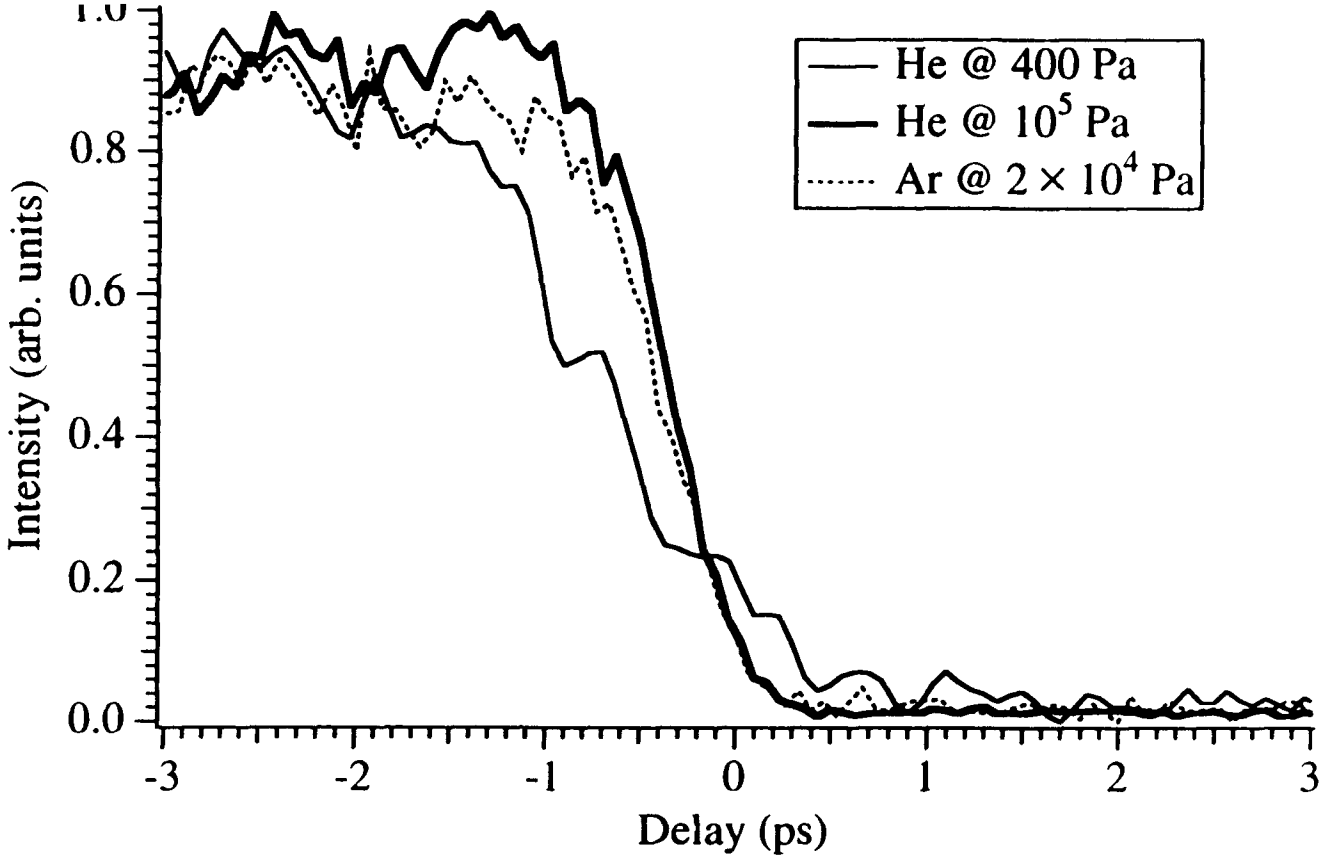
He @ 400 Pa
He @ 10^5 Pa
Ar @ 2 × 10^4 Pa
Intensity (arb. units)
0.0
0.2
0.4
0.6
0.8
-3
-2
-1
0
1
2
3
Delay (ps)

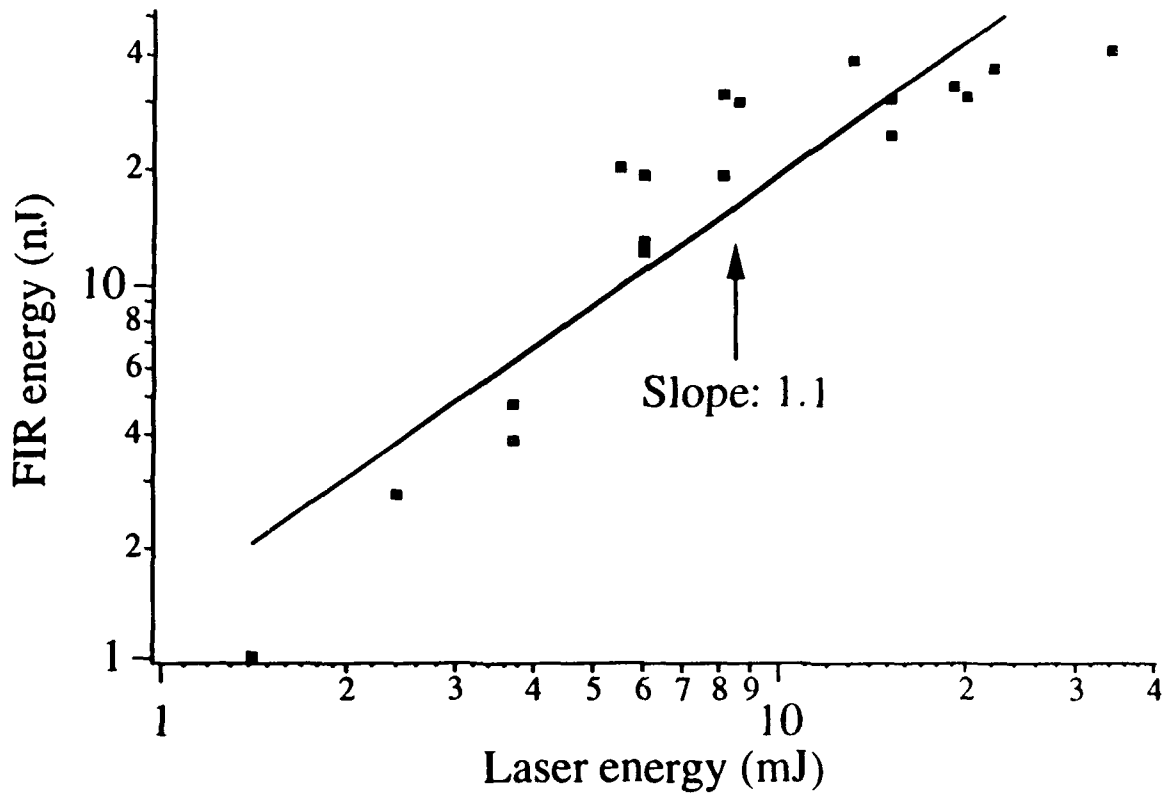
FIR energy (nJ)
4
2
10
8
6
4
2
1
Slope: 1.1
1
2
3
4
5
6
7
8
9
10
2
3
4
Laser energy (mJ)

Figure 8

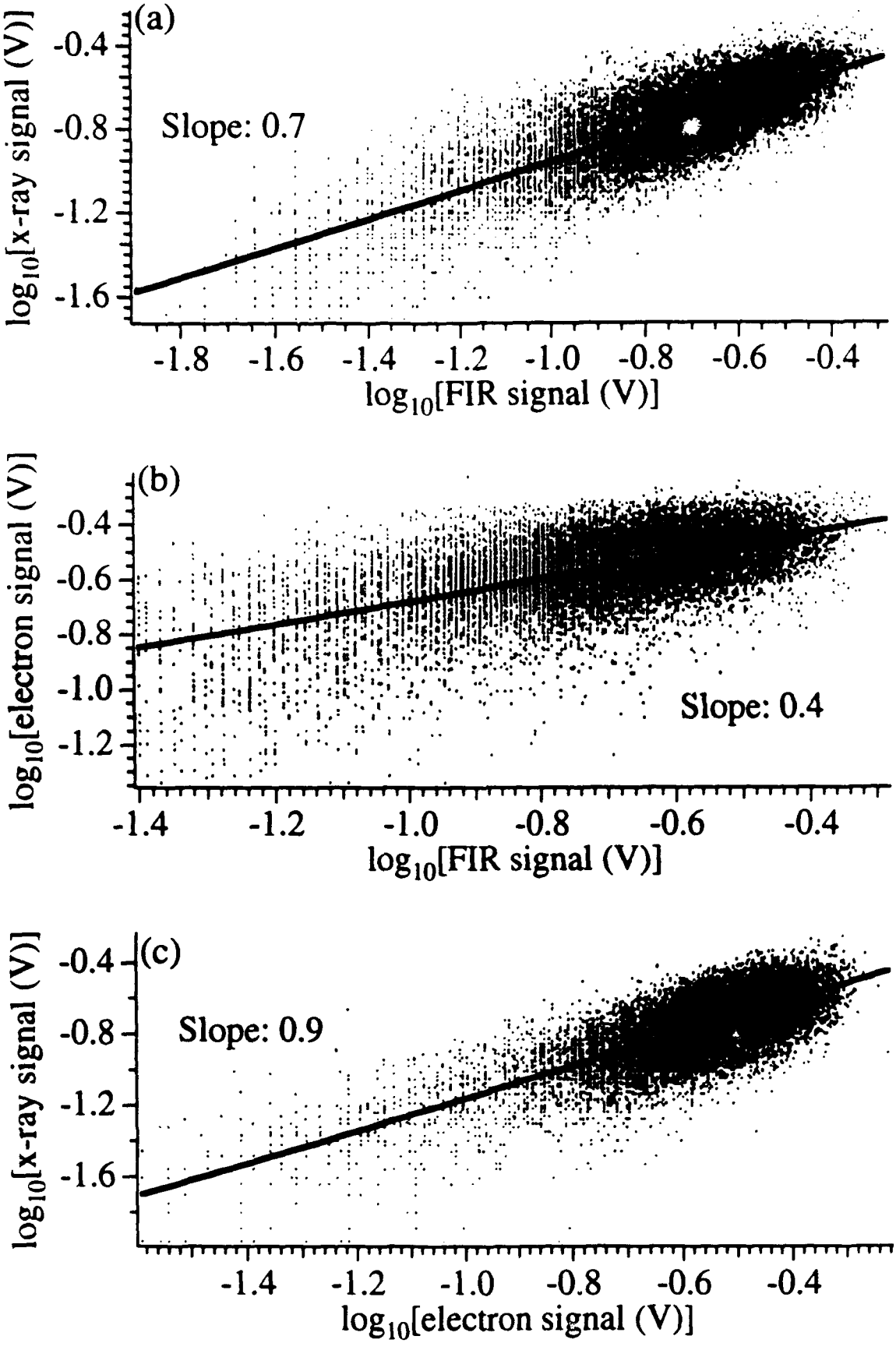
(a)
Slope: 0.7
log10[x-ray signal (V)]
-0.4
-0.8
-1.2
-1.6
-1.8
-1.6
-1.4
-1.2
-1.0
-0.8
-0.6
-0.4
log10[FIR signal (V)]
(b)
Slope: 0.4
log10[electron signal (V)]
-0.4
-0.6
-0.8
-1.0
-1.2
-1.4
-1.2
-1.0
-0.8
-0.6
-0.4
log10[FIR signal (V)]
(c)
Slope: 0.9
log10[x-ray signal (V)]
-0.4
-0.8
-1.2
-1.6
-1.4
-1.2
-1.0
-0.8
-0.6
-0.4
log10[electron signal (V)]

Figure 9

#29

X-rays from Microstructured Targets Heated by Femtosecond Lasers

S.P. Gordon, T. Donnelly, A. Sullivan, H. Hamster, and R.W. Falcone

Department of Physics

University of California at Berkeley

Berkeley, CA 94720

(510) 642-8916

We have demonstrated efficient conversion of ultrashort-pulse laser energy to x-rays above 1 keV using laser-produced plasmas generated on a variety of microstructured surfaces. Lithographically-produced grating targets generated 0.1 mJ of keV x-rays and porous gold and aluminum targets emitted 1 mJ. This represents an improvement of a factor of 100 over flat targets. The K-shell emission spectrum of porous aluminum was primarily composed of helium-like spectral lines.

Sub-picosecond x-ray pulses have applications as short wavelength flashlamps for photoionization-pumped x-ray lasers[1, 2] and as sources for time-resolved x-ray scattering experiments.[3, 4] Instrument-limited, picosecond bursts of x-rays have been measured from the near-solid density plasmas produced by intense, ultrashort-pulse lasers focused on solid metal targets.[5-7] The resulting plasmas cool rapidly due to heat conduction into the underlying cold solid and expansion into the vacuum, thereby abruptly quenching x-ray emission.

Unfortunately, solid density plasmas reflect most of the incident laser radiation due to the high refractive index at the target surface. Somewhat increased absorption can be achieved with p-polarized laser light, incident at an angle with respect to the surface normal, due to resonance absorption and vacuum heating;[8-11] however, with flat targets, this implies a reduction of the incident laser intensity. Since the conversion efficiency of laser energy to x-rays in solid plasmas increases with intensity,[12] normal incidence is desirable. The optimal target should therefore be structured to employ these absorption mechanisms with a normally incident beam.

Enhanced absorption by gratings and porous targets has been previously demonstrated at laser intensities up to 10^{16} W/cm^2.[13] The work described here, and related work at Lawrence Livermore National Laboratory,[14] extend the study of these interactions up to intensities of 10^{18} W/cm^2. Our laser system uses a self-modelocked Ti:Al_2O_3 oscillator which is amplified as described in Ref. 15; it generates pulses with 130 fs duration and 200 mJ at 0.8 μm. These pulses were focused at a 10° incidence angle with a 15 cm off-axis parabolic mirror to a 9 μm focal spot on target. X-ray emission above 1 keV was monitored with an x-ray diode (UDT X-UV100) filtered by

25 μm of Be. A 0.7 tesla magnetic deflector was used to avoid spurious signals from hot electrons. Spectra of x-rays between 1.45 and 2.1 keV were obtained with a KAP spectrometer in a von Hamos configuration.

The first targets employed in these studies were gratings produced by photolithographic techniques. They effectively absorb laser light if the light is polarized perpendicular to the grating grooves. Since the light is p-polarized with respect to the walls of the grating, absorption can be significant, even for the steep plasma gradients expected in ultrashort-pulse experiments. Rae and Burnett[11] have shown theoretically that a plasma with a surface density gradient 100 times shorter than the laser wavelength is capable of absorbing one-half of the energy of an obliquely-incident, intense laser pulse. Assuming that light propagating in the grating grooves is subject to this absorption on the grating walls, we can estimate the absorption depth δ of the laser in the grooves. The energy loss at the surface may be written as $\partial E/\partial A \approx -0.5\ E_0/A$, where ∂A is a surface area element, E_0 is the incident energy, and A is the beam area. For a structure with a volume-to-surface area ratio (V/SA) which is constant as a function of depth z, $\partial A = (SA/V)\partial V = (SA/V)\ A\partial z$. The differential equation for energy loss then becomes $\partial E/\partial z \approx -0.5(SA/V)\ E_0$. Thus, the absorption depth δ is approximately given by 2V/SA.

For a grating, $V/SA=(l\Lambda d)/(2ld)=\Lambda/2$, where d is groove depth, l is length of the exposed area, and Λ is the period; so $\delta\approx\Lambda$. The absorption depth is therefore expected to be insensitive to target composition and fill factor, which is consistent with the results of previous experiments.[13] However, if the thickness of the walls is small compared to the nominal heat penetration depth during the laser pulse ($\geq$50 nm)[12], such gratings should reach higher temperatures than massive targets, thus further enhancing the emitted x-ray efficiency. The optimal grating target has a small period and thin walls.

X-ray output versus incident laser energy for a 0.6 μm period grating overcoated with 60 nm of aluminum is shown in Fig. 1. For comparison, the output from an aluminum-coated glass slide and from a polished silicon wafer is also shown. A 30% larger signal was obtained from the same grating coated with 50 nm of gold and from a 0.7 μm period grating coated with silver. The somewhat enhanced emission of the aluminum-coated slide, compared to the silicon wafer, can most likely be attributed to a small amount of surface roughness.

Our second type of target is a porous form of metal that appears black. In particular, porous gold, called 'gold black' or 'gold smoke', absorbs well throughout the visible and into the infrared.[16, 17] This material is produced by evaporation of the metal in a few torr of argon or nitrogen, and has an average density 400 times below solid. It is composed of micron-sized fractal clusters formed by diffusive growth of 10 nm particles. Theories of infrared absorption by this material at room temperature require detailed knowledge of its fractal structure,[18] or at a least rudimentary accounting for the proximity and connectedness of neighboring particles.[19-21]

When this material becomes hot due to laser absorption, these cluster effects are likewise expected to be important. However, it is possible to estimate the absorption coefficient in the same manner as for the gratings by assuming absorption is predominantly a surface effect. In this case, $V/SA=V_c/NA_p$ where V_c is the cluster volume ($4\pi R_c^3/3$), A_p is the surface area/particle ($4\pi R_p^2$), and N is the number of particles/cluster. For a fractal, $N=(R_c/R_p)^D$, where R_c is the cluster radius, R_p is the particle radius, and D is the fractal dimension.[18] D may be estimated by using the average density $\bar{\rho}=\rho_s(R_c/R_p)^{D-3}$, where ρ_s is solid density. This simple treatment predicts an absorption depth of $\delta\approx R_c^{3-D}/R_p^{2-D}$. Typically, $R_c\approx 1$ μm, $R_p\approx 5$ nm, and

D≈1.9, so the absorption depth is expected to be approximately 2 μm. As a result of the long thermal gradient, thermal conduction during the laser pulse is not important. Since a 2 μm absorption depth in porous gold contains as many atoms as a 5 nm depth of solid, the heated mass of material in the porous target would be 10 times smaller than that in the flat target and could therefore become up to 10 times hotter.

Black gold emitted > 1 mJ of x-rays above 1 keV with 200 mJ on target. No variation of x-ray intensity was detected with the diode placed at various angles within $\pm\pi/4$ radians from the normal. Flat gold, for comparison, was 100 times less efficient. Figure 2 shows the measured output as a function of incident laser energy for porous and flat gold targets. A target characterized by a gradually increasing gold black depth was used to determine the absorption depth of this material. The x-ray output of this target reached 90% of its asymptotic value at a depth of 1 to 2 μm; this measurement approximates the expected depth as calculated above.

If a porous target was prepulsed with amplified spontaneous emission from the laser amplifiers with sufficient energy to damage the structure before the arrival of the main energy pulse, the x-ray output was reduced by a factor of 20. Thus the actual microscopic structure of these targets, and not merely the low average atom density, is important to their effectiveness. Measurement of the x-rays transmitted through progressively higher atomic number filters revealed extremely non-thermal emission; emission between 2 and 10 keV was characterized by a 700 eV temperature, and between 10 and 30 keV by a 3 keV temperature. The emission from solid gold was similarly non-thermal, with a 1 keV fit between 2 and 10 keV.

It is possible to produce other porous materials with the same evaporation technique used for gold. Since K-shell spectra from a variety of aluminum plasmas have been published,[6, 7, 22] we examined porous aluminum which had a density 1.5% that of solid. This material generated x-rays above a kilovolt almost as efficiently as the gold, and was likewise shown to be much more efficient than a flat aluminum target. With 150 mJ on target, porous aluminum emitted > 0.5 mJ, compared to 3 μJ from solid aluminum. A thin porous aluminum target with a depth gradient was employed to determine the approximate absorption depth; in this case the measured depth was 15 to 20 μm. The absorption depth theory described above does not seem to explain this order of magnitude increase of δ over gold black.

We modeled the temperature and density of aluminum black as a function of time assuming an initial heated depth of 20 μm and ionization to the helium-like stage. We used flux limited thermal diffusion at the average density of the structure and isentropic expansion of the particles following the laser pulse. Radiation cooling was found to be minimal. Assuming the average density of the structure, the cluster radius, and the fractal dimension remain constant, expansion into the voids implies cooling according to:

$$T \propto \rho_p^{\gamma-1} \propto R_p^{0.67(D-3)},$$

where T is the temperature, ρ_p is the particle density (initially solid density), and $\gamma = 5/3$ is the specific heat ratio. This calculation predicts a peak temperature during the laser pulse of 4 keV, with rapid cooling in the following picosecond to 500 eV. The local electron density at this time has dropped to 4×10^{22}/cc — an order of magnitude below solid density. Cooling and expansion then continue at a slower pace, reaching 200 eV and 1.5×10^{22}/cc after 4 ps.

A spectrum of porous aluminum emission is shown in Fig. 3. The dominant emission lines are the He-like (Al^{11+}) series and H-like (Al^{12+}) 2p-1s line. The presence of the intercombination line indicates below-solid densities. Comparison of the relative intensities and Stark broadening of the 1snp - $1s^2$ (n = 4-7) lines with those predicted by the RATION plasma code indicates a density near $3x10^{22}$ electrons/cc and a temperature of 300 eV. The Kα line from unionized aluminum is conspicuously absent from these spectra; this line is usually present in solid density plasmas because hot electrons excite the underlying cold material. We looked for this interaction in a separate experiment using a target composed of thin gold black deposited on solid aluminum; again, the Kα line was not present. This implies that forward-directed superthermal electrons are not generated in the porous material.

In summary, we have demonstrated enhanced x-ray emission by gratings and porous targets up to incident laser intensities of 10^{18} W/cm^2. We measured 1 mJ of x-rays above 1 keV emitted in a broad bandwidth from porous gold, and 0.5 mJ in K-shell lines from porous aluminum.

This work was supported by the U.S. Air Force Office of Scientific Research and through a collaboration with Lawrence Livermore National Laboratory under contract W-7405-ENG-48. We wish to thank R.L. Shepherd and D.F. Price for useful conversations, R.W. Lee for the use of his RATION plasma code, M.D. Perry and S.R.J. Brueck for production of grating targets, and D.W. Phillion for providing software to analyze the x-ray film data.

References

1. H. C. Kapteyn, Appl. Opt. **31**, 4931 (1992).

2. D. C. Eder, G. L. Strobel, R. A. London, M. D. Rosen, R. W. Falcone and S. P. Gordon, *"Photo-Ionized Inner-Shell X-Ray Lasers"* in *Short Wavelength V: Physics with Intense Lasers* (OSA, Washington, D.C., 1993), to be published.

3. J. Z. Tischler, B. C. Larson and D. M. Mills, Appl. Phys. Lett. **52**, 1785 (1988).

4. K. Murakami, H. C. Gerritsen, H. van Brug, F. Bijkerk, F. W. Saris and M. J. van der Wiel, Phys. Rev. Lett. **56**, 655 (1986).

5. M. M. Murnane, H. C. Kapteyn, M. D. Rosen and R. W. Falcone, Science **251**, 531 (1991).

6. P. Audebert, J. P. Geindre, J. C. Gauthier, A. Mysyrowicz, J. P. Chambaret and A. Antonetti, Europhys. Lett. **19**, 189 (1992).

7. J. C. Kieffer, M. Chaker, J. P. Matte, H. Pepin, C. Y. Cote, Y. Beaudoin, T. W. Johnston, C. Y. Chien, S. Coe, G. Mourou and O. Peyrusse, Phys. Fluids B **5**, 2676 (1993).

8. F. Brunel, Phys. Rev. Lett. **59**, 52 (1987).

9. P. Gibbon and A. R. Bell, Phys. Rev. Lett. **68**, 1535 (1992).

10. U. Teubner, J. Bergmann, B. van Wonterghem, F. P. Schafer and R. Sauerbrey, Phys. Rev. Lett. **70**, 794 (1993).

11. S. C. Rae and K. Burnett, Phys. Rev. A **44**, 3835 (1991).

12. M. D. Rosen, *"Scaling Laws for Femtosecond Laser-Plasma Interactions"* in *Femtosecond to Nanosecond High-Intensity Lasers and Applications* (SPIE, Bellingham, 1990) Vol. 1229, p. 160.

13. M. M. Murnane, H. C. Kapteyn, S. P. Gordon, J. Bokor, E. N. Glytsis and R. W. Falcone, Appl. Phys. Lett. **62**, 1068 (1993).

14. R. Shepherd, D. Price, W. White, A. Osterheld, R. Walling, W. Goldstein, R. Stewart and S. P. Gordon, *"Characterization of Short Pulse Laser-Produced Plasmas at the Lawrence Livermore National Laboratory Ultrashort-Pulse Laser"* in *Short-Pulse High-Intensity Lasers and Applications II* (SPIE, Bellingham, 1993) Vol. 1860, p. 123.

15. A. Sullivan, H. Hamster, H. C. Kapteyn, S. Gordon, W. White, H. Nathel, R. J. Blair and R. W. Falcone, Opt. Lett. **16**, 1406 (1991).

16. C. G. Granqvist and O. Hunderi, Phys. Rev. B **16**, 3513 (1977).

17. L. Harris and J. K. Beasley, J. Opt. Soc. Am. **42**, 134 (1952).

18. V. A. Markel, L. S. Muratov, M. I. Stockman and T. F. George, Phys. Rev. B **43**, 8183 (1991).

19. P. O'Neill and A. Ignatiev, Phys. Rev. B **18**, 6540 (1978).

20. U. Kreibig, A. Althoff and H. Pressmann, Surf. Sci. **106**, 308 (1981).

21. G. Zaeschmar and A. Nedoluha, J. Opt. Soc. Am. **62**, 348 (1972).

22. G. A. Kyrala, R. D. Fulton, E. K. Wahlin, L. A. Jones, G. T. Schappert, J. A. Cobble and A. J. Taylor, Appl. Phys. Lett. **60**, 2195 (1992).

Figure Captions

Figure 1. X-ray emission above 1 keV versus laser energy from an Al-coated grating (*), flat Al (x), and a Si wafer (+). The grating data is fit to a power law with an exponent of 1.1, and both solid targets to 2.1.

Figure 2. X-ray emission above 1 keV versus laser energy from porous Au and flat Au. The black Au data is fit to a power law with an exponent of 1.5, and the solid target to 1.7.

Figure 3. K-shell spectrum of porous Al taken at 10^{18} W/cm^2.

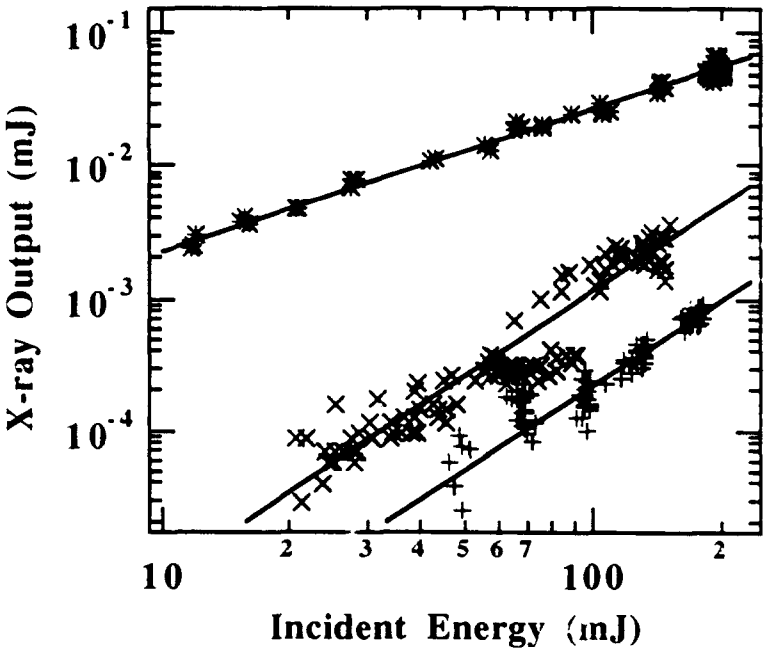
X-ray Output (mJ)
10^-1
10^-2
10^-3
10^-4
2
3
4
5
6
7
10
100
2
Incident Energy (mJ)

Figure 1

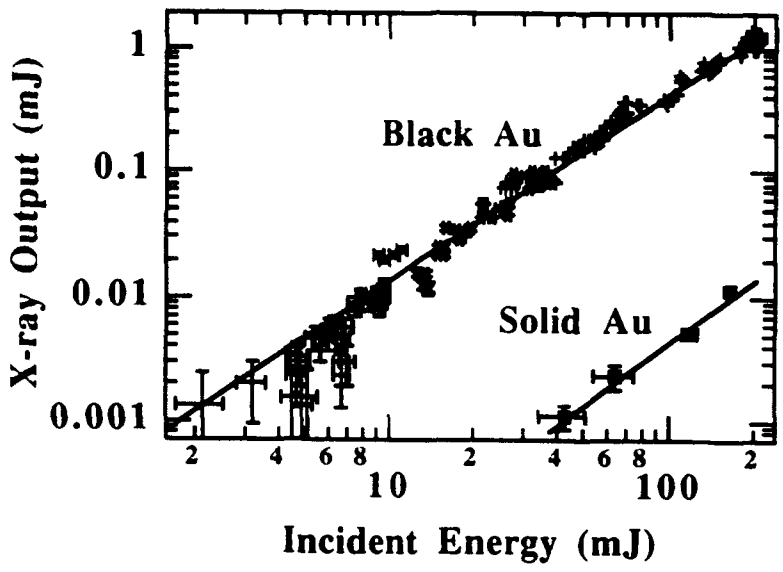
X-ray Output (mJ)
1
0.1
0.01
0.001
Black Au
Solid Au
2
4
6
8
10
2
4
6
8
100
2
Incident Energy (mJ)

Figure 2

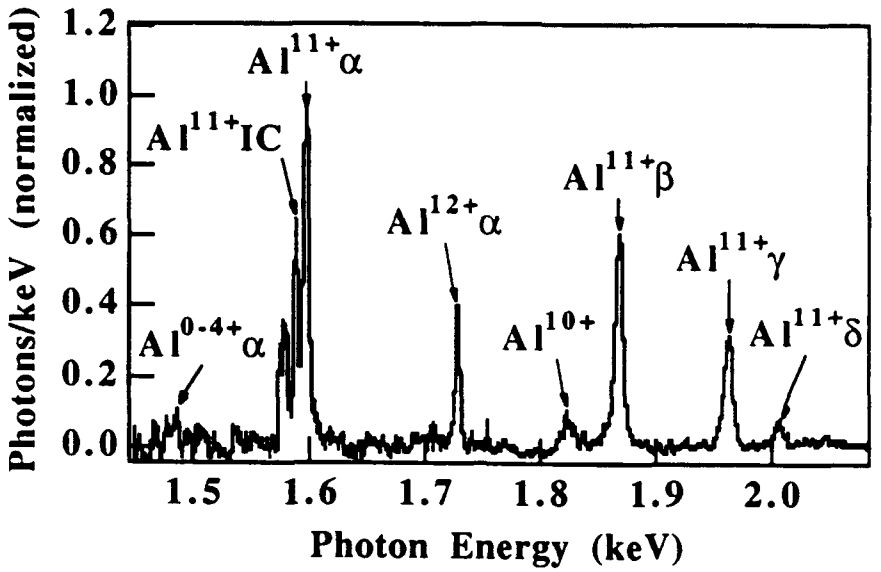
Photons/keV (normalized)
1.2
1.0
0.8
0.6
0.4
0.2
0.0
$Al^{11+}\alpha$
$Al^{11+}IC$
$Al^{12+}\alpha$
$Al^{11+}\beta$
$Al^{11+}\gamma$
$Al^{0-4+}\alpha$
Al^{10+}
$Al^{11+}\delta$
1.5
1.6
1.7
1.8
1.9
2.0
Photon Energy (keV)

Figure 3

#30

Propagation of Intense, Ultrashort Laser Pulses in Plasmas

A. Sullivan, H. Hamster, S.P. Gordon, H. Nathel,[a] and R.W. Falcone

Department of Physics
University of California at Berkeley
Berkeley, CA 94720
(510) 642-8916

We have investigated the propagation of terawatt-power laser pulses in gases. The spatial distribution of focused radiation is modified by refraction that results from the spatially inhomogeneous refractive index of the plasma generated by high-field ionization. We observe Thomson scattering, stimulated Raman scattering, and strong wavelength shifting of the laser light.

PACS numbers: 52.40.Nk, 42.65.Jx, 52.35.Mw

Recent work involving the propagation of high-intensity laser pulses in dense plasmas results from an interest in exciting extended lengths of atoms and ions using nonlinear processes.[1,2] For example, multiphoton-ionized, recombination-pumped x-ray lasers require long lengths of the gain media.[3] Here we report experiments that examined the propagation of ultrashort-duration, high-intensity laser pulses and, specifically, the predicted phenomenon of self-channeling in plasmas formed under conditions of rapid ionization.

Self-channeling of laser light in plasmas has been predicted to occur under certain restrictive conditions.[2,4,5] Channeling is expected due to modifications of the refractive index of the plasma that result from intense laser interaction with electrons. At high intensities ($\approx 10^{19}$ W/cm^2 at near-infrared wavelengths) the oscillatory electron motion becomes relativistic, with a corresponding increase in the effective electron mass. Additionally, intense laser radiation drives electrons out of the focal region due to ponderomotive forces. These effects act to reduce the plasma frequency and increase the refractive index where the laser is most intense. The positive lens thus formed should counteract diffraction and result in collimated propagation over extended lengths.

The threshold power, P_{crit}, for self-channeling of lasers in a plasma is given by[5]

$$P_{crit}(W) = 1.6 \times 10^{10} \frac{n_{crit}}{n_e} \qquad (1)$$

where n_{crit} is the critical electron density (a function of the laser wavelength) and n_e is the electron density of the plasma. At a wavelength of 804 nm (the wavelength in our experiment), $n_{crit} = 1.7 \times 10^{21}$ cm^{-3}. For a laser power of 2.3 TW (the peak power in our experiment) the requirement on the electron density to produce channeling is then $n_e > 1.2 \times 10^{19}$ cm^{-3}.

Self-channeling is expected to be limited by a variety of effects. For example, channel length will be limited by erosion of energy caused by diffraction of the below-threshold leading edge of the pulse, and by depletion of the trailing edge by stimulated Raman scattering (SRS).[4,6,7] The loss of energy from the leading edge propagates

backward through the pulse due to the formation of short temporal structure which does not channel.[7]

If the transition from non-ionized gas (or vacuum) to plasma is not sufficiently abrupt, radial refractive index gradients can cause the beam to defocus.[1,8] For example, for a Gaussian intensity profile, the radial phase variation due to the plasma will cause initially concave (focusing) phase fronts to become convex (defocusing). An estimate of electron density at which this defocusing effect becomes important is[8]

$$n_e > n_{crit}\,\theta^2 \qquad (2)$$

where θ is the half-angle of a focused Gaussian beam. For our 804 nm laser and tight focusing conditions, the maximum allowable electron density (given by Eqn. (2)) before refractive defocusing occurs is approximately the same as the minimum electron density required for self-channeling of our 2.3 TW laser pulses (given by Eqn. (1)).

In our experiment, a plasma is produced by focusing an intense laser pulse into a gas. The laser pulse is produced by chirped-pulse-amplification in a titanium-doped-sapphire laser system (similar to the laser described in Ref. 9) and has a duration of 120 fs, a peak power of 2.3 TW, and a central wavelength of 804 nm. In vacuum, the pulse focuses to a peak intensity of 9×10^{18} W/cm^2 using an f/3 off-axis parabolic mirror; this intensity was determined by imaging the focus spot. In order to observe the propagation of the laser in a plasma, we image spectrally-filtered, Thomson-scattered radiation from the pulse at 90° to the propagation direction. A magnified image of the focal region is projected onto a charge-coupled-device (CCD) camera which is connected to a computer. The microscope-objective-based imaging system results in a calibration of 2 μm per CCD pixel; the resolution is 8 μm with a typical field of view of 200 × 1150 μm.

We note that images of plasma fluorescence are much larger than Thomson images due to hydrodynamic expansion that occurs during the comparatively long fluorescence emission time. Plasma images therefore don't reveal the actual laser intensity distribution and are less useful in studies of laser propagation.

We performed experiments with three different gas distribution techniques: static-filled target chamber, pulsed jet, and differentially-pumped cell. The target chamber can be filled up to atmospheric density. With the jet we obtain gas densities up to $5 \times 10^{18}\,cm^{-3}$. With the differentially-pumped cell we obtain gas densities up to $5 \times 10^{19}\,cm^{-3}$; the cell has a 50 μm aperture through which the laser enters. The jet and cell each provide increasingly abrupt boundaries to the gas region and limit the effects of refractive defocusing.

Figure 1 shows a typical spectrum of the side-scattered radiation from the static-filled chamber. The scattered light spectrum is composed of two components: a linear Thomson-scattered component, which is centered at 804 nm, and an intense stimulated Raman scattered component (SRS), which is shifted from the laser wavelength by approximately the plasma frequency. At relatively low laser intensity or low gas density, the Thomson component of the spectrum replicates the input laser spectrum and increases linearly in intensity with density. However, at higher intensity and density, both the transmitted and scattered light are blue-shifted and broadened due to the rapid change in refractive index during ionization.[10] We note that this effect can lead to considerable spatial and temporal variations of the laser wavelength during the pulse which may affect propagation. A simple interpretation of the radially dependent blue-shift suggests a positive lens which may enhance self-channeling. More complete theoretical analysis is needed of the effects of extreme blue-shifts that result from the focusing of ultrashort lasers in ionizing gases; the resulting radial index variations are comparable to those predicted from charge displacement.

The scattered signal is dominated by SRS at high pressure and high laser power. SRS was observed to be up to 6 orders of magnitude more intense than the linear Thomson-scattered radiation, and was seen to originate primarily from spots on either side of the laser focus. Our observation of SRS is important since it provides evidence of driven plasma waves that could prevent channeling.[6,7]

Figure 2 shows a series of images of laser propagation in N_2 (using the jet) as the gas density is increased. The peak power of the laser exceeded the critical power by up to a factor of 4 at the highest pressures. Due to the extreme brightness of the SRS signal, it was masked in the plane of the camera to prevent saturation of the CCD and allow observation of the linearly scattered Thomson radiation on either side of the focus. The middle images shown in Fig. 2 include the SRS block near the image of the laser focus. As the gas density is increased beyond that predicted to induce self channeling (35 torr), no evidence of self-channeling is observed. At the highest densities, the beam shows considerable reduction in its on-axis intensity (as also indicated by a reduction in SRS) and is observed to break up into filaments that appear to originate in the focal region. This behavior appears universal and was also observed in He and Ar gas.

With the differentially-pumped gas cell we obtain a more abrupt vacuum-plasma interface and are able to reach an electron density of 9×10^{19} cm^{-3} in Ar before beam breakup occurs. At the highest density, the peak power of the laser exceeded the critical power by a factor of 30; channeling was not observed in either Ar, N_2, or He.

In an additional experiment, an aperture was used to constrict the diameter of the laser beam before the focusing optic. The partially closed aperture had the effect of reducing the laser power to 0.5 TW, decreasing the focusing angle, increasing the focused spot size to 5 μm, and reducing the focused intensity to 2×10^{18} W/cm^2. SRS was greatly attenuated due to the reduction in the laser intensity. At a pressure of 100 torr of He ($n_e = 7 \times 10^{18}$ cm^{-3}) we observed that the focused laser remained collimated over a distance approximately three times the Rayleigh range measured at low gas pressure. This result was surprising since the electron density was an order of magnitude below the threshold density for self-channeling at this laser power. Figure 3 shows the Thomson-scattered laser profiles in this experiment at low pressure (30 torr, Fig. 3a) and high pressure (100 torr, Fig. 3b). In Fig. 4, the full-widths at half-maximum of those beams are plotted versus propagation distance.

An important aspect of this experiment is the empirically determined requirement that we employ an aperture in the laser beam in order to observe extended propagation. The aperture may act to increase coupling of energy into a channeled mode by adjusting the focusing angle of the laser. Alternatively, the resulting flat-topped laser profile may reduce the effects of refraction and defocusing which occur during plasma formation. Since the uniform, circular intensity profile produced by the aperture yields a region between the lens and the Airy pattern at the focus that has a donut-shaped mode with a central, low-intensity region near the optical axis, the resulting positive curvature of the plasma distribution near the axis may allow energy to refract inward and initiate the collimated propagation we observe. The length of collimated propagation decreases with reduced laser energy.[11]

In summary, we observe that ionization dynamics and plasma refraction play a critical role in the propagation of intense, ultrashort laser pulses in plasmas. By going to more confined gas geometries we achieve higher gas density before strong refraction and beam breakup into filaments occurs. In our search for self-channeling we obtain a null result even when the laser power exceeds the critical power by more than an order of magnitude. We observe strong spectral modification of the propagating laser pulse and suggest that the resulting spatial and temporal wavelength variations affect pulse propagation through the wavelength dependence of the plasma refractive index. Finally, we observe propagation of the laser pulse over extended lengths using a focused, flat-topped laser profile at intensities below calculated thresholds for channeling.

This work was supported by the US Air Force Office of Scientific Research and through a collaboration with Lawrence Livermore National Laboratory under contract W-7405-ENG-48.

(a) Lawrence Livermore National Laboratory, Livermore, CA 94550

References

[1] P. Monot, T. Auguste, L.A. Lompre, G. Mainfray, and C. Manus, J. Opt. Soc. Am. B, **9**, 1579 (1992).

[2] A.B. Borisov, A.V. Borovskiy, V.V. Korobkin, A.M. Prokhorov, O.B. Shiryaev, X.M. Shi, T.S. Luk, A. McPherson, J.C. Solem, K. Boyer, and C.K. Rhodes, Phys. Rev. Lett., **68**, 2309 (1992).

[3] P. Amendt, D.C. Eder and S.C. Wilks, Phys. Rev. Lett., **66**, 2589 (1991); N.H. Burnett and G.D. Enright, IEEE J. Quantum Electron., **26**, 1797 (1990).

[4] P. Sprangle, E. Esarey and A. Ting, Phys. Rev. A, **41**, 4463 (1990).

[5] G.Z. Sun, E. Ott, Y.C. Lee, and P. Guzdar, Phys. Fluids, **30**, 526 (1987).

[6] T.M. Antonsen and P. Mora, Phys. Rev. Lett., **69**, 2204 (1992).

[7] P. Sprangle, E. Esarey, J. Krall, and G. Joyce, Phys. Rev. Lett., **69**, 2200 (1992).

[8] R. Rankin, C.E. Kapjack, N.H. Burnett, and P.B. Corkum, Opt. Lett., **16**, 835 (1991).

[9] A. Sullivan, H. Hamster, H.C. Kapteyn, S. Gordon, W. White, H. Nathel, R.J. Blair, and R.W. Falcone, Opt. Lett., **16**, 1406 (1991).

[10] S.C. Rae and K. Burnett, Phys. Rev. A, **46**, 1084 (1992); W.M. Wood, C.W. Siders and M.C. Downer, Phys. Rev. Lett., **67**, 3523 (1991).

[11] A. Sullivan, "Propagation of High-Intensity, Ultrashort Laser Pulses in Plasmas," Ph.D. Thesis, University of California at Berkeley, Berkeley, California (1993).

Figure Captions

Figure 1. Side scattered spectrum showing the linear Thomson and stimulated Raman components at 30 and 90 torr of He. At 90 torr the Thomson component shows strong blue-shifting due to rapid index changes associated with the ionization process.

Figure 2. Images of laser propagation in the gas jet as the N_2 gas density is increased. The equivalent pressure of N_2 is indicated in the right margin in units of torr. The threshold pressure for self-channeling is 35 torr for five times ionized N_2 at a power of 2.3 TW.

Figure 3a. Image of laser propagation in 30 torr of He. The laser intensity is approximately 2×10^{18} W/cm^2 and the dimensions of the image are 200 x 1140 μm.

Figure 3b. Same conditions as Fig. 3a except 100 torr of He. Enhanced collimation is seen beyond the focus as compared to propagation at the lower pressure shown in Fig. 3a.

Figure 4. Beam full-width at half-maximum (FWHM) versus propagation distance from the data shown in Fig. 3. The dotted line indicates a Gaussian fit with approximately same divergence angle as the unchanneled beam.

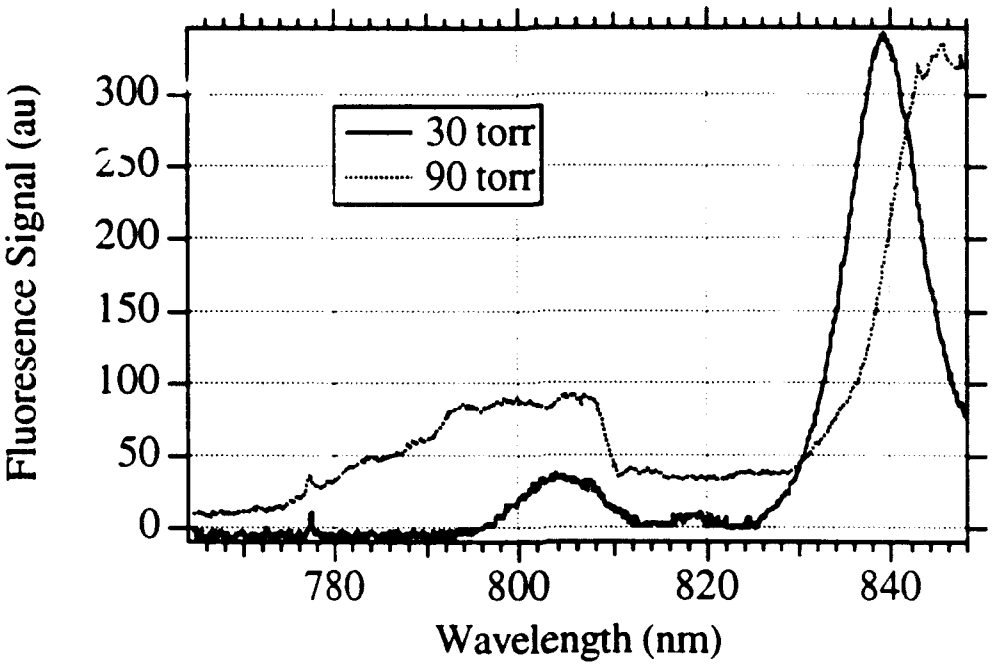
Fluoresence Signal (au)
300
250
200
150
100
50
0
30 torr
90 torr
780
800
820
840
Wavelength (nm)

Figure 1.

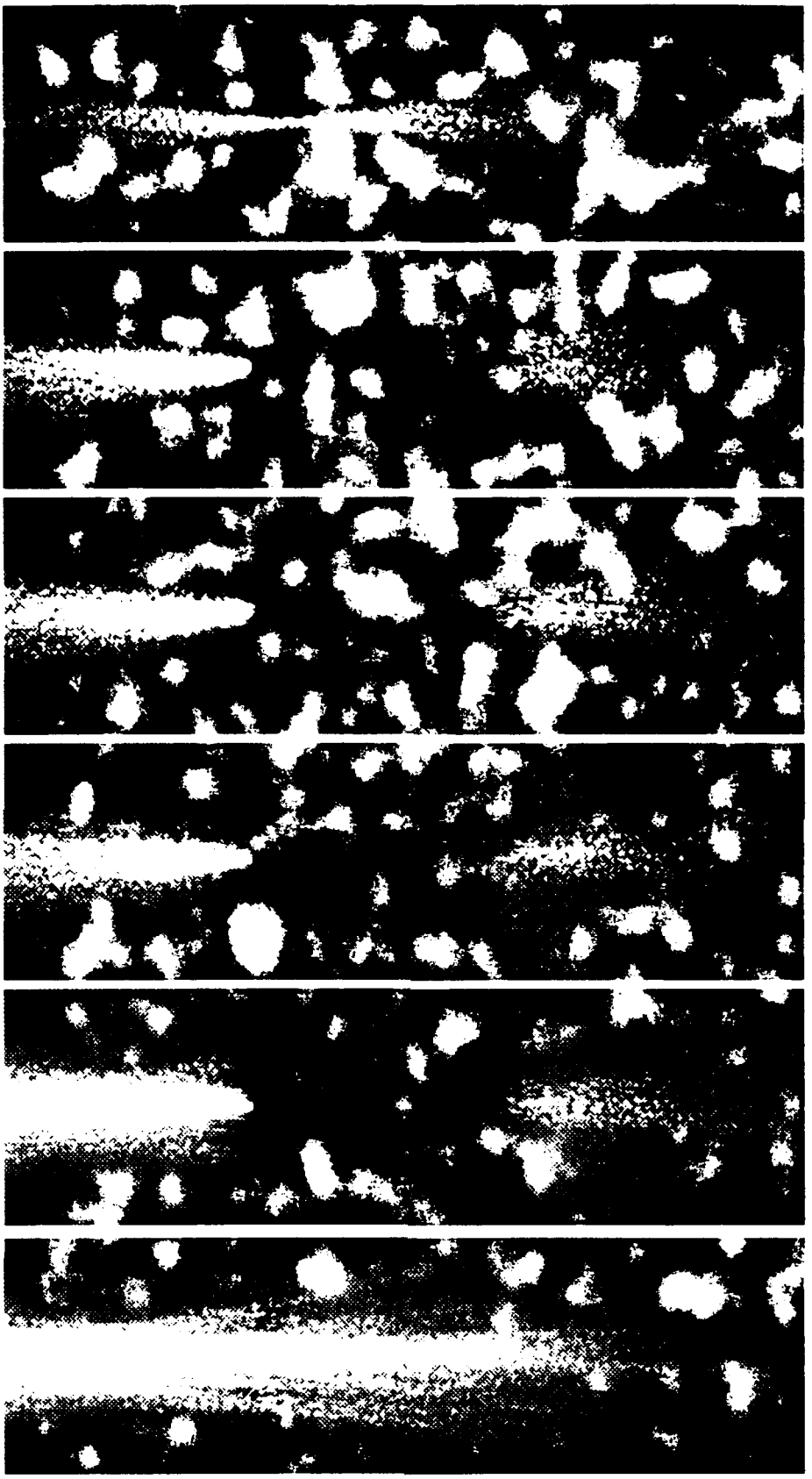
10
25
75
100
120
150

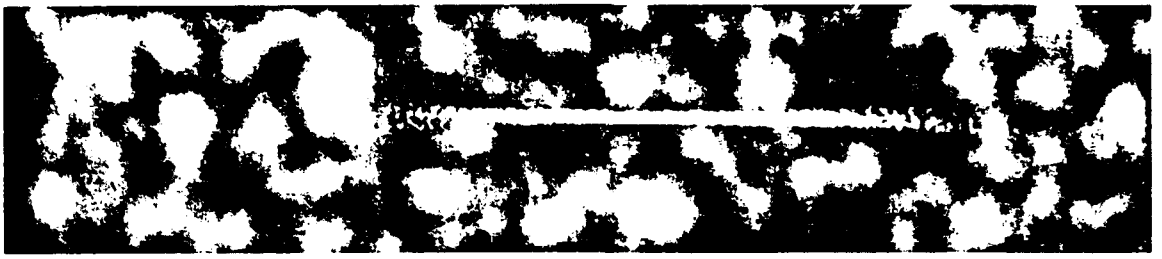

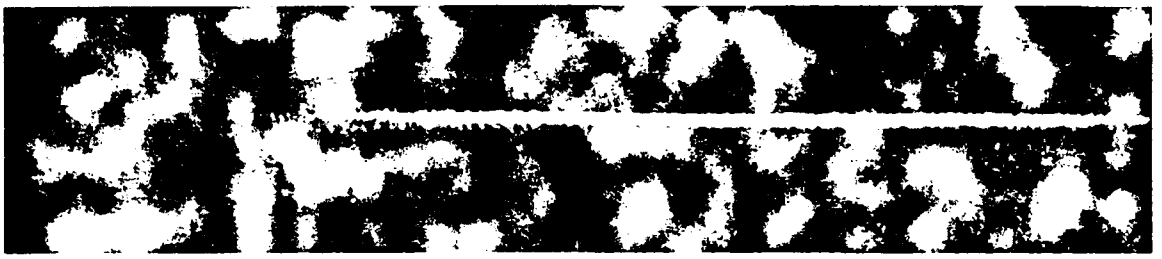

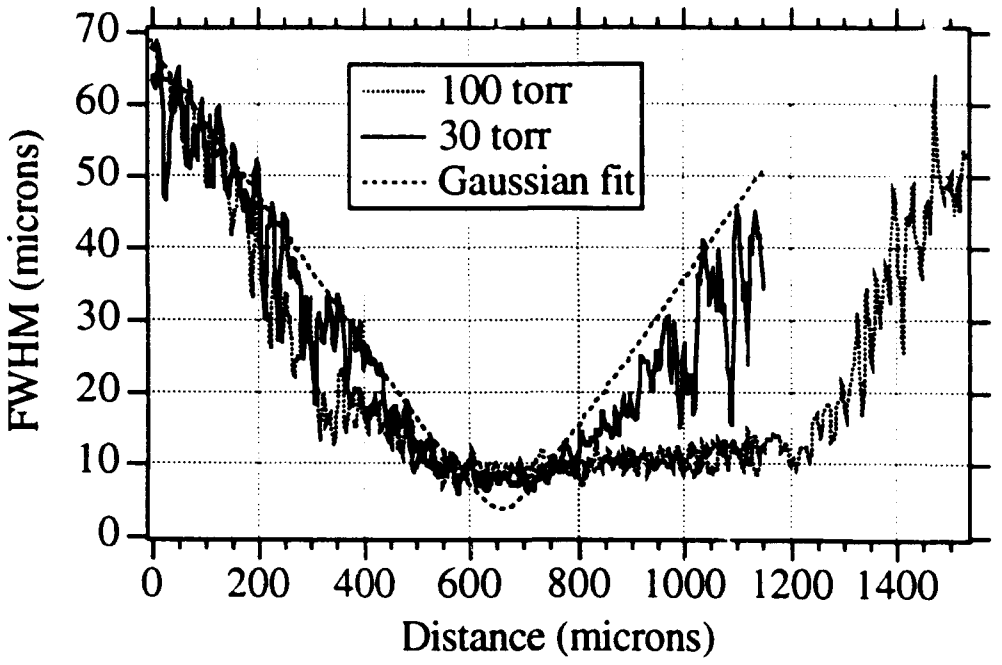
70
60
50
40
30
20
10
0
FWHM (microns)
100 torr
30 torr
Gaussian fit
0
200
400
600
800
1000
1200
1400
Distance (microns)

Figure 4.

#31

Sub-Picosecond Thomson-Scattering Measurements of Optically Ionized Helium Plasmas

T.E. Glover, T.D. Donnelly, E.A. Lipman, A. Sullivan and R.W. Falcone

Department of Physics, University of California at Berkeley
Berkeley, California 94720

ABSTRACT

We present the first sub-picosecond, time-resolved temperature measurements of gaseous plasmas produced by high-intensity optical ionization. Thomson-scattering is used to measure electron and ion temperatures of helium plasmas created by 125 fs, 800 nm laser pulses focused to an intensity of 2×10^{17} W/cm^2. We find that the *electron* temperature is accurately predicted by a tunneling ionization model. The measured *ion* temperature is significantly above ambient room temperature and is consistent with direct heating by the laser pulse.

PACS numbers: 52.40.Nk, 52.25.Rv, 52.50.Jm

Several authors have recently suggested that x-ray lasers pumped by electron-ion recombination are feasible if cold electrons can be produced from the interaction of a high-intensity laser pulse with a gas sample [1]. Burnett and Corkum [2] have used a model based on tunneling ionization and the resulting drift energy to predict that relatively cold electrons can be produced from such an interaction. Initial experimental tests of this prediction produced conflicting results. Corkum, *et al.* [3] concluded that electron energies are reasonably well predicted by the tunneling model, while Mohideen, *et al.* [4] concluded that the tunneling model significantly underestimates average electron energies. Both of these experiments were performed at low gas density ($< 10^{11}$ /cc). Recombination lasers, however, require relatively high gas density ($> 10^{18}$ /cc) which may result in additional heating mechanisms [5]. Experiments performed at high density [6,7] have utilized longer laser pulses than optimal for transient recombination lasers. The Thomson-scattering measurements of Offenberger, *et al.* [6] were performed using 12 ps pulses; inverse bremsstrahlung (IB) dominated the electron heating and thermal conduction significantly modified the measured temperatures. The accuracy of the tunneling model, therefore, could not be assessed by these experiments. Similarly, the measurements of Leemans, *et al.* [7] were performed with 500 ps laser pulses; therefore, the plasma was not probed on a time-scale relevant to transient recombination lasers.

In this work we use Thomson-scattering to determine electron and ion temperatures of moderately high density helium plasmas. We use a two-pulse technique to create and then probe the plasma on a time-scale short enough that no significant plasma cooling occurs. Our experiments, performed in a regime where ionization heating determines electron energies, test the accuracy of the tunneling model at densities and on time-scales relevant to recombination lasers.

The experimental apparatus is shown in Fig. 1. An initial laser pulse (125 fs, 30 mJ, 800 nm) ionizes helium gas and a second, co-linear pulse at 400 nm probes the preformed plasma. The probe pulse is produced by frequency doubling the 800 nm pulse in a 1 mm KDP crystal. We calculate that the wavelength dependent index of refraction in KDP results in a maximum pump-probe delay of 80 fs. We vary this delay up to 1 ps by passing both pulses through a glass window. This two-pulse technique avoids complications that could arise from modification of the laser spectrum due to ionization induced blue-shifting [8]. Such modifications could complicate interpretation of the Thomson-scattered spectrum and are minimized in these experiments because, at focus, our probe pulse sees a fully-ionized He^{2+} plasma. As expected, measurements of the transmitted probe pulse spectrum revealed no spectral modification. Our peak ionizing laser intensity (2×10^{17} W/cm^2) is a factor of twenty in excess of the intensity necessary [9] to produce He^{2+}, which insures that He is fully ionized over the spatial dimension of our focused probe pulse. The pump and probe pulses are focused to spot sizes of 6.5 μm x 5 μm and 5 μm x 3 μm respectively using an 8 cm focal length off-axis, parabolic mirror. We determined that the probe beam was contained within the focus of the ionizing beam by imaging the focal regions of both beams simultaneously using a CCD camera. The peak intensity of the probe pulse was 2×10^{16} W/cm^2.

Thomson-scattered light was collected over a f/3 collection angle using a 5X microscope objective which viewed a black surface (Wood's horn) behind the laser focus. The microscope objective formed an image of the focus outside of the static-gas-filled target chamber; occulters at this image plane allowed us to spatially discriminate against Thomson-scattered light originating from regions of incompletely ionized He. A second lens imaged the Thomson-scattered light through a crossed Czerny-Turner spectrometer (1/8 m, 1200 g/mm grating) followed by a gated microchannel plate intensifier (MCP) and optical multichannel analyzer. The gated MCP collected light for approximately 10 ns; however, the effective time resolution for probing the plasma was the 125 fs duration

of our probe pulse. We gated the MCP to avoid interference from line emission in He ions; line emission dominated the detected light at late time. Care was taken to eliminate stray laser scatter from the chamber walls and from mirror imperfections; our levels of stray scatter were typically less than 1% of the peak Thomson signal.

Thomson-scattered light was collected at an angle (θ) of 60 degrees with respect to the propagation vector of the 400 nm laser (k_o). The pump laser was polarized parallel to, and the probe laser was polarized perpendicular to, the scattering plane. Accordingly, we probed density fluctuations with wavenumber, $2k_o \times \sin(\theta/2) \cong k_o$. Spectra were taken over a pressure range from 3 -75 torr at a pump-probe delay of 1 ps. Spectra were also taken at a pump-probe delay of < 80 fs (no window) and we found no statistically significant temperature difference from the 1 ps data; we therefore confirmed that plasma cooling was insignificant on the time-scale of our experiments.

Spectra taken at gas densities of 10, 25 and 50 torr are shown in Fig. 2. The central feature at 400 nm (discussed below) is called [10] the "ion feature." The "electron features" (on either side of the ion feature) result from scattering due to electron density fluctuations associated with electron plasma waves modified by thermal motion. The data shown in Fig. 2 have been fit to theoretical Thomson scattering spectra convolved with both the spectral response of the spectrometer and the spectral distribution of the probe laser. The theoretical spectra assume Maxwellian electron distributions [10]. We find good agreement between theoretical and experimental spectra at all pressures. The measurements of Mohideen also show that the form of the initial He distribution function produced from a laser pulse similar to ours is well approximated by a Maxwellian distribution [4]. All fits are consistent with doubly ionized He at the specified density. Best fits are obtained for electron temperatures of nominally 40 eV.

While fits to the short wavelength side of the data in Fig. 2 are good, we note an asymmetry in the electron feature and consequently a poor fit on the long wavelength side

of the data. We believe this asymmetry is due to the presence of near-threshold, stimulated-Raman-scattering (SRS). We find that we are able to significantly modify and/or enhance this long wavelength electron feature (in comparison to the short wavelength feature) by collecting light from different spatial regions of the plasma. The spatial dependence of this enhancement, along with the observation that the magnitude of the enhancement decreases with laser intensity, suggests that it is due to SRS. In our laboratory, SRS has been observed to have strong spatial and laser-intensity dependencies[11].

Experimentally measured temperatures are unaffected by the presence or absence of the observed SRS component. Furthermore, we observe that reduction of the pump laser intensity by 50% does not change the electron temperature (as determined by the electron feature on the short wavelength side of the central ion peak) and this suggests that SRS does not significantly affect our temperatures. Wilks, *et al.* [12] have investigated the influence of the SRS backscattering instability on the electron temperature for short-pulse, laser-ionized plasmas; we calculate that SRS elevates the electron temperature by ≈ 10%, so that we do not expect it to significantly effect the measured temperature.

Also of significance in the spectra of Fig. 2 is the central scattering feature at 400 nm. This "ion feature" is associated with electron density fluctuations caused by ions [10]. The spectral width of a short-pulse laser is always large in comparison with the inherent width of this feature so that we are insensitive to the spectral form of the ion feature and instead sample its integrated power due to convolution with the laser pulse. For low ion temperatures (high values of ZTe/Ti), the ion feature is a double peaked structure about the central laser frequency, and is due to electron density fluctuations associated with ion acoustic waves. For high ion temperatures (low ZTe/Ti), the ion feature is approximately Gaussian, centered at the central laser frequency, and reflects the

ion thermal spread. Without resolution of the ion feature, an experimental spectrum taken at one collection angle does not specify which of these ion scattering situations dominates. This results from the fact that the intensity of the unresolved ion feature is a double valued function of ion temperature. The ion temperature (and subsequent specification of acoustic versus thermal scatter) can be uniquely determined from Thomson scattering spectra taken at two different collection angles. A change in the collection angle changes the propagation vector of the fluctuations probed and therefore specifies the ion temperature. Spectra taken at collection angles of both $\theta = 60$ and 120 degrees indicate that the ion scattering is dominated by fluctuations associated with acoustic waves. The ion temperatures (see Fig. 3) range from 0.7 eV at 3 torr to 4.4 eV at 75 torr. Finally, we note that the height of the central ion feature was not a sensitive function of the spatial plasma region viewed, as was the case for the SRS component of the electron feature. We also observed that the ion feature height was insensitive to the presence or absence of an enhanced SRS component in the electron feature. These observations, along with the absence of a significant variation in relative ion feature height with a 50% reduction in laser intensity, also suggest that stimulated Brillouin scattering (SBS) did not significantly effect our ion feature height.

The variation in measured electron temperature with gas density is also shown in Fig. 3. Electron and ion temperatures were assigned by finding best theoretical fits to several experimental spectra at each gas pressure and then taking the average of these fits. Error bars were determined by the range of temperatures that could reasonably fit the data. The electron temperatures are 40 eV (3 torr), 50 eV (10 torr), 40 eV (25 torr), 38 eV (50 torr) and 36 eV (75 torr). The nominal 10 eV variation of the 10 torr data from all other data is within the error of our measurement (typically 10% for pressures above 25 torr and 20% for pressures below 25 torr). Within this error, we find that the electron temperature does not change over a 3-75 torr pressure range. The Thomson-scattering experiments of Ref. 6 show an increase in the (He) electron temperature from 21 eV at

20 torr to 36 eV at 100 torr; these experiments were performed with longer laser pulses than those used in our experiments so that IB heating and thermal conduction dominated the electron energy. We calculate that IB heating is unimportant for our experiments (< 2 eV heating at 50 torr). We calculate heating due to tunneling ionization using rates given by Ammosov [13]; the distribution function of residual electron energies was calculated using the classical approach of Corkum [3] and equivalent temperatures were defined as two-thirds the predicted average energy. The predicted temperature for a 125 fs pulse at 800 nm focused to 2×10^{17} W/cm^2 is 40 eV, in good agreement with our measured temperatures.

In contrast to our results, the measurements of Mohideen [4] indicate that the tunneling model significantly underestimates electron energies. These short-pulse experiments yielded electron temperatures in He of 37 eV for removal of the first electron and 140 eV for removal of the second electron. This implies an average, thermalized electron temperature in He^{2+} of approximately 90 eV. We calculate that for Mohideen's laser parameters (820 nm, 180 fs, 2.5×10^{16} W/cm^2), the tunneling model predicts temperatures approximately a factor of 3 lower than those measured in his experiments. We consider the possibility that our experimental spectra preferentially reveal a colder (37 eV) distribution while masking a hotter (140 eV) distribution. We calculate the Thomson-scattering spectra from 37 eV and 140 eV electron distributions and sum the predicted spectra. The resulting theoretical curve at 50 torr indicates distinct peaks due to a 140 eV distribution (at 413 nm and 387 nm) which are a factor of 2 lower than the peaks due to a 37 eV distribution (at 411 nm and 389 nm). The peak due to the 140 eV distribution would be observable (on the short wavelength side of the ion scattering peak), but it is not present in the data.

While the origin of the discrepancy between our data and Ref. 4 is unknown, we note that time-resolved continuum slope measurements performed in our laboratory [14]

support our conclusion that the electron temperature in He^{2+} is accurately predicted by the tunneling ionization model. These continuum slope measurements were performed using 160 fs, 616 nm laser pulses focused to an intensity of 2×10^{16} W/cm^2. Using this technique, we measured a temperature of 22 eV $\pm$ 4 eV compared to the tunneling model prediction of 21 eV for these laser parameters.

Measured ion temperatures indicate a gradual increase with density as shown in Fig. 3. This is consistent with heating expected from ion-ion collisions in the laser field. Low ion temperature leads to high (ion-ion) collisionality so that the ions are heated by ion-ion collisions more efficiently than by electron-ion collisions. We calculate this heating using the Spitzer [15] ion-ion collision frequency at an effective energy which is the sum of the ion thermal and the ponderomotive energies. The thermal component of this effective temperature increases as the ions gain energy via collisions in the laser field; this has the effect of saturating the energy gain because the temperature dependence of the collision frequency leads to a decrease in the heating rate for higher energy ions. The expected heating is, therefore, not strictly linear in gas density. The predicted ion temperatures are compared to the experimental values in Fig. 3 and we note good agreement between theory and experiment.

In conclusion, we have used Thomson scattering to measure electron and ion temperatures in He plasmas produced by high intensity optical ionization. The measured ion temperatures varied from 0.7 eV to 4.4 eV (increasing with gas density) and are consistent with direct heating by ion-ion collisions in the laser field. The measured electron temperatures did not vary significantly over a pressure range from 3 torr to 75 torr. This result is consistent with our expectation that we are operating in a parameter space, favorable for recombination lasers, where electron temperatures are primarily determined by the optical ionization process. Contrary to the conclusions reached in Ref. 4, we find that the electron temperature is in good agreement with temperature

predictions based on the tunneling ionization model. This conclusion implies that electrons can be produced with sufficiently low residual energies to make recombination pumped x-ray lasers feasible.

The authors would like to thank Hector Baldis, Wim Leemans, Umar Mohideen, Allan Offenberger, David Villeneuve, and Scott Wilks for useful discussions and comments on our work, and Frank Patterson for loan of the OMA detector. T.E.G. would like to acknowledge support of an AT&T CRFP fellowship. E.A.L. would like to acknowledge support of an NSF graduate fellowship. This work was supported by the U.S. Air Force Office of Scientific Research and through a collaboration with Lawrence Livermore National Laboratory under contract W-7405-ENG-48.

Figure Captions

Figure 1. Experimental layout. An initial laser pulse at 800 nm fully ionized He gas and a second pulse at 400 nm probed the resulting plasma.

Figure 2. Thomson spectra in He. (---- experimental data; —— theory)

(a) 50 torr: fit to 40 eV electron temperature and 3.6 eV ion temperature;

(b) 25 torr: fit to 40 eV electron temperature and 2.8 eV ion temperature;

(c) 10 torr: fit to 50 eV electron temperature and 2.5 eV ion temperature.

Figure 3. Measured and predicted electron and ion temperatures as functions of pressure. Electron temperatures are calculated using the tunneling ionization model while ion temperatures are calculated from ion-ion collisional heating in the laser field.

References

[1] P. Amendt, D. C. Eder, and S. C. Wilks, Phys. Rev. Lett. **66**, 2589 (1991); N. H. Burnett and G. D. Enright, IEEE J. Quantum Electron. **26**, 1797 (1990); Y. Nagata, *et al.* Phys. Rev. Lett. **71**, 3774 (1993).

[2] N. H. Burnett and P. B. Corkum, J. Opt. Soc. Am. B **6**, 1195 (1989).

[3] P. B. Corkum, N. H. Burnett and F. Brunel, Phys. Rev. Lett. **62**, 1259 (1989).

[4] U. Mohideen, *et al.*, Phys. Rev. Lett. **71**, 509 (1993); U. Mohideen, Ph.D. thesis, Columbia University (1993).

[5] B. M. Penetrante and J. N. Bardsley, Phys. Rev. A **43**, 3100 (1991).

[6] A. A. Offenberger, *et al.*, Phys. Rev. Lett. **71**, 3983 (1993).

[7] W. P. Leemans, *et al.*, Phys. Rev. Lett. **68**, 321 (1992).

[8] W. M. Wood, C.W. Siders and M. C. Downer, Phys. Rev. Lett. **67**, 3523 (1991).

[9] Augst, *et al.*, Phys. Rev. Lett. **63**, 2212 (1989).

[10] J. Sheffield, *Plasma Scattering of Electromagnetic Radiation*, (Academic Press, New York, 1975).

[11] A. Sullivan, Ph.D. thesis, University of California at Berkeley (1993), available from University Microfilms Inc., 300 North Zeed Road, Ann Arbor, MI 48106-1346.

[12] S. C. Wilks, personal communication; Wilks, *et al.* (to be published).

[13] M.V. Ammosov, N.B. Delone and V.P. Krainov, Sov. Phys. JETP. **64** , 1191 (1986).

[14] T. E. Glover, Ph.D. thesis, University of California at Berkeley (1993), available from University Microfilms Inc., 300 North Zeed Road, Ann Arbor, MI 48106-1346.

[15] F. F. Chen, *Introduction To Plasma Physics and Controlled Fusion*, (Plenum Press, New York, 1990).

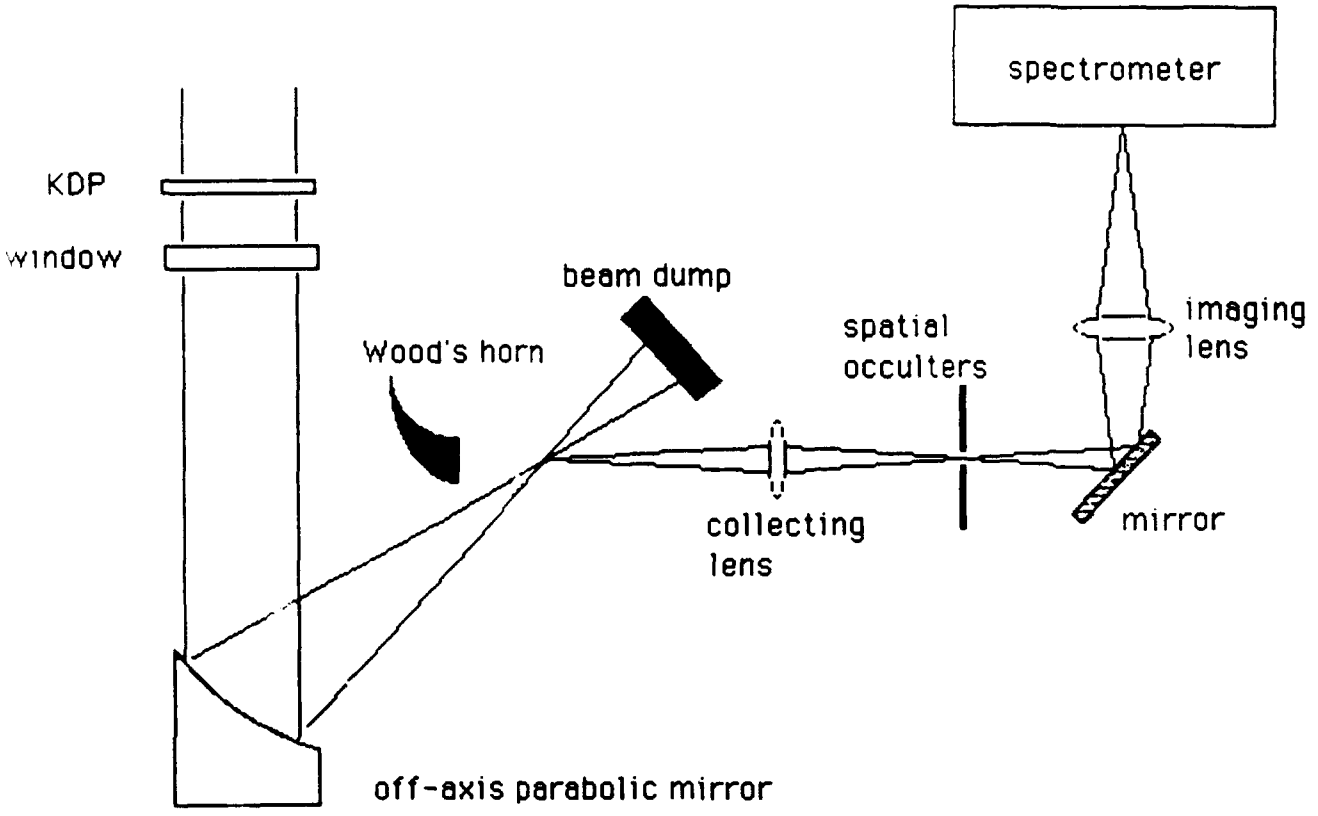

EXPANDED VIEW OF FOCAL REGION

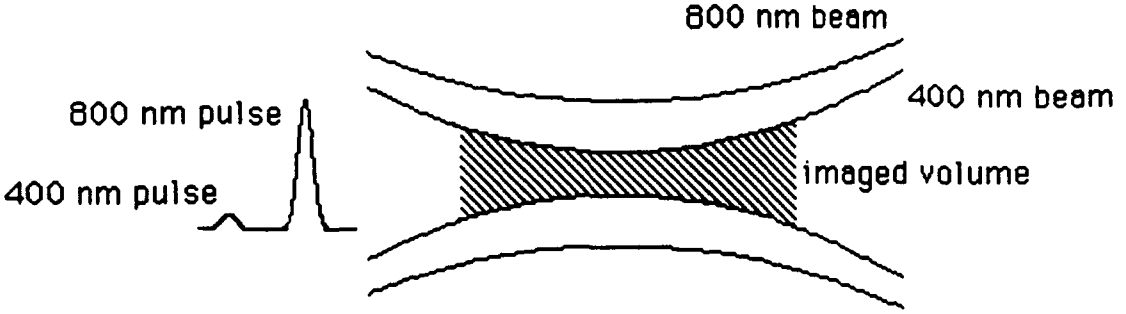

Figure 1

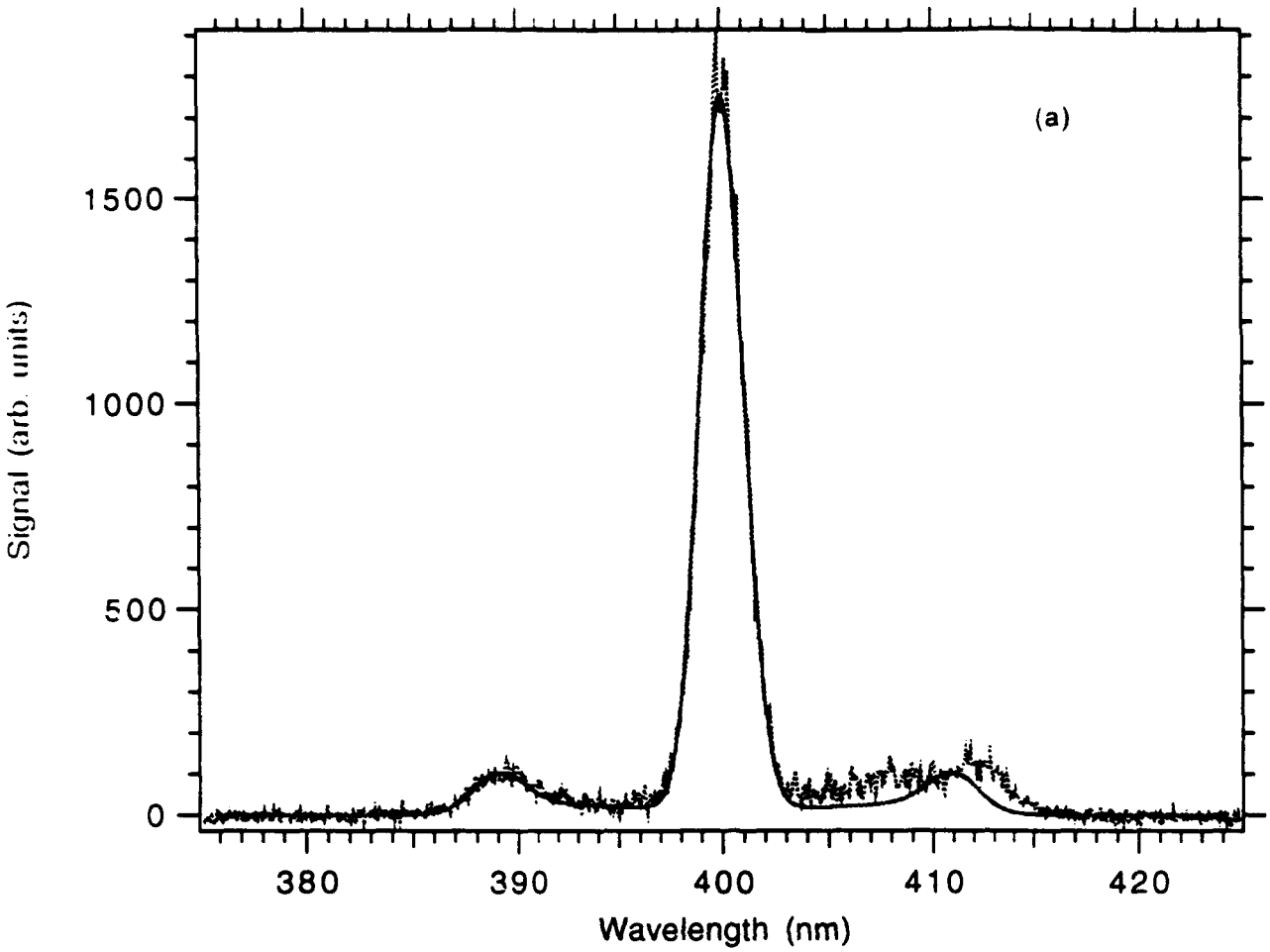
(a)
1500
1000
500
0
Signal (arb. units)
380
390
400
410
420
Wavelength (nm)

Figure 2a

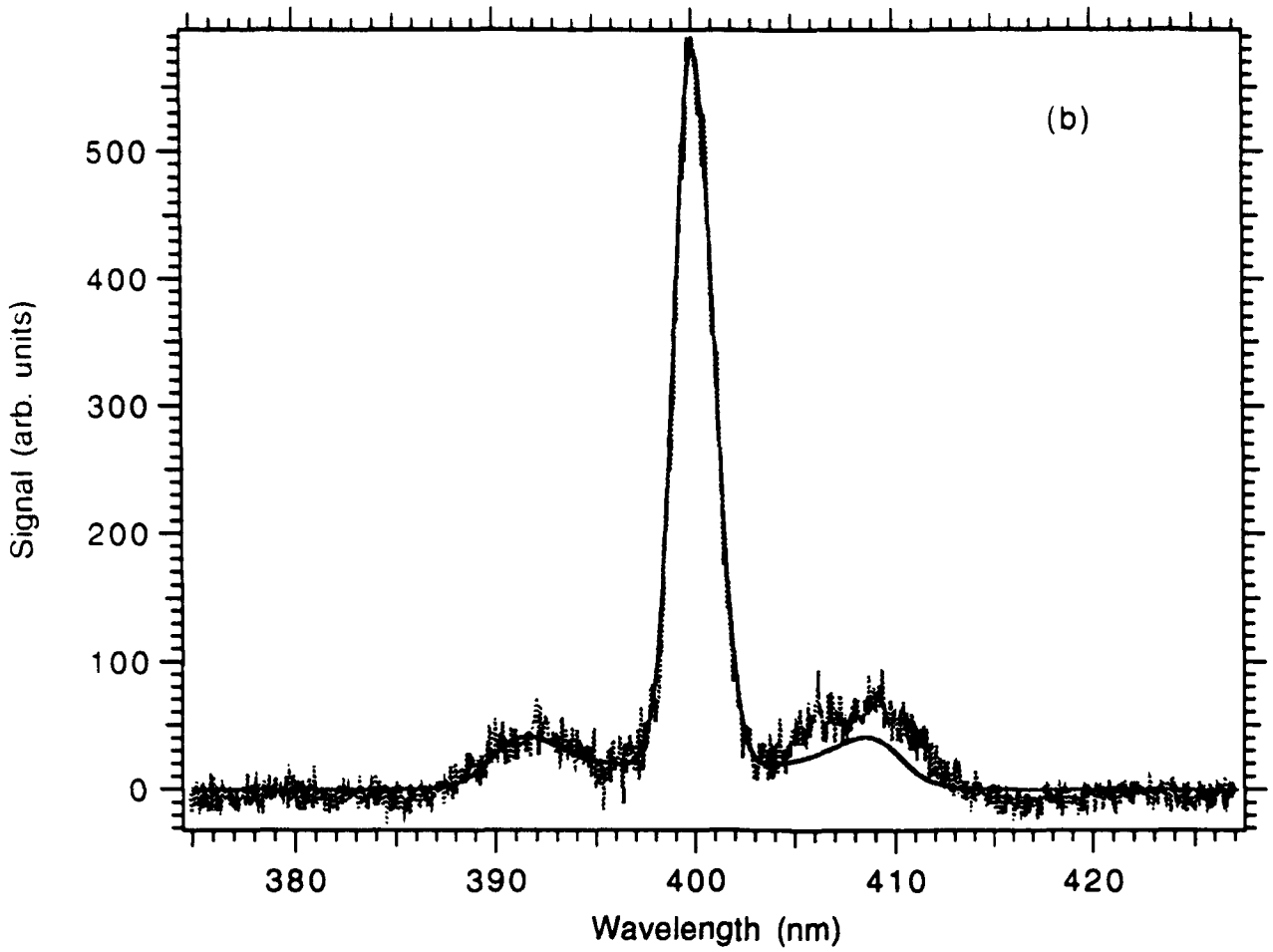
(b)
Signal (arb. units)
500
400
300
200
100
0
380
390
400
410
420
Wavelength (nm)

Figure 2b

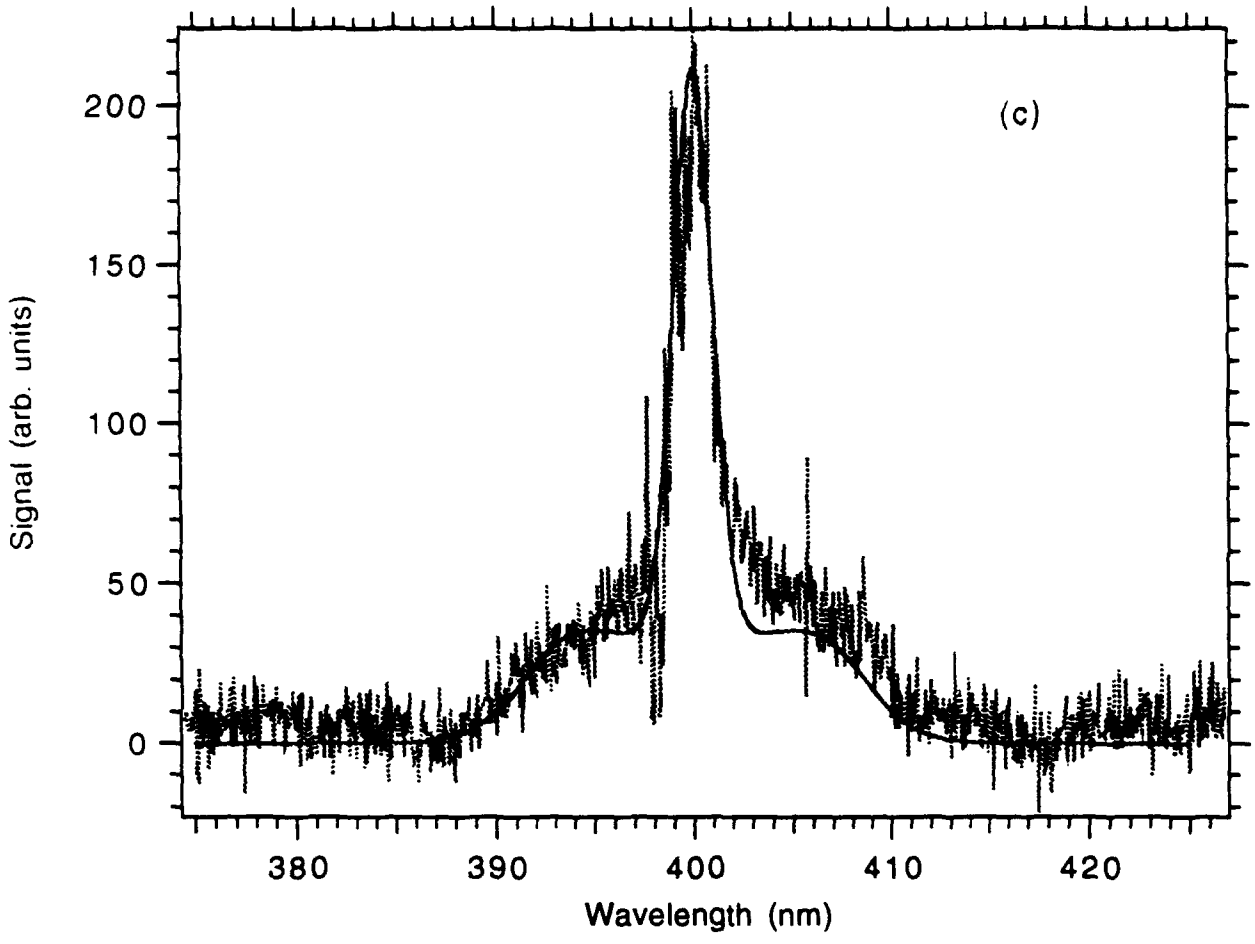
(c)
Signal (arb. units)
200
150
100
50
0
380
390
400
410
420
Wavelength (nm)

Figure 2c

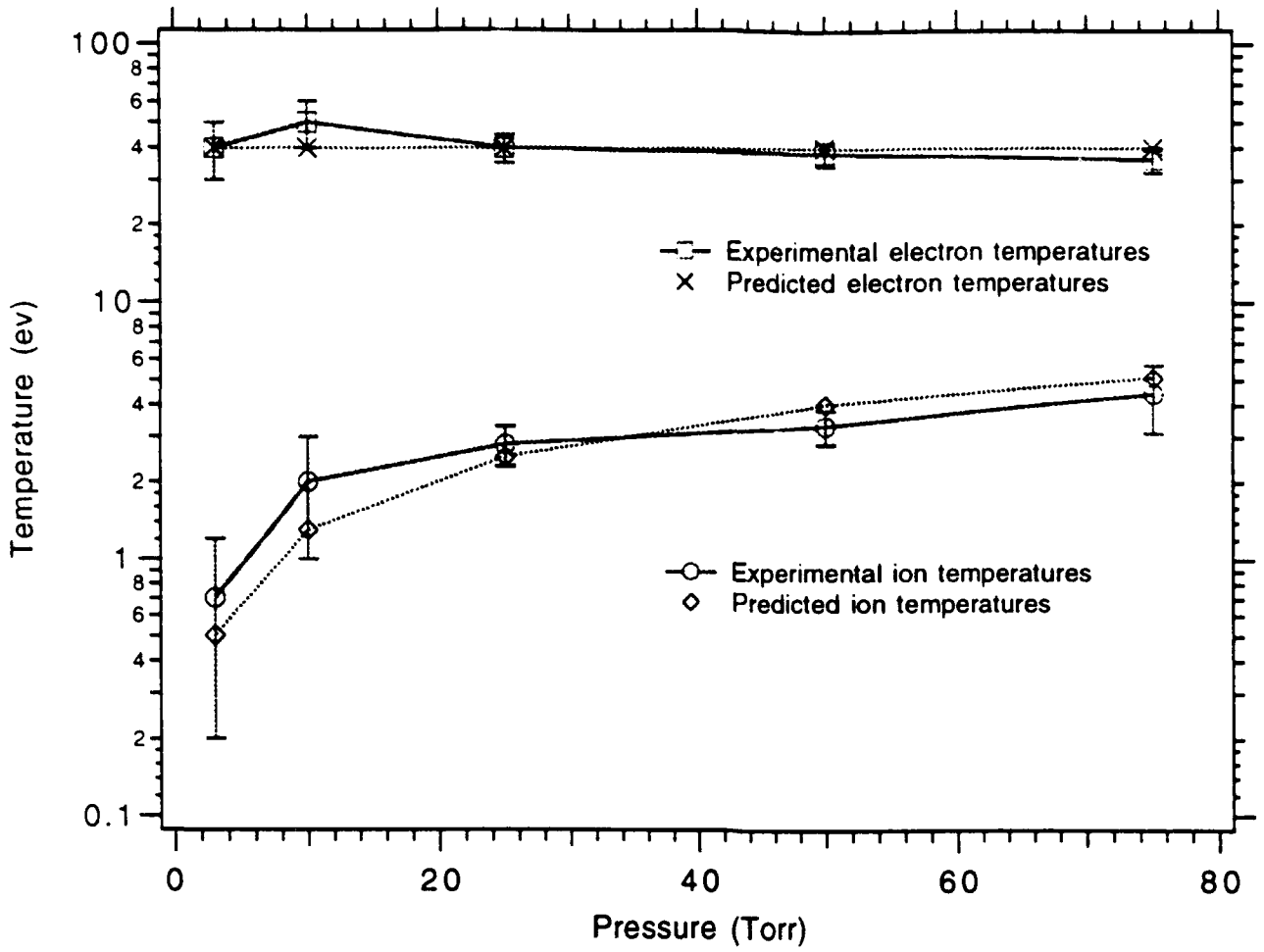
Temperature (ev)
100
8
6
4
2
10
8
6
4
2
1
8
6
4
2
0.1
0
20
40
60
80
Pressure (Torr)
Experimental electron temperatures
Predicted electron temperatures
Experimental ion temperatures
Predicted ion temperatures

Figure 3

Approved for public release;
distribution unlimited.

AIR FORCE OF SCIENTIFIC RESEARCH (AFSC)
NOTICE OF TRANSMITTAL TO DTIC
This technical report has been reviewed and is
approved for public release IAW AFR 190-12
Distribution is unlimited.
John [illegible]
STINFO Program Manager